Dissertation

Continuous **Focal** Drug Delivery to Assess the Pharmacological Role of **Liraglutide** on Energy Homeostasis in the **Hypothalamus**

submitted by

MSc, BSc

Katrin Kaineder

for the Academic Degree of

Doctor of Philosophy

(PhD)

at the

Medical University of Graz

Department of Internal Medicine

Division of Endocrinology and Diabetology

under the Supervision of

Univ.-Prof. Dr. med. univ. Thomas R. Pieber

2017

Statutory Declaration

I hereby declare that this dissertation is my own original work and that I have fully acknowledged by name all of those individuals and organisations that have contributed to the research for this dissertation. Due acknowledgement has been made in the text to all other material used. Throughout this dissertation and in all related publications I followed the guidelines of “Good Scientific Practice and Ombuds Committee at the Medical University of Graz”.

Parts of this thesis are adapted from the publication Kaineder et al. “Continuous intrahypothalamic rather than subcutaneous liraglutide administration leads to reduced body weight gain and stimulation of melanocortin system”, published 2017 in the *International Journal of Obesity*.

Date:

Acknowledgements

The accomplishment of my PhD-thesis would not have been possible without the encouragement and support of many amazing people, whom I had the honor to meet during these four years.

First I want to honestly thank my supervisor, without whom this thesis could not have been done. Thank you, Thomas Pieber for your constructive criticism and your undoubted support in every situation.

Special thanks goes to my awesome Upper Austrian friends Thomas and Selma, for their great help during the development of my PhD project, and for giving me amazing advice and suggestions for all my scientific publications. With their convincing words they kept me going during doubtful situations.

Of course, I want to thank my labmates. Together we are the basic research unit (BRUT) at the Divison for Endocrinology and Diabetology. We started as a very small group, Alexandra, Mina, Barbara and me and ended in a group of eight people, Petra, Julia, Jasmin, Ceren, Lukas, Kaddour, and Rokhsareh, who rule the lab no matter what. Special thanks to Petra for motivation and encouragement during the last tough year. I want thank Julia and Kaddour, who helped me a lot with experiments and analysis. To my dearest office partners, Ceren and Mina, thank you for your patience, cheering words and our coffee breaks, which I already miss. You are all amazing people, and I am grateful that I had the chance to meet every single one of you.

I am very thankful to my parents, Karin and Fritz, my grandpa Karl and my uncle Karl-Heinz, who actually convinced me to do a PhD. Without these amazing and great people I would not have gotten so far in my career. I love you.

My last thank is directed to Matthias, who supported me with his great serenity and comfort in critical situations. Thank you for the laughs and fun we shared.

Special thanks to everybody from the DK-MOLIN for making this PhD thesis possible. I am very thankful for all the new amazing people I got to know from all over the world because of the DK.

I also want to thank Signe Sørensen Torekov, Jens Holst, and Bolette Hartmann for giving me the chance to stay at their lab to discuss the study design and hypothesis of my project. I thank all the members of Signe's and Jens lab for the warm welcome in Copenhagen and for the fun we shared on conferences. Special thanks to Eva, I had a wonderful time with you, and I am very thankful that you allowed me to get an insight in clinical studies.

This study has been funded by the Medical University of Graz through the PhD Program Molecular Fundamentals of Inflammation (DK-MOLIN) via the Austrian Science Fund (FWF, project number W1241).

Table of Contents

Abbreviations and Definitions

3V	Third ventricle
ACSF	Artificial cerebrospinal fluid
ADRβ1	Adrenergic receptor β1
AGRP	Agouti related protein
AMPK	AMP-activated protein kinase
α-MSH	α- melanocyte stimulating hormone
AP	Anterior - Posterior
ARC	Arcuate nucleus
AT	Adipose tissue
BBB	Blood brain barrier
BDNF	Brain derived neurotrophic factor
BMI	Body mass index
BMP7	Bone morphogenetic protein 7
CART	Cocaine and amphetamine regulated transcript
CCK	Cholecystokinin
CDNA	Complementary Deoxyribonucleic acid
CIDEA	Cell death-inducing DFFA-like effector a
COFM	Cerebral open flow microperfusion
CRH	Corticotropin-releasing hormone
CVO	Circumventricular organs
DIO2	Type II iodothyronine deiodinase
DMN	Dorsomedial nucleus
DPPIV	Dipeptidyl peptidase IV
DV	Dorsal-Ventral
EMA	European Medicines Agency
EWAT	Epididymal brown adipose tissue
FDA	Food and Drug Administration
FFM	Free fat mass
FG	Free glycerol
FGF21	Fibroblast growth factor 21
GABA	Gamma aminobutyric acid
GFAP	Glial fibrillary acidic protein

GLP-1	Glucagon-like peptide
GLP-1R	Glucagon-like peptide 1 receptor
H&E	Haematoxylin & eosin
I.D.	Inner diameter
IBAT	Interscapular brown adipose tissue
ICV	Intracerebroventricular
IH	Intrahypothalamic
IWAT	Inguinal white adipose tissue
LHA	Lateral hypothalamus
MC3R	Melanocortin 3 receptor
MC4R	Melanocortin 4 receptor
MCH	Melanin-concentrating hormone
ME	Median eminence
Micro-CT	Micro-computer tomography
ML	Midline
MTII	Melanotan II
NAC	Nucleus accumbens
NaCl	Sodium chloride
NaF	Sodium fluorescein
NEFA	Non-esterified fatty acid
NEP	Neprilysin
NPY	Neuropeptide Y
O.D.	Outer diameter
OCT	Optimal cutting temperature
PBS	Phosphate buffered saline
PEEK	Polyether ether ketone
PFA	Paraformaldehyde
PLH	Posterior lateral hypothalamus
POMC	Proopiomelanocortin
PPARGC1a	Peroxisome proliferator-activated receptor gama coactivator 1-alpha
PRDM16	PR containing domain 16
PVN	Paraventricular nucleus
PYY	Polypeptide Y
qPCR	Quantitative Polymerase chain reaction
REE	Resting energy expenditure

RNA	Ribonucleic acid
S.D.	Sprague Dawley
SAT	Subcutaneous adipose tissue
SC	Subcutaneous
SF1	Steroidogenic factor 1
T2D	Type 2 diabetes
T3	Triiodothyronine
T4	Thyroxine
TAG	Triglycerides
TNFRSF9	Tumor necrosis factor receptor superfamily, member 9
TRH	Thyrotropin-releasing hormone
TRKB	Tropomyosin receptor kinase B
TSH	Thyroid stimulating hormone
UCP1	Uncoupling protein 1
VAT	Visceral adipose tissue
VMN	Ventromedial nucleus
VTA	Ventral tegmental area
ZIC1	Zinc finger of the cerebellum 1

Zusammenfassung

Liraglutid ist ein Glukagon-like Peptid-1-Rezeptor (GLP-1R) Agonist, welcher von der FDA und EMA für die chronische Gewichtsbehandlung und die glykämische Kontrolle zugelassen ist. Seinen anorektischen Effekt übt Liraglutid möglicherweise über den GLP-1R im Hypothalamus aus. Der Hypothalamus spielt durch die Regulierung des Appetits und des Energieverbrauchs eine zentrale Rolle bei der Aufrechterhaltung des Körpergewichts. In Tierversuchen wurde gezeigt, dass die akute Liraglutid Behandlung zu Sättigung und Gewichtsverlust führt und außerdem Thermogenese im Fettgewebe stimuliert. Allerdings müssen die präzisen Mechanismen, die dem chronischen Liraglutid-induzierten Gewichtsverlust zugrunde liegen, noch untersucht werden.

In dieser Studie wollen wir den Unterschied zwischen peripher (subkutanem - SC) und zentral (intrahypothalamisch - IH) injiziertem Liraglutid auf den Körpergewichtsverlauf in chronischer und akuter Behandlung zu erforschen. Wir untersuchten, ob dem Gewichtsverlust ein erhöhter Energieverbrauch im Fettgewebe oder eine Stimulierung hypothalamischer Appetit-Zentren zugrunde liegt.

Gesunde und dünne männliche Sprague Dawley Ratten (N=32) wurden in 4 Gruppen, 2 Behandlungs- und 2 Kontrollgruppen unterteilt. Wir verabreichten Liraglutid kontinuierlich entweder intrahypothalamisch (IH; 10 µg/Tag) oder subkutan (SC; 200 µg/kg/Tag) für 28 Tage. Für die 24-stündige Akut-Studie injizierten wir Liraglutid (IH Liraglutid) oder ein Plazebo (IH Kontrolle) einmalig in den Hypothalamus von gesunden Ratten (N=16). In beiden Studien wurden Körpergewicht und Fettgewebsmasse gemessen. Die Adipozytengröße von 3 verschiedenen Fettdepots wurde für die chronische Liraglutidverabreichung ausgewertet. Die Verteilung des subkutanen und des viszeralen Fettgewebe nach der chronischen Liraglutid-Verabreichung wurde unter Verwendung von einem bildgebenden Verfahren (Mikro-Computer Tomographie) analysiert. In beiden Studien untersuchten wir die Genexpression von validierten Markern für Browning-, Thermogenese- und Adipozyten-Differenzierung in drei verschiedenen Fettdepots sowie die Genexpression von Markern, die spezifisch für die hypothalamische Appetitregelung sind.

Die chronische IH Liraglutid Verabreichung induzierte eine 8%ige Körpergewichtsreduktion am Tag 9 im Vergleich zur entsprechenden Kontrollgruppe

(*P*<0,01) und einen Körpergewichtsverlust von 7% am Tag 9 im Vergleich zur SC-Liraglutid Behandlung (*P*<0,01). Es zeigte sich eine Reduktion des epididymalen und inguinalen Fettgewebes nach chronischer IH Liraglutid Behandlung im Vergleich zur Kontrollgruppe (*P*<0,05). Durch die chronische IH Liraglutid Behandlung konnten wir eine 18-fache Induktion von mRNA des hypothalamischen Melanokortin-4-Rezeptors (*P*<0,01) erzielen. Blutparameter für Glukose und Fettstoffwechsel wurden von beiden Behandlungen nicht beeinflusst, mit Ausnahme einer signifikanten Erhöhung des Thyroxinspiegels im Plasma (*P*<0,05) nach chronischer IH Liraglutid Behandlung. Wir konnten keinen anorektischen Effekt nach akuter IH und chronischer SC Liraglutid Behandlung beobachten.

Zusammengefasst erzielte eine chronische Verabreichung von Liraglutid in den Hypothalamus eine höhere Reduktion des Körpergewichts und verschiedener Fettdepots als die eine periphere Verabreichung von Liraglutid. Die Körpergewichtsreduktion wird von einer Aktivierung des Melanokortin Systems im Hypothalamus begleitet und somit schließen wir Thermogenese und Browning als gewichtsreduzierende Faktoren aus. Grundsätzlich zeigte sich in dieser Studie, dass eine chronische Stimulierung des GLP-1R im Hypothalamus mit Liraglutid zu einer erheblichen Reduktion des Körpergewichts führt. Weitere Studien müssen folgen, um die zentrale Rolle des GLP-1R in Bezug auf die Regulierung des Körpergewichts genauer zu erforschen.

Abstract

Liraglutide is a glucagon-like peptide-1 receptor (GLP-1R) agonist and is approved by the FDA and EMA for use in chronic weight management and glycaemic control. Liraglutide possibly exerts its anorectic effects via the GLP-1R in the brain, especially in the hypothalamus. The hypothalamus plays a pivotal role in the maintenance of body weight by regulating appetite and energy expenditure. Animal studies show that acute liraglutide treatment triggers satiety, weight loss and activates thermogenesis in adipose tissue. However, the precise mechanisms underlying the chronic liraglutide-induced weight loss are still under investigation.

In this study, we aimed to evaluate the difference between peripherally (subcutaneous – SC) and centrally (intrahypothalamic – IH) injected liraglutide on body weight regulation in both a chronic and an acute administration. We examined whether energy expenditure, in terms of thermogenesis and browning of adipose tissue or hypothalamic appetite centres are involved in the liraglutide-induced weight loss.

Therefore, healthy and lean male Sprague Dawley rats (N=32) were separated in 4 groups, 2 treatment and 2 control groups. For the chronic study design, we continuously administered liraglutide either intrahypothalamically (IH; 10 µg/day) or subcutaneously (SC; 200 µg/kg/day) for 28 days. For the 24-hours acute study we injected liraglutide (IH liraglutide) or placebo (IH control) once into the hypothalamus of healthy lean rats (N=16). For both studies, we assessed changes in body weight and adipose tissue mass. Adipocyte size of three different adipose tissue depots was evaluated for the chronic study setup. The distribution of subcutaneous and visceral adipose tissues after chronic liraglutide administration was analysed by using micro-CT. For both studies, we examined mRNA signature of markers for browning, thermogenic and adipocyte differentiation in adipose tissue depots as well as markers specific for neurons regulating appetite.

The results show that chronic IH liraglutide administration induced an 8% body weight reduction at day 9 compared to the corresponding control group (P<0.01) and a 7% body weight loss at day 9 compared to SC liraglutide treatment (P<0.01). Epididymal and inguinal adipose tissue mass were significantly reduced after chronic IH liraglutide treatment compared to the control group (P<0.05). Moreover, our data show that chronic IH liraglutide treatment triggered an 18-fold induction of the

hypothalamic *melanocortin 4 receptor* ($P<0.01$). Circulating plasma parameters for glucose and fat metabolism were unaffected by both treatments, apart from a significant increase of circulating thyroxine levels ($P<0.05$) after chronic IH liraglutide treatment. Both acute IH and chronic SC liraglutide treatment were did not trigger an anorectic effect.

Thus we conclude that chronic IH liraglutide is more effective than SC liraglutide treatment in triggering an anorectic effect, by reducing body weight and adipose tissue mass. We further state that this profound reduction in body weight and adipose tissue mass is most likely mediated by the hypothalamic melanocortin 4 receptor system rather than by improved thermogenesis. Further investigations will be needed to assess the role of the central GLP-1R in the regulation of body weight.

GENERAL INTRODUCTION

1 Epidemiology of obesity

Obesity is stated as one of the top ten global health problems by the World Health Organization[1]. In the past three decades, the prevalence of obesity increased two-fold, with currently 600 million adults and already 41 million children classified as obese[1–4]. If this trend continues, an estimated one-third of the world's adult population will be overweight (body mass index, BMI ≥25.0 kg/m^2) and another 20% will be obese (BMI ≥30.0 kg/m^2) by 2030[5]. In Austria, 51.7% of adults (20 years or older) are obese or overweight, and already 22.9% of children (0-9 years) are classified as obese or overweight[6].

Overweight and obesity are no longer limited to high-income countries, but also pose a challenge to low– and middle-income countries[1]. In Africa, the prevalence of childhood obesity has nearly doubled in the last two decades[1]. This enormous worldwide increase of obesity is considered to be a major health concern with a significant economic burden to all health care systems[7]. The rapid increase is mainly regarded to be a result of modern western sedentary lifestyle[8,9]. Distinct genetic variations increase obesity prevalence but obesity and overweight are mostly initiated by an imbalance in energy homeostasis when energy intake exceeds energy expenditure[8,9]. Obesity and its associated comorbidities, such as type 2 diabetes, coronary heart disease, ischemic stroke and several types of cancer request discovery of new targets and identification of molecular mechanisms responsible for body energy homeostasis[10,11]. Energy homeostasis is the control of energy balance in the human body and involves the coordinated homeostatic regulation of food intake and energy expenditure to sustain weight control.

1.1 Energy homeostasis

Energy homeostasis is a biological process that involves the coordinated homeostatic regulation of energy intake (food intake) and energy expenditure (resting metabolic rate, physical activity)[12]. Energy homeostasis matches intake to expenditure and is thus balancing body weight and body fat content in healthy normal weight individuals[13]. Changes in the circulating concentrations of metabolites and hormones that are involved in whole-body energy homeostasis are indicative of energy imbalances. In a situation of energy surplus, circulating anorexigenic factors such as leptin, insulin, glucagon-like peptide-1 (GLP-1), peptide YY_{3-36} (PYY_{3-36}) or glucose are increased, whereas orexigenic factors such as ghrelin are decreased[14].

Under steady-state conditions, all ingested nutrients are normally metabolized to maintain a basic metabolic rate, thermogenesis, and muscle action (energy expenditure). Excess energy is stored as glycogen and fat for food deprivation[15]. To maintain an energy balance, a neural regulator senses nutrient availability in the internal milieu (a process referred to as “adiposity negative feedback”) and generates appropriate signals to the neural circuits controlling appetite and energy expenditure, usually referred to as homeostatic regulation of adiposity and body weight[15]. Leptin is the major mediator of “adiposity negative feedback” and is secreted in direct proportion from adipose tissue[12]. Upon food ingestion leptin is secreted from adipose tissue enters the brain and stimulates satiety via activation of hypothalamic satiety neurons[12]. Beside “adiposity negative feedback” signals numerous hormonal and nutrient-related signals influence appetite. Gut peptides such as PYY_{3-36}, GLP-1, or cholecystokinin are responsible for induction of satiety after food ingestion. In contrast, the gut hormone ghrelin is responsible for the stimulation of food intake and is therefore secreted before meal onset[16]. Ghrelin inhibits the activity of satiety neurons by activating appetite stimulating neurons in the hypothalamus[17].

1.2 Energy homeostasis regulated in the hypothalamus

Neurons in the hypothalamus are involved in sensing humoral and local energy signals, which transmit information about the energy status of each individuum[14]. Previous animal studies have shown that the hypothalamus contains neuronal centers (nuclei) which regulate whole-body energy balance. These hypothalamic centers include nuclei such as the arcuate nucleus (ARC), the paraventricular nucleus (PVN), and the ventromedial hypothalamus (VMH) among others[14]. Activation or inhibition of those hypothalamic nuclei leads to a change in food intake which results either in weight gain or in weight loss[18–20].

Anorexigenic and orexigenic neuronal populations are abundant in the ARC and are regulated by peripheral hormones. Neurons that co-express agouti-related protein (AGRP) and neuropeptide Y (NPY) exert orexigenic effects[21]. Neurons that co-express α-melanocyte stimulating hormone (α-MSH; product of proopiomelanocortin (POMC) cleavage) and cocaine-and-amphetamine-regulated transcript (CART) exert anorexigenic effects[21]. Selective ablation of AGRP/NPY neurons in the ARC has led to a reduction in food intake and subsequent weight loss (anorexigenic)[22,23], while ablation of POMC/CART neurons causes hyperphagia and weight gain (orexigenic)[24,25]. Studies on lean and obese animal models have shown that genetic deletion of *Agrp* – and *Npy* expressing neurons did not affect body weight or food intake[26–28]. Genetic deletion of the *Pomc* expressing neurons resulted in hyperphagia, increased fat mass and increased body length[28]. Even though studies have shown that genetic deletion of AGRP/NPY neurons did not affect energy homeostasis, it is beyond doubt that AGRP/NPY as well as POMC/CART neurons are critical for the regulation of appetite and energy homeostasis[22]. AGRP/NPY neurons express receptors for peripheral appetite hormones such as insulin, leptin, and ghrelin[29–31]. Stimulation of the specific receptor leads to coordinated physiological responses that regulate energy homeostasis through modulation of appetite and/or energy expenditure[14]. Insulin is secreted from pancreatic ß-cells after feeding, which reduces energy intake by targeting the hypothalamic orexigenic AGRP/NPY and anorexigenic POMC/CART neurons. Leptin is secreted from adipocytes proportional to fat mass and targets the hypothalamic orexigenic and anorexigenic neurons which leads to the reduction of food intake[32,33]. Ghrelin, another important humoral factor, is released from the stomach during fasting

periods. After a prolonged fasting period (sleep), ghrelin stimulates the orexigenic AGRP/NPY neurons in the hypothalamus and thereby induces appetite and food intake[34]. AGRP/NPY neurons inhibit POMC/CART neurons by releasing the neurotransmitter GABA (gamma-aminobutyric acid)[35]. The inhibition of POMC/CART neurons by GABA prevents satiety[35–37]. An animal study has shown that the orexigenic effect of ghrelin was dependent on GABA release from AGRP neurons[36].

The hypothalamus consists of so-called first and second order neurons, which communicate with each other. The first order AGRP/NPY and POMC/CART neurons of the ARC send neuronal projections to the PVN where they stimulate second order neurons of the melanocortin system[29,38,39]. The POMC/CART neurons in the ARC together with the second order neurons in the PVN constitute the hypothalamic anorexigenic melanocortin system. The melanocortin system in the PVN includes the melanocortin 3 and 4 receptors (MC3R and MC4R). Beside the MC3R and MC4R expressing neurons, other neurons, which release appetite suppressants such as thyrotropin-releasing hormone are present in the PVN[40,41]. The anorexigenic melanocortin system in the hypothalamic PVN[42] is stimulated by the peptide α-MSH released from POMC/CART neurons in the ARC[33]. The binding and activation of the MC4R by α-MSH lead to weight loss and suppression of food intake[24,43]. Inactivation of the MC4R by genetic deletion results in severe obesity[44]. In rodents, it has been shown that intracerebroventricular administration of a common MC4R agonist (MTII) resulted in a decrease of food intake, this effect was blocked by the administration of the MC4R antagonist (SHU9119)[43,44] proving that the suppression of food intake is dependent on MC4R activation. MC4R probably exerts its anorexigenic effects by regulating the expression of brain-derived neurotrophic factor (BDNF) and the AMP-activated protein kinase in the VMH[14,38,45]. The VMH has been shown to play a major role in appetite regulation and in addition regulates energy balance by regulating thermogenesis in brown and white adipose tissue depots[38,39]. A study performed in conditional knock-out mice has shown that BDNF expressing neurons control energy balance[14]. Genetic deletion of BDNF has led to hyperphagia and obesity in humans and mice whereas administration of BDNF has led to body weight loss and reduction in food intake through MC4R signaling[45].

Altogether, the melanocortin system controls appetite in a highly ordered manner by stimulating or inhibiting different brain areas that regulate appetite, energy

expenditure, and energy balance by synergizing metabolism, cognition, and reward[15]. These brain systems are closely connected to each other and communicate via neuronal projections[15]. Energy homeostasis is regulated by the hypothalamus and the pituitary gland (pituitary-hypothalamic axis), the reward system includes the nucleus accumbens and the ventral tegmental area, the cognitive part is regulated by the hippocampus, amygdala and the thalamus[15]. This complexity and variety in systems involved in appetite regulation indicate that energy homeostasis consists of tightly regulated and conserved mechanisms.

2 Liraglutide as an anti-obesity drug

Liraglutide is a long-acting glucagon-like peptide-1 (GLP-1) analogue and has been approved by FDA and EMA for type 2 diabetes and obesity[7]. Liraglutide, as an anti-obesity drug was approved for adults with a BMI of 30 or higher or for adults with a BMI of 27 or higher who have at least one weight-related comorbid condition (type 2 diabetes, hypertension, elevated cholesterol)[7]. Liraglutide shares 97% structural homology with the human endogenous peptide GLP-1, which is secreted from enteroendocrine L-cells in the gut in the distal ileum and jejunum in response to nutrient ingestion[46]. Upon stimulation (food ingestion) GLP-1 is secreted from L-cells and amplifies pancreatic insulin secretion from ß-cells and decreases glucagon secretion in a glucose-dependent manner thereby lowering blood glucose levels[46–48]. Numerous studies have demonstrated that peripheral administration of GLP-1 or GLP-1 analogues decreases food intake and reduces body weight through the induction of satiety[35,49–51]. Because GLP-1 analogues stimulate insulin secretion and inhibit glucagon secretion exclusively in a glucose-dependent manner, the risk of developing hypoglycaemia is very low, which favours these agents as treatment for obesity and type 2 diabetes mellitus[52].

2.1 Pharmacokinetics of liraglutide (Adsorption, Distribution, Metabolism, Toxicity – ADMET)

Since endogenous GLP-1 is quickly (half-life of approx. 2 minutes) enzymatically degraded by dipeptidyl peptidase IV (DPP-IV) and cleared by the kidneys, long-acting GLP-1 analogues, such as liraglutide were developed[46]. Liraglutide has an elimination half-life of 10-14 hours due to modification of the peptide with an amino acid substitution at position 34 (replacing lysine with arginine) and the addition of a 16-carbon fatty acid chain to lysine at position 26[52]. These modifications allow the prolonged activity of liraglutide, by forming heptamers in solution as well as through a high binding affinity (>98%) to albumin in the circulation, thus making it relatively resistant to degradation by DPP-IV[7,53]. Bioavailability for subcutaneously administered liraglutide is ~55% resulting in the maximum concentration at 11 hours, allowing for once-daily dosing in humans[52]. After subcutaneous administration of 3 mg liraglutide, the volume of distribution is about 20–25 L, which means that liraglutide is mainly distributed throughout the circulation[52]. In contrast to the native

GLP-1, liraglutide is taken up by multiple organs and degraded enzymatically by neprilysin and DPP-IV[54–56]. Liraglutide has a favourable safety profile with mild to moderate side effects like vomiting, nausea, and diarrhoea which can be eliminated by slow uptitration of liraglutide dosing[52].

2.2 Liraglutide and energy homeostasis

Liraglutide mediates its actions through the G-protein coupled GLP-1 receptor (GLP-1R). The GLP-1R is expressed in pancreatic islets, enteric nervous tissue, lung, heart, kidney, small and large intestine, stomach and in the brain[57,58]. In the brain, the GLP-1R occurs in regions that control energy homeostasis (food intake, energy expenditure), such as the brainstem and the hypothalamus[57,59]. Native GLP-1 and liraglutide induce satiety via the GLP-1R at different sites in the body. This has been shown in studies in which centrally or peripherally expressed GLP-1R were pharmacologically antagonized or genetically deleted and stimulated either with peripherally injected GLP-1 or liraglutide. These studies have demonstrated that native GLP-1 exerts its anorexigenic effects on food intake via peripherally expressed GLP-1 receptors, whereas liraglutide seems to act through central GLP-1 receptors[60–63].

The potential for peripherally administered GLP-1 as anti-obesity drug has been first shown in humans in acute studies with exogenous GLP-1 administration[35,64,65]. GLP-1 reduced caloric intake by regulating all components of appetite regulation: increased satiety and decreased hunger[35,64,65]. In a clinical phase 2 trial, including obese patients with a BMI ≥ 30 kg/m^2, liraglutide reduced body weight in a dose-dependent fashion, with the highest dose (3 mg) resulting in the greatest body weight reduction (7.2 kg)[66]. In addition, clinical phase 3 studies have demonstrated a body weight loss of 5 to 10% in obese patients treated over 56 weeks with liraglutide (3 mg)[67–69]. The liraglutide-induced body weight loss was caused by a substantial loss of body fat of approximately 15%[7]. Liraglutide has beneficial effects on body weight, cardiovascular outcomes, and glycaemic control, but it was assumed that its long-term use could result in pancreatitis and thyroid cancer caused by stimulation of ß-cell and C-cell proliferation in rodents[7,70]. Nevertheless, in humans, the development of pancreatitis and thyroid cancer has not been reported because human ß-cells and thyroid C-cells express the GLP-1R at a much lower density than rodents[71].

Animal and human studies have shown that liraglutide treatment leads to body weight loss, but data on possible mechanisms underlying the chronic body weight management of liraglutide are still limited[7]. A recent clinical study in obese non-diabetic subjects examined the mechanisms behind the liraglutide-induced weight loss over 5 weeks[72]. Patients either received subcutaneous liraglutide with a dose of 1.8 mg (the dose approved for diabetes treatment), 3 mg (the dose approved for obesity treatment) or placebo[72]. The effect of liraglutide on energy intake and energy expenditure was assessed. After 5 weeks of liraglutide treatment (3 mg), a reduction in energy intake, and an increase in satiety rather than increased energy expenditure have been attributed to the observed liraglutide-induced weight loss[72]. In contrast, a recent study has elucidated the role of energy expenditure in liraglutide-induced weight loss in obese type 2 diabetic (T2D) patients treated with metformin in combination with liraglutide[38]. The 1-year combinational therapy has resulted in a significant increase in resting energy expenditure relative to free fat mass and a decrease in BMI[38]. The apparent discrepancies between studies have been explained by the length of the treatment period (4-12 weeks vs. 1 year)[38].

In addition to the action of liraglutide on centres in the brain responsible for energy homeostasis, such as the hypothalamus and the brainstem it has been reported that liraglutide also stimulates the central reward system[73]. Acute studies in obese T2D patients and rodents have demonstrated that GLP-1R agonists promote weight loss and reduction in food intake through the activation of appetite – and reward-related brain areas[74,75]. Appetite –and reward related brain areas such as amygdala play an important role in the GLP-1R-induced satiety[75]. This has been demonstrated in a human psychological study, where the GLP-1R antagonist, exendin 9-39 blocked the response to food-related images in obese T2D subjects, supporting the view that GLP-1R agonists promote weight loss by reducing the hyperresponsiveness to pictures of high-caloric food[7,75]. The putative role of GLP-1R in the brain is further supported by studies in rodents, in which acute intracerebroventricular GLP-1 administration has shown that GLP-1 potently inhibits food intake[76,77]. On the other hand, in humans subcutaneously administered liraglutide in a dose of 30 - 40 nM was not detected in cerebrospinal fluid (CSF). Liraglutide is mainly bound to albumin in the circulation and only small amounts are freely available and ready to cross the blood-brain barrier (BBB)[78,79]. Furthermore, there was no correlation between body weight loss observed upon subcutaneous liraglutide administration and

concentrations of liraglutide found in CSF[78]. Based on the concept of albumin binding, it is not likely that liraglutide crosses the BBB to a larger extent. However, an acute study in rodents has demonstrated that subcutaneously administered liraglutide accumulates in some areas in the brain[35]. The access of liraglutide to different brain areas has been shown after injecting fluorescently labelled liraglutide (400 µg/kg) subcutaneously in mice[35]. In the mouse brain, labelled liraglutide was observed in all circumventricular organs, including the media eminence, the subfornical organ, the organum vasculosum of the lamina terminalis and the choroid plexus[35]. Liraglutide has also been observed within the hypothalamic regions protected by the BBB, including the arcuate nucleus (ARC) and the paraventricular nucleus (PVN)[35]. A recent study identified more specifically the anorexigenic POMC/CART neurons in the ARC of the hypothalamus as the main mediators of liraglutide-induced weight and appetite reducing effects[35]. The inconsistency among human and rodent studies may come from different dosing (3 mg/day vs. 200 µg/kg/BID), and the shorter half-life of liraglutide in rodents[80]. The observed distribution pattern of fluorescently labelled liraglutide has shown a pivotal role of the central GLP-1R in the regulation of energy homeostasis. Acute studies in rodents directly targeting specific hypothalamic nuclei revealed that the ARC, the PVN, and the VMH mediate the body weight -and appetite-reducing effects of liraglutide[38]. The GLP-1R in the hypothalamus is essential for liraglutide-induced appetite signalling. Studies in diet-induced obese mice have shown that pharmacologic blockade or genetic deletion of the central GLP-1R lead to reduced ability to maintain body weight and an increase in food intake[60,81]. A recent acute study in rodents, where stimulation of GLP-1 receptors in the VMH has resulted in body weight loss independent of caloric intake, has shown that loss in body weight is due to the activation of the AMPK pathway in the VMH[38]. The AMPK pathway in the VMH stimulates energy expenditure in terms of increased thermogenesis and browning prevalence in brown and white adipose tissue[38].

Aim of the study

After careful revising the literature still several questions remain open. The aim of my PhD project was to elucidate the following questions.

1. What is the difference between central and peripheral delivery of liraglutide on energy homeostasis?
2. What is the difference between acute and chronic central delivery of liraglutide on energy homeostasis?
3. What are the underlying mechanisms of chronic central liraglutide-induced weight loss?
    a. Does chronic central liraglutide treatment induce thermogenesis and increase browning of white and brown adipose tissue?
    b. Are there direct pharmacological effects on the brain? We hypothesized that the hypothalamic melanocortin system might be involved.

We aimed to evaluate if either central or peripheral chronic administration of liraglutide induce sustained weight loss through increased thermogenesis and to which extent the hypothalamic melanocortin system is involved in the liraglutide-induced weight loss in healthy lean rats on a normal diet.

CHAPTER 1

Establishment of a focal drug delivery system to the hypothalamus

3 Establishment of a focal drug delivery system to the hypothalamus

3.1 Abstract

The hypothalamus is located above the midbrain and below the thalamus and both together construct the ventral diencephalon of the brain. Because of the hypothalamus' position, it is difficult to target the hypothalamus without causing severe damage to other brain areas. Energy homeostasis is regulated by different appetite regulating neurons, each triggering different physiological responses. These neurons constantly communicate with the endocrine system and compensate for metabolic imbalances. To examine the specific neuronal role in energy homeostasis, a focal drug delivery system is essential to continuously and directly target these neuronal centres without glial scar formation.

We aimed to establish such a focal drug delivery system for continuous and chronic drug delivery directly to the hypothalamus. We started by evaluating three different materials (stainless steel, Teflon, polyether ether ketone - PEEK), for their usage as material for implanted brain cannulae. We investigated the effect of these materials on body weight and the effect of PEEK on tissue damage by staining inflammatory cell markers and marker for reactive astrogliosis. We determined the body weight daily to assess interferences from the used material or implantation on body weight development. We evaluated successful substance delivery to the hypothalamus by injecting sodium fluorescein as a marker via the brain cannula. Sodium fluorescein concentrations were spectrophotometrically analysed in the supernatant of hypothalamic tissue homogenates.

We evaluated if substance delivery to the hypothalamus was successful by injecting the marker sodium fluorescein via the brain cannula and spectrophotometrically analysed the concentration of sodium fluorescein in the supernatant of hypothalamic tissue homogenates.

The low abundance of macrophages and microglia in the tissue surrounding the cannula indicated that PEEK is biocompatible. We did not observe any changes to the material surface upon cannula removal which indicates that PEEK is mechanically stable to the brain's micro-motion over 14 days of cannula implantation. We did not observe any change in body weight development during the implantation

of the PEEK cannula and were able to demonstrate that substance delivery to the hypothalamus was not hindered by astrogliosis and resulting glial scar formation.

3.2 Aim

In this project we aimed to identify the most suitable cannula material for focal drug delivery system to the hypothalamus. We intended to identify which focal drug delivery system for chronic and continuous intrahypothalamic drug administration does not cause severe damage to the surrounding brain areas and guarantees successful substance delivery. We also investigated if the cannula material is compatible with micro-computer tomography imaging.

3.3 Introduction

Specific brain regions can be studied by targeted delivery of pharmacological agents to these regions. Targeted delivery to a specific brain site guarantees the study of precise neuronal activities and difficulties with the permeability across the blood brain barrier is avoided. This approach can be applied in multiple ways in neuroscience such as investigating the actions of psychotropic agents[82–84], providing controlled models of brain inflammation[85–87], enabling chronic administration of trophic factors[84,88,89,] and examining the central control of energy homeostasis[38,39,90,91].

The focal delivery of substances to the hypothalamus is challenging. One of the main challenges is to reach the hypothalamus, without causing severe damage of other brain regions. Therefore a well-established and appropriate method is needed to deliver substances directly to the site of interest. Targeted delivery of pharmaceutical agents to examine their pharmacodynamics in the hypothalamus requires a biocompatible focal drug delivery system, which provokes minimal damage in surrounding brain areas. To guarantee minimal damage, the cannula should be small in size and robust, but flexible enough to withstand brain's micro-motions[92]. The cannula material should be resistant to material degradation and suitable for long-lasting implantations[92].

The response of the central nervous system to tissue damage is unique and includes the proliferation and activation of microglia and astrocytes[93]. Microglia are derived from the monocyte lineage and immunologically resemble macrophages[94]. They are immunologically active within minutes upon tissue damage and start to proliferate, phagocytose invading pathogens, remove debris, secrete mediators that promote astrocytosis and induce neuronal degeneration[94]. The second immunologically response to tissue damage is the activation of astrocytes which play an essential role in the healing phase following tissue damage. The excessive proliferation of astrocytes, termed reactive astrogliosis, can be visualised by staining for glial fibrillary acidic protein (GFAP), a cytoskeletal marker for astrocytes[95,93]. The induction of reactive astrogliosis and its resulting glial scar formation are the reason for the limited application time of most membrane-based brain cannula systems[96]. Glial scar formation hinders the chronic application of pharmaceutical substances to specific brain regions through membrane-based cannula systems[96]. Therefore, avoiding membrane-based cannula system minimizes adhesion of cells and substances to the

cannula surface (biofouling) and reduces damage to the tissue surrounding the cannula for 30 days of implantation[96].

Stainless steel has been associated with tissue reactions in bone and soft tissues and has been found to undergo corrosion and toxic ion release *in vivo* and *in vitro* models[97–99]. Additionally, there is potential carcinogenicity associated with long-term implants of stainless steel[100].

3.4 Research design and methods

3.4.1 Animal Models

Male Sprague-Dawley (S.D.) rats (12–15 weeks old, 320–450 g; Harlan Laboratories, Udine, Italy) were housed under conditions of controlled temperature (23°C) and illumination (12-h light/dark cycle). Rats were allowed ad libitum access to water and standard laboratory chow. Animals were sacrificed by decapitation. The brain was removed immediately after transcardial perfusion. All animal experiments were approved by the Austrian Federal Government (BMWF-66.010/0003-II/10b/2010) and were performed in consent with Directive 2010/63/EU on the protection of animals used for scientific purposes.

3.4.2 Study design

Male Sprague Dawley rats were randomly assigned to one of three groups (each N=3) (Table 1). We implanted brain cannulae (Bilaney Consultants, Düsseldorf, Germany) composed of different material into the hypothalamus of three different rat groups (Table 2). The brain cannulae were inserted to the dorsal part of the paraventricular nucleus of the hypothalamus (stereotactic coordinates: 0.6 mm right from midline, 1.7 mm posterior to bregma and 7.6 mm from skull surface). We assessed the body weight of all rats daily for 14-days cannula implantation. Rats were checked daily for behaviour changes, suggestive of neurotoxicity. At day 14 rats were sacrificed and brain tissue was extracted.

Table 1 – Material and position of implanted cannulae. Each group included three rats and the study duration was 14 days. AP (anterior -posterior), ML (medial – lateral), DV (dorsal – ventral);

Group number	Cannula material	Stereotactic coordinates [mm]
1	Stainless steel	AP – 1.7, ML – 0.6, DV – 7.6
2	Teflon	AP – 1.7, ML – 0.6, DV – 7.6
3	PEEK	AP – 1.7, ML – 0.6, DV – 7.6

Table 2 – Technical specifications of implanted cannulae. O.D. (outer diameter), I.D. (inner diameter);

Part number	Cannula size [gauge]	Cannula size [mm]	Cannula length below pedestal [mm]	Cannula material
328OP/SP	28	O.D. 0.36 I.D. 0.18	7.6	Stainless steel
328OPT/SP	28	O.D. 0.36 I.D. 0.18	7.6	Teflon
328OP/PK/SP	28	O.D. 0.36 I.D. 0.18	7.6	PEEK

3.4.3 Surgical implantation of three different brain cannulae into the hypothalamus

Before implantation, rats were individually placed in an anesthesia induction chamber (Rothacher, Heitenried, Switzerland). Anesthesia was induced with 4 vol% isoflurane (Isoflo, Esteve Farma, Carnaxide, Portugal) in 100% oxygen with a flow rate of 5 l/min until loss of righting reflex. Anesthesia was maintained with an injectable anaesthetic (0.1 ml/kg; 0.5 mg/kg Midazolam, 5 µg/kg Fentanyl, 5 mg/kg Domitor; 1mL/1kg body weight, ERWO Pharma GmbH, Hameln pharma plus GmbH, Vienna, Austria). Anesthesia was maintained with isoflurane in 100% oxygen at a flow rate of 1.5 l/min. The head was fixed in a stereotactic frame (KOPF Instruments, CA, USA) and rats were prepared for surgery by shaving the head and disinfecting the skin with 70% ethanol. A spherical dental drill was used to drill a 1 mm hole into the skull leaving the dura intact. The dura was then punctured with fine forceps in order to create a defined opening of the meninges[96]. Cannulae made of different material (PlasticsOne, Bilaney Consultants, Düsseldorf, Germany) were inserted slowly to a depth of 7.6 mm 1.7 mm posterior to the bregma and 0.6 mm from midline (AP – 1.7 mm; ML – 0.6 mm; DV – 7.6 mm) and fixed to the skull using four anchor screws and biocompatible dental cement (iCEM Self-Adhesive; Heraeus, Hanau, Germany). After surgery, rats received analgesics and anti-inflammatory treatment for the following

two days (50 mg/kg Claforan, Sanofi-Aventis GmbH, Vienna, Austria; 50 mg/ml Carprofen; Pfizer Corporation Austria GmbH, Vienna, Austria).

3.4.4 Stereotactic coordinates

The stereotactic coordinates to reach the dorsal part of the paraventricular nucleus of the hypothalamus were determined using the dimensions of the coronal sections from the rat brain atlas (Figure 1)[101].

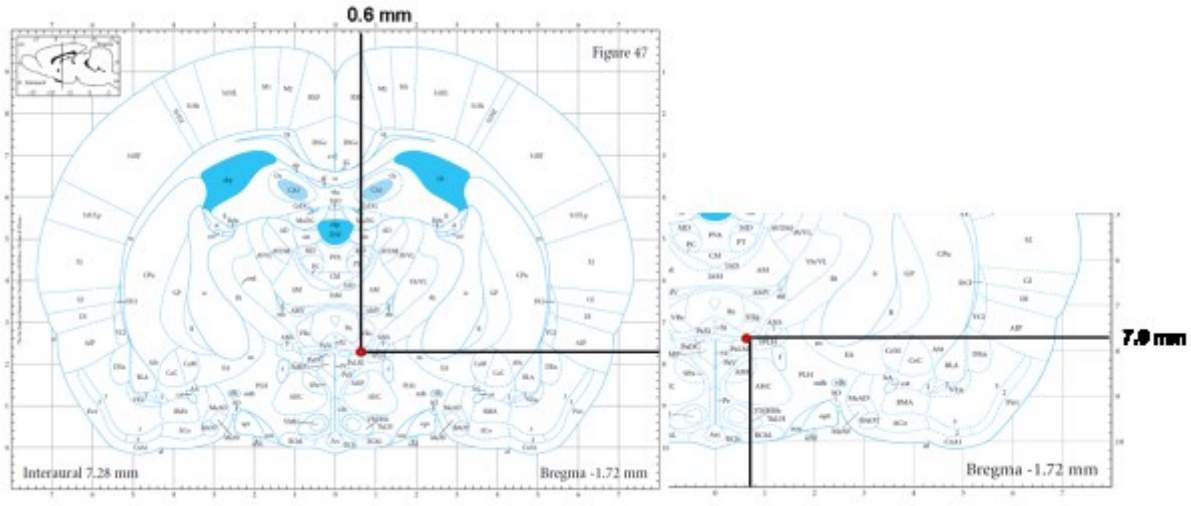

Figure 1 – Coronal section of the rat brain indicating the stereotactic coordinates. The left picture shows the coronal section of the rat brain 1.72 mm posterior to bregma, and the right image is its enlargement. The tip of the implanted cannula is indicated by the red dot at the paraventricular dorsal part of the hypothalamus. The black lines indicate the position from bregma (0.6 mm) and from skull surface (7.6 mm)[101]. Figure modified from Paxinos and Watson[101].

3.4.5 Evaluating the effect of three different implantation materials on body weight

Rats were weighed daily for 14 days on a precise laboratory scale (Competence CP3202S-0CE, Sartorius AG, Göttingen, Germany).

3.4.6 Immunohistochemical analysis of reactive astrogliosis, microglial activation, and thymocyte infiltration

The brain was fixed in 4% paraformaldehyde in 0.1 M phosphate buffered saline pH 7.2 (PBS) over night at room temperature and further processed and embedded in paraffin by using the Sakura Tissue Tek working station (VIP 5E-F2, Sanova Diagnostics, Vienna, Austria). Brains were sectioned (section thickness 1.5 µm) around the implantation site and were examined by haematoxylin and eosin (H&E) staining. Diaminobenzidine immunohistochemistry and heat mediated antigen

retrieval with citrate buffer (pH 6) was performed to detect expression of markers for thymocyte infiltration (W3/13) (1:100, ab33885, Abcam, Cambridge, UK), for reactive astrogliosis (GFAP) (1:1000, ab7260, Abcam, Cambridge, UK) and for active microglia/macrophages (ED1) (1:100, ab31630, Abcam, Cambridge, UK).

For H&E staining, brains were fixed in 4% PFA over night at 4°C, washed three times with PBS and incubated in freshly prepared 20% sucrose in PBS over night at 4°C. Brains were stored at -20°C in TissueTek wells embedded in OCT solution till cryocutting and staining.

3.4.7 Histological and spectrophotometrical verification of correct substance delivery and placement of the brain cannula

Induction of anesthesia is described in section 3.4.3. The cannula was inserted into the rat brain directly to the paraventricular dorsal part of the hypothalamus according to the rat brain stereotactic coordinates mentioned above (AP – 1.7 mm; ML – 0.6 mm; DV – 7.6 mm). To remove residual blood from the inner surface of the cannula and the surrounding brain tissue, the cannula was rinsed with 2 µL of 0.9% phosphate buffered saline (PBS) upon implantation. A volume of 3 µl of sodium fluorescein (NaF; 7.5 mg/mL diluted in saline) was injected through the cannula into the hypothalamus for 30 min (approx. flow rate 0.1 µl/min). After sacrification by decapitation, brains were excised, and the hypothalamus was dissected. Part of the frontal cortex was dissected, and served as control tissue. Tissues were stored in 1.5 ml test tubes and weighed on an analytical balance (M-Power AZ214, Sartorius AG, Göttingen, Germany). Tissues were dissolved in sterile water (w/v) (Aqua-bidest, Fresenius Kabi, Graz, Austria) and homogenized by vortexing. The tissue homogenates were stored in the fridge at 4°C over night to allow diffusion of the marker sodium fluorescein to the aqueous phase. After 24 hours the test tubes were centrifuged and the supernatant was transferred to new 1.5 ml test tubes. The increase in fluorescence intensity of sodium fluorescein was measured spectrophotometrically in the supernatants via Microplate Reader Synergy HT (Biotek, Vienna, Austria) (emission wavelength of 485 nm) at Joanneum Research HEALTH (Graz, Austria).

3.5 Results

3.5.1 Body weight development was unaffected for 14-days PEEK cannula implantation

We observed that rats implanted with stainless steel cannulae had an increased body weight loss of 3% at day 1 compared to baseline (Figure 2). Rats implanted with a stainless steel cannula reached baseline at day 4 (Figure 2). We showed that PEEK cannula implantation led to body weight reduction of 1% at day (Figure 2). Teflon did not trigger a postsurgical body weight loss compared to baseline (Figure 2). Rats with PEEK and Teflon implanted cannulae reached their initial pre-surgical weight at day 2 (Figure 2). Rats implanted with PEEK or Teflon brain cannulae showed a body weight gain of 10% at the day 12 compared to baseline (Figure 2). Teflon and PEEK showed almost the same body weight development (Figure 2).

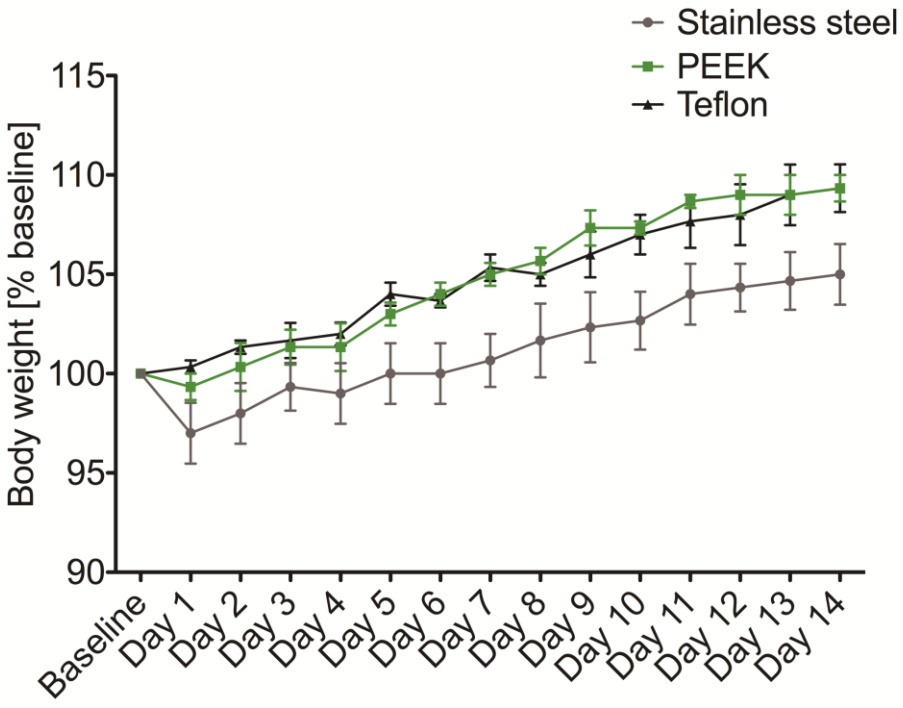

Figure 2 – PEEK leads to a modest and normal body weight gain. The effect of stainless steel (gray), Teflon (black) and PEEK (green) on change of body weight over 14 days cannula implantation to the hypothalamus. Body weight was normalized to baseline (before surgery). N=3 each group. Data is given as mean ± SEM.

3.5.2 Glial scar formation and thymocyte infiltration after 14-days implantation of PEEK cannula are mild

We observed low expression of the microglia marker ED1 in close vicinity to the implantation site 14 days after PEEK cannula implantation (Figure 3). After 14 days

of PEEK cannula implantation, we observed no qualitative difference in expression of the astrocyte marker GFAP at the cannula implantation site compared to the rest of the hypothalamic tissue (Figure 4). We observed no infiltration of thymocytes to the surrounding tissue of the PEEK cannula implantation site after 14 days compared to the rest of the hypothalamic tissue (Figure 5).

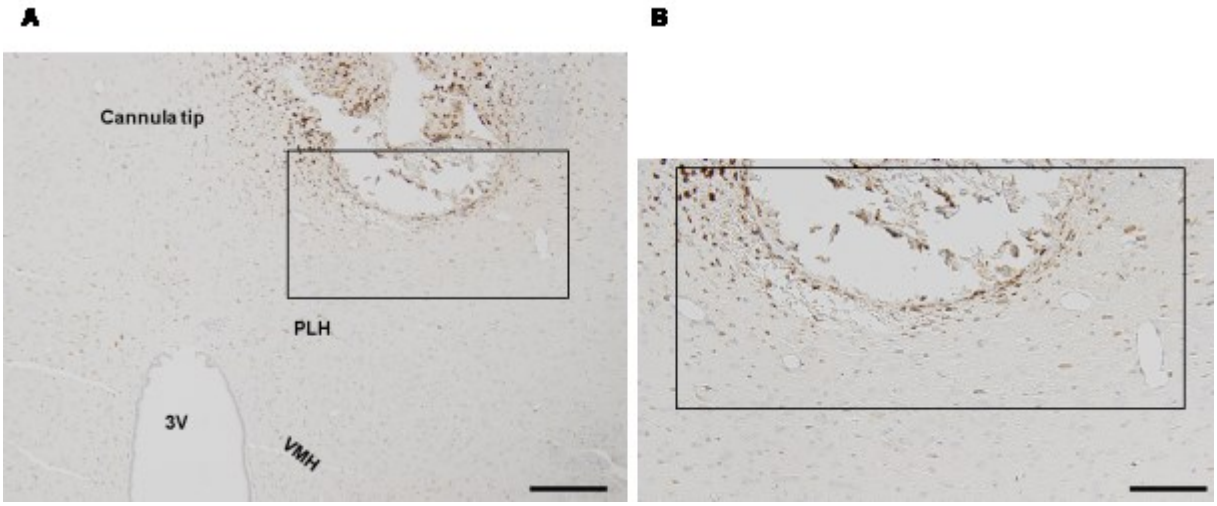

Figure 3 – PEEK causes a slight infiltration of microglia to the site of cannula implantation. (A) Brightfield immunohistochemistry for ED1 counterstained with haematoxylin in rat brain specimens, overview with details (boxed areas). **(B)** The detailed histological appearance of microglia after 14 days cannula implantation (hypothalamus). *Scale bars* surveys = 200 µm, details = 100 µm; 3V = third ventricle; VMH = ventromedial hypothalamus; PLH = posterior lateral hypothalamus;

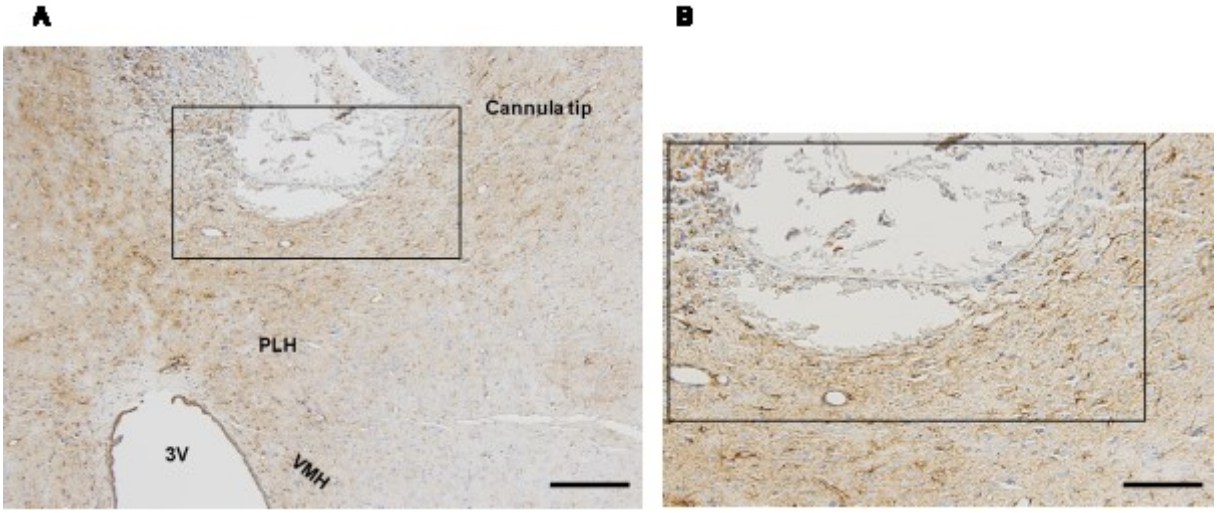

Figure 4 – PEEK causes no reactive astrogliosis after 14 days of cannula implantation. (A) Brightfield immunohistochemistry for GFAP counterstained with haematoxylin in rat brain specimens, overview with details (boxed areas). **(B)** Detailed histological appearance of reactive astrocytes after 14 days of cannula implantation (hypothalamus). *Scale bars* surveys = 200 µm, details = 100 µm; 3V = third ventricle; VMH = ventromedial hypothalamus; PLH = posterior lateral hypothalamus;

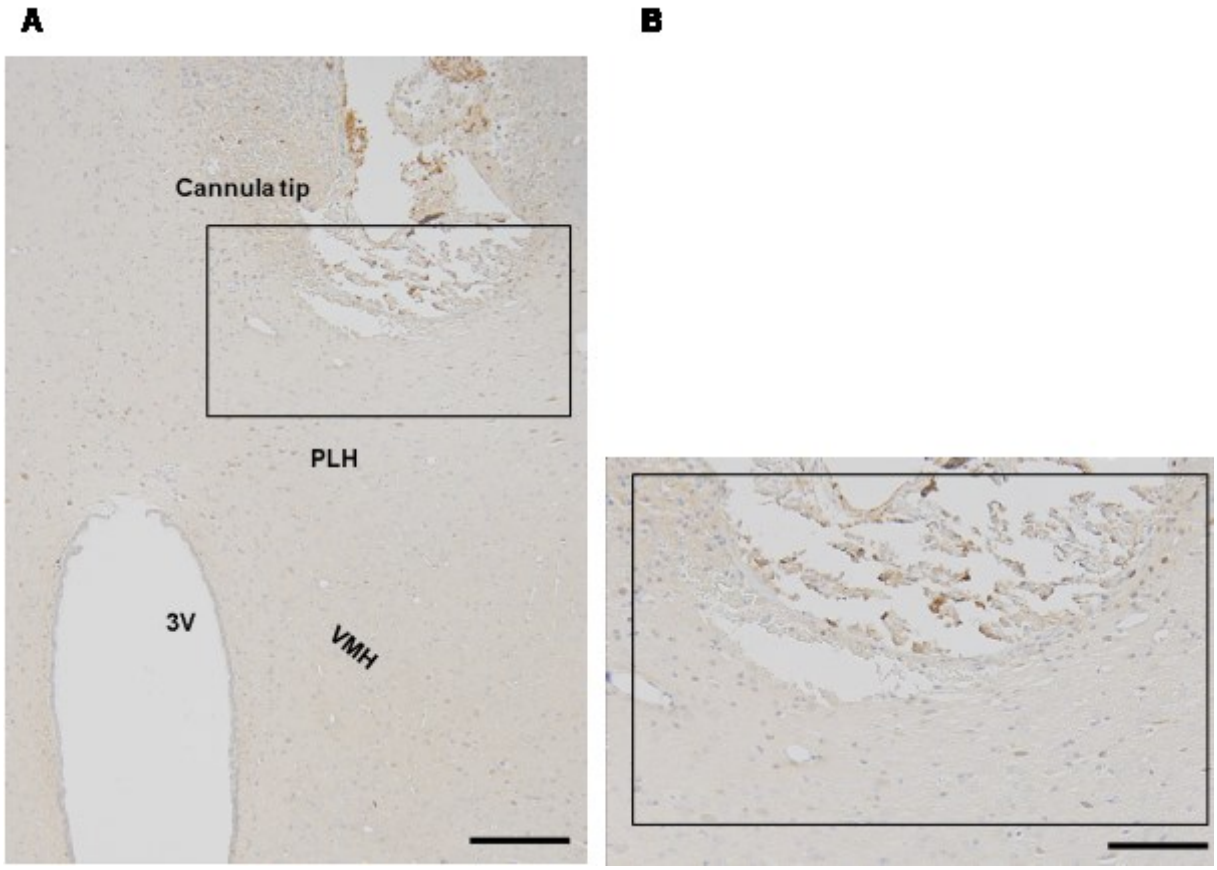

Figure 5 – PEEK does not stimulate thymocyte infiltration after 14 days of cannula implantation. **(A)** Brightfield immunohistochemistry for W3/13 counterstained with haematoxylin in rat brain specimens, overview with details (boxed areas). **(B)** Detailed histological appearance of thymocytes after 14 days of cannula implantation (hypothalamus). *Scale bars* surveys = 200 µm, details = 100 µm; 3V = third ventricle; VMH = ventromedial hypothalamus; PLH = posterior lateral hypothalamus;

3.5.3 Verification of cannula placement and successful substance delivery to the hypothalamus

The brain cannula was implanted correctly to the paraventricular dorsal part of the hypothalamus indicated by the probe tip (Figure 6A). We visualised the insertion channel by injecting the dye Evans Blue (Figure 6B). We observed the correct insertion of the brain cannula by visualising the insertion channel by injecting the dye Evans Blue (Figure 6B). We quantitatively showed that delivery of sodium fluorescein was specific to the hypothalamus compared to the control region, which is indicated by a higher fluorescence intensity (Figure 6C).

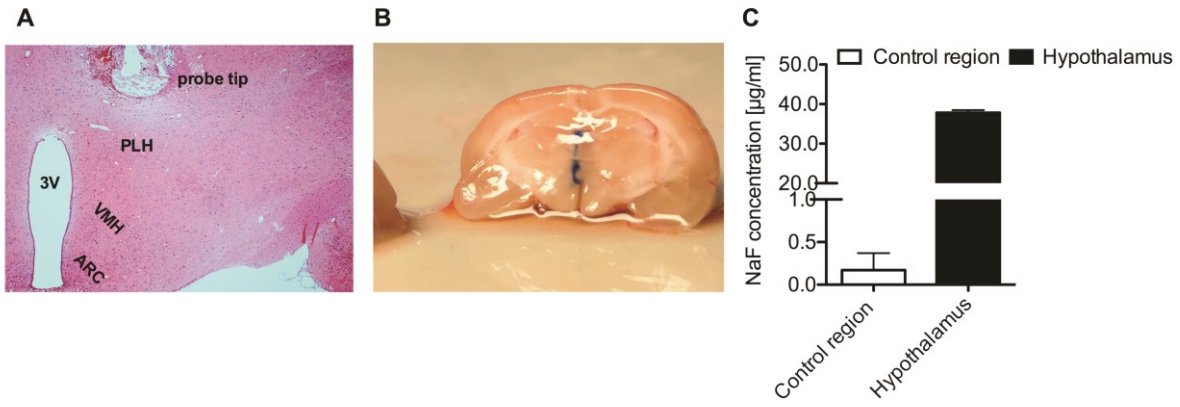

Figure 6 – Substance delivery to the hypothalamus. (A) H&E staining of a 5-µm thick coronal section of the rat hypothalamus with the indicated correct placement of the implanted PEEK cannula tip (AP - 1.7; ML - 0.6; DV - 7.6 mm); **(B)** Stained (blue line) cannula channel and cannula tip in the rat brain by using Evans Blue as marker. **(C)** Quantitative assessment of intrahypothalamic NaF (sodium fluorescein) administration via PEEK brain cannula. PLH (peduncular part of the lateral hypothalamus), VMH (ventromedial hypothalamus), ARC (arcuate nucleus), 3V (third ventricle); (Kaineder et al, 2017, unpublished results)

3.6 Discussion

Three different materials were tested for their biocompatibility, immunoreactivity, and suitability for chronic substance delivery to the hypothalamus. The implantation of PEEK cannulae did not influence body weight development throughout the study period of 14 days. PEEK stimulated only a mild increase in microglia and astrocyte infiltration in close vicinity of the cannula tip and did not affect thymocyte infiltration after 14 days of cannula implantation. The mild increase in the expression of astrogliosis markers showed low accumulation of astrocytes, which did not hinder substance delivery to the hypothalamus.

Body weight was our read out parameter of choice in terms of representing the health status of the rats and to ensure that cannula implantation to the hypothalamus itself does not lead to body weight loss. We showed that stainless steel led to the highest body weight loss after surgery and reduced gain in body weight after 14 days cannula implantation compared to PEEK and Teflon. Stainless steel is suggested to be the most suitable cannula material for stereotactic implantation at specific coordinates in the CNS[102] but it is known that soft tissues are sensitive to metal reactions and it has been found that stainless steel undergoes corrosion and toxic ion release *in vivo* and *in vitro*[97– 99]. In addition, chronic tissue implantation of stainless steel has been associated with potential carcinogenicity[100] and is also not compatible with radiographic imaging (micro-CT). Our data indicated that neither implantation of PEEK nor Teflon induced a significant body weight loss and that the body weight gain was similar for both materials. PEEK and Teflon share similar material characteristics and are both FDA approved as medical implants[103]. They share characteristics such as good chemical resistance and good dielectric strength (electrical insulation)[103]. But PEEK has higher flexural modulus (bending stiffness) of 590,000 psi than Teflon (72,000 psi) and a higher tensile strength (14,000 psi vs. 1,500 – 3,000 psi), it is stronger, stiffer and still flexible enough for deep brain tissue implantation[103], such as implantation into the hypothalamus. The brain is continually pulsating due to vascular and respiratory oscillations, and small relative movement (micro-motion) between cannula and tissue induces some level of strain[104]. Therefore the cannula material has to be flexible to prevent shear forces on the brain tissue. We assume that flexibility reduces mechanical stress caused by micro-motions of the brain floating in cerebrospinal fluid while the cannula is fixed to the skull. In contrast, material stiffness facilitates the focal insertion of the cannula to the hypothalamus.

Because PEEK shows a remarkable combination of flexibility, strength, and stiffness properties[105], we chose to further investigate the histopathological effects of PEEK on the surrounding brain tissue after 14 days implantation.

As expected, we observed only low abundance of microglia after 14 days of PEEK cannula implantation, because resting microglia react to brain injury within a few minutes[94]. We observed newly activated, rod like, phagocytic microglia in close vicinity to the cannula channel and less active microglia surrounding the cannula tip after 14 days of implantation. This ensured free substance diffusion to the hypothalamus. In accordance with data from another animal study, in which we compared membrane-based (microdialysis) with non-membrane based (cerebral open flow microperfusion) brain cannula systems[96], we observed no microglia activation in areas more distant from the cannula tip. The implantation of the cannula triggered only mild thymocyte infiltration to the cannula tip. PEEK seemed to be an immunological inert material, indicated by the slight thymocyte infiltration after 14 days of implantation. We noticed reactive astrocytes close to the cannula tip, but we suggest that they only form mild to moderate astrogliosis without any scar formation as we did not have any problems with substance delivery to the hypothalamus, demonstrated by successful sodium fluorescein administration via the cannula.

Our data showed that delivery of sodium fluorescein to the hypothalamus via PEEK cannulae was successful. We observed higher concentration of sodium fluorescein in hypothalamic extracts compared to the control group. Therefore, we assume that sodium fluorescein was directly delivered to the hypothalamus by the used cannula system.

Considering our results, we chose PEEK as material for the brain cannula experiments, because it did not influence normal body weight development, was biocompatible with surrounding brain tissue, provided successful drug delivery and was compatible to be used with micro-CT imaging.

The established continuous focal drug delivery system to the hypothalamus is important for our next study, which aimed to investigate the chronic effect of liraglutide (Victoza, Novo Nordisk) on energy homeostasis in the hypothalamus.

CHAPTER 2

The chronic effect of continuous liraglutide treatment on energy homeostasis

4 The chronic effect of continuous liraglutide treatment on energy homeostasis

4.1 Abstract

The hypothalamus regulates energy homeostasis by responding to neuropeptides, such as GLP-1. Since GLP-1 is rapidly degraded, liraglutide a GLP-1 receptor agonist is marketed for chronic obesity treatment. Liraglutide induces body weight reduction possibly via stimulation of the GLP-1 receptor (GLP-1R), which is expressed in the hypothalamus. In animal studies, acute liraglutide treatment triggers weight loss, satiety and stimulates thermogenesis in adipose tissue. The precise mechanisms how liraglutide particularly affects chronic weight loss are still under investigation.

We evaluated whether chronic hypothalamic (central) or chronic subcutaneous (peripheral) administration of liraglutide induce sustained weight loss through altered adipose tissue function and to which extent hypothalamic neuronal appetite regulators are involved in the liraglutide-induced weight loss in healthy lean rats on normal diet. We continuously administered liraglutide either intrahypothalamically (IH) (10 µg/day) or subcutaneously (SC) (200 µg/kg/day) for 28 days to lean Sprague Dawley rats (N=8 each) via ALZET osmotic pumps. We analysed body weight continuously for 28 days. Adipose tissue mass and adipocyte size of three different fat depots were examined. Subcutaneous and visceral adipose tissue volumes in the abdominal region were measured by using micro-CT. We examined genetic expression patterns of browning, thermogenic and adipocyte differentiation markers in three different adipose tissue depots as well as particular neuronal markers for appetite neurons in the hypothalamus.

Central (IH) liraglutide administration induced an 8% body weight reduction at day 9 compared to the control group (P<0.01) and a 7% body weight loss at day 9 compared to peripheral (SC) liraglutide treatment (P<0.01). This data was in line with a significant reduction of adipose tissue mass and adipose tissue volume with central liraglutide treatment (P<0.05). Our data show that chronic central liraglutide treatment triggered an 18-fold induction of the hypothalamic *mc4r* gene (P<0.01). We observed a significant increase in circulating thyroxine (T4) levels (P<0.05).

Chronic central liraglutide administration resulted in profound reduction in body weight and reduction in fat mass most likely mediated by the anorexigenic

hypothalamic melanocortin system (MC4R) rather than by adipose tissue browning or enhanced thermogenesis of evaluated adipose tissue.

4.2 Aim

We aimed to investigate the chronic effects of central (IH) and peripheral (SC) liraglutide treatment on body weight development, adipose tissue distribution, glucose and fatty acid metabolism, and molecular mechanisms regulating energy homeostasis in one single study. We intended to study the potency of the peripherally and centrally expressed GLP-1R in terms of body weight reduction.

4.3 Introduction

Liraglutide (Victoza®, Novo Nordisk) was approved for the treatment of type 2 diabetes mellitus in Europe in 2009 and in the USA in 2010[107]. In 2014, liraglutide (Saxenda®, Novo Nordisk) was approved by the FDA and in 2015 by the EMA as chronic obesity treatment for adults with a BMI ≥ 30 or a BMI ≥ 27 who have at least one weight-related comorbid condition, such as hypertension, type 2 diabetes, or elevated cholesterol levels[7]. Liraglutide reduces caloric intake and subsequently leads to moderate but sustained weight loss[66]. The underlying mechanisms mediating the chronic anorectic and body weight-reducing effects are not clear[79].

It was reported that genetically modified mice, which lack the GLP-1 receptor in the brain, lose their ability to induce satiety and maintain body weight after subcutaneous liraglutide administration[60]. In addition, pharmacologically antagonizing the GLP-1R in the brain of rats resulted in a reduced ability to induce satiety and induce weight loss[81]. These studies identified the GLP-1R in the brain as major player in the regulation of appetite and body weight.

Acute central liraglutide treatment in rodents has been shown to result in body weight loss independent of food intake[38]. Instead, body weight loss has been attributed to the stimulation of thermogenesis in the brown adipose tissue (BAT) and browning of white adipose tissue (WAT) via the hypothalamic AMP-activated protein kinase (AMPK) pathway in the VMH[38]. A recent study identified the hypothalamic POMC/CART neurons in the ARC as the main mediators of the liraglutide-induced weight loss after peripheral liraglutide administration[35]. It was shown, at least in animals that peripherally injected liraglutide was transported to regions in the brain which are protected by the blood brain barrier (BBB)[35], such as the ARC. In contrast, in humans it has been reported that peripheral liraglutide administration often leads to only limited effects mediated in the brain because only small amounts (~1-2%) of the large liraglutide-albumin complex can freely cross the BBB[79]. In humans, peripherally administered liraglutide transported to the brain did not correlate with the observed weight loss[78].

A direct comparison of chronic central and chronic peripheral liraglutide administration in a single study would help to link existing studies investigating either central or peripheral administration of liraglutide and would clarify whether liraglutide is more effective centrally or in the periphery. Such comparative data on chronic central and peripheral effects of liraglutide are necessary to identify new pathways to

improve the pharmacological benefits of chronic obesity treatment. (Kaineder et al., IJO 2017, unpublished results).

Parts of this thesis are adapted from the publication Kaineder et al. "Continuous intrahypothalamic rather than subcutaneous liraglutide administration leads to reduced body weight gain and stimulation of melanocortin system", published 2017 in the *International Journal of Obesity*.

Research design and methods

4.3.1 Animal models

Male Sprague Dawley (S.D.) rats (12–15 weeks old, 400–450 g; Charles River Laboratories) were housed under conditions of controlled temperature (23°C) and illumination (12-h light/dark cycle). Rats were allowed ad libitum access to water and standard laboratory chow diet. Animals were sacrificed by decapitation and tissues (hypothalamus, adipose tissue depots) were immediately removed, snap frozen and stored at -80°C for further analysis. All animal experiments were approved by the Austrian Federal Government (BMWF-66.010/0010-WF/V/3b/2015) and were performed in consent with Directive 2010/63/EU on the protection of animals used for scientific purposes. (Kaineder et al., IJO, 2017, unpublished results)

4.3.2 Study Design

The study design was non-blinded and based on four groups (each N=8). Two groups received treatment (liraglutide) either intrahypothalamically (IH) or subcutaneously (SC) and two groups received placebo, aCSF for IH control and 0.9% NaCl for SC control group. Group 1: IH liraglutide; Group 2: IH control (aCSF); Group 3: SC liraglutide; Group 4: SC control (NaCl). Group 2 and group 4 (treated with placebo) served as control groups (Table 3). (Kaineder et al., IJO 2017, unpublished results).

For chronic administration, rats were continuously treated for 28 days with either 10 µg/day IH liraglutide or with 200 µg/kg/day SC liraglutide via osmotic pumps. The administered dose of IH liraglutide was chosen on its ability to significantly inhibit feeding and induce body weight loss[76,77]. The dose of SC administration was chosen to minimize the transfer effect from periphery to the hypothalamus[35], to ensure differentiation between a central and peripheral effect of liraglutide. (Kaineder et al., IJO 2017, unpublished results).

Table 3 – Treatment and application site of four different groups. Each group was comprised of 8 rats and was treated continuously for 28 days. Stereotactic coordinates for hypothalamic application: AP – 1.7, ML 0.6, DV – 7.6 mm; AP (anterior -posterior), ML (medial – lateral), DV (dorsal – ventral), aCSF (artificial cerebrospinal fluid);

Group number	Group name	Treatment	Application site
1	IH liraglutide	Liraglutide 10 µg/day	Hypothalamus
2	IH control	aCSF	Hypothalamus
3	SC liraglutide	Liraglutide 200 µg/kg/day	Subcutaneous
4	SC control	0.9% NaCl	Subcutaneous

4.3.3 Surgical implantation of osmotic pumps

Before implantation, rats were individually placed in an anesthesia induction chamber (Rothacher, Heitenried, Switzerland) induced with 4 vol% isoflurane (Isoflo, Esteve Farma, Carnaxide, Portugal) in 100% oxygen with a delivery rate of 5 l/min until loss of righting reflex. Rats were anesthetized using an injectable anaesthetic (0.1 ml/kg; 0.5 mg/kg Midazolam, 5 µg/kg Fentanyl, 5 mg/kg Domitor; ERWO Pharma GmbH, Hameln pharma plus GmbH, Vienna, Austria). Anesthesia was maintained with isoflurane in 100% oxygen at a flow of 1.5 l/min. For a 28 days continuous drug administration we chose the pump models 2ML4 for SC (subcutaneous) and the model 2004 for IH (intrahypothalamic) administration (ALZET Durect, Cupertino, California, USA) (Table 4). The osmotic pumps were implanted on the back of the rats slightly posterior to the scapulae. Osmotic pumps were implanted according to manufacturer's instructions by creating a pocket at the mid-scapular region using a hemostat and inserting the filled pump in the pocket. (Kaineder et al., IJO 2017, unpublished results).

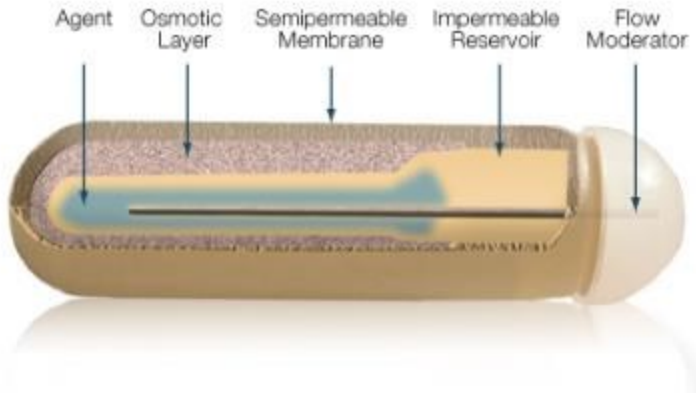

Figure 7 – Schematic representation and working principle of ALZET osmotic pumps. ALZET pumps work by osmotic pressure difference between the osmotic layer and the tissue environment surrounding the pump. An influx of water from the tissue environment through the semipermeable membrane is caused by the high osmolality of the osmotic layer. The flexible reservoir, which concludes the test agent, is compressed by the water entering the pump. The compression of the reservoir is predetermined and controls the delivery rate of the test agent.[110],[111]; Picture taken from the homepage of ALZET

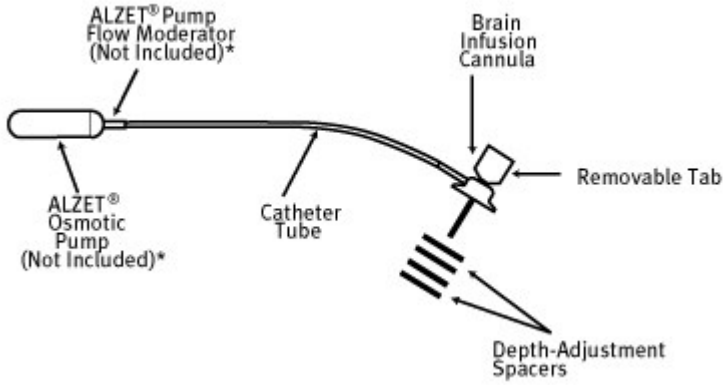

Figure 8 – An ALZET osmotic pump and components of the brain cannula system assembled before implantation. The ALZET Flow Moderator is connected to the osmotic pump and the catheter tubing connects the pump with the brain cannula system. The brain cannula system is implanted to the hypothalamus.[112];Picture taken from the homepage of ALZET

Table 4 – Technical description of the ALZET osmotic pumps. IH – intrahypothalamic; SC-Subcutaneous;

	Pumping rate [µl/h]	Pumping duration [days]	Reservoir volume [µl]
Model 2004 (IH)	0.22 ± 0.05	42	234
Model 2ML4 (SC)	2.55 ± 0.05	31	1997.2

4.3.4 Surgical implantation of intrahypothalamic cannula

Induction of anesthesia for stereotactic surgery was the same as for the implantation of osmotic pumps as described before. The head was fixed in a small animal stereotactic frame (Model 900, David Kopf Instruments, California, USA) and rats were prepared for surgery by shaving the head and disinfecting the skin with 70% ethanol. A spherical dental drill was used to drill a 1 mm hole into the skull leaving the dura intact. The dura was then punctured with fine forceps in order to create a defined opening of the meninges[96]. The cannula (PlasticsOne, Bilaney Consultants, Düsseldorf, Germany) was inserted slowly to a depth of 7.6 mm (intrahypothalamically) via a 1 mm hole drilled into the skull 1.7 mm lateral to the bregma and 0.6 mm from midline and fixed to the skull using four anchor screws and biocompatible dental cement (iCEM Self Adhesive; Heraeus, Hanau, Germany). After surgery, rats received analgesics and anti-inflammatory drugs for the following three days (50 mg/kg Claforan, Sanofi-Aventis GmbH, Vienna, Austria; 50 mg/ml Carprofen; Pfizer Corporation Austria GmbH, Vienna, Austria). The cannula was connected to an osmotic pump filled with liraglutide dissolved in artificial cerebrospinal fluid (aCSF; Harvard Apparatus, Germany), and the pump was implanted subcutaneously. (Kaineder et al., IJO 2017, unpublished results).

4.3.5 Assessment of body weight, adipose tissue mass and size

Body weight was continuously assessed on a precise laboratory scale (Competence CP3202S-0CE, Sartorius AG, Göttingen, Germany). After 28 days rats were sacrificed and freshly excised adipose tissue depots (inguinal WAT, epididymal WAT, interscapular BAT) were weighed on an analytical balance (M-Power AZ214, Sartorius AG, Göttingen, Germany). Epididymal (eWAT) and inguinal (iWAT) white adipose tissue and interscapular brown adipose tissue (iBAT) were isolated, fixed in 4% paraformaldehyde over night at room temperature and embedded in paraffin. Embedded tissues were cut in 5-µm-thick sections and stained with haematoxylin and eosin (H&E). Adipose tissue sections were evaluated using the Olympus BX51 microscope and representative areas from these sections were captured by using the Olympus camera 4A14690. The images were acquired with a standard X20-microscope objective lens. The imaging area was selected according to a high prevalence of adipocytes with an intact cell membrane and minimal adjacent tissues such as blood vessels, muscle and inflammatory cells. Adipocytes with unclear cell borders were excluded from analysis. Image annotation was performed manually by

using the Olympus Analysis Five Software and the mean adipocyte size was calculated for each type of adipose tissue. (Kaineder et al., IJO 2017, unpublished results).

4.3.6 Assessment of abdominal visceral and subcutaneous fat composition

Abdominal adipose tissue (AT) volumes of visceral (VAT) and subcutaneous (SAT) depots were measured with a micro-CT scanner (Siemens Inveon micro CT, Siemens Healthcare GmbH, Erlangen, Germany; energy settings: 200 mA, 80kV, 1200 ms) with Siemens Inveon Acquisition Workplace software (version 1.2.2.2) before (baseline) drug treatment and after 28 days of chronic infusion of liraglutide or placebo. Data was reconstructed using filtered back projection and algorithm of Feldkamp in Siemens Inveon Acquisition workplace. The reconstructed datasets were exported to DICOM format using Siemens Inveon Research Workplace and post processed regarding adipose tissue volumes using Materialise MIMICS v.19 (Materialise, Leuven, Belgium). We focused on the abdominal region, since scanning the abdominal adipose depots provides sufficient information to estimate total body fat and monitor site-specific changes in adiposity and reduces scanning time[113]. (Kaineder et al., IJO 2017, unpublished results).

4.3.7 RNA isolation, cDNA transcription and RT-qPCR

QIAzol Lysis Reagent (QIAGEN GmbH, Hilden, Germany) was used for tissue lysis. Total RNA content was isolated from homogenized adipose and hypothalamic tissue by using the RNeasy Mini Kit (QIAGEN GmbH, Hilden, Germany) including on-column DNase I treatment. RNA quantity was measured on NanoDrop (NanoDrop 2000c, ThermoFisherScientific GmbH, Vienna, Austria) and 1 µg total RNA was reversely transcribed by using the iScript advanced cDNA synthesis kit (Bio-Rad Laboratories, Vienna, Austria). Gene expression analysis via qPCR was performed using TaqMan Universal PCR Master Mix (Life Technologies, Carlsbad, California, USA) or LightCycler 480 SYBR Green I Master Mix (Roche, Vienna, Austria) according to the manufacturer's instructions on a Roche LightCycler 480 Instrument (Roche Austria, Vienna, Austria). Sequences of primers and probes are listed in Appendix. (Kaineder et al., IJO 2017, unpublished results).

4.3.8 Examination of metabolic and hormonal parameters

Plasma glucose levels were assessed by using the Accu-Check Performa system (Roche Diabetes Care Austria GmbH, Vienna, Austria). Non-esterified free fatty acids

(NEFA) were measured via the enzymatic colorimetric NEFA-HR(2) assay kit (WAKO Diagnostics, Richmond, Virginia, USA). Plasma free glycerol (FG) content was quantified colorimetrically using free glycerol reagent (Sigma Aldrich, Vienna, Austria). Plasma triacylglycerol levels (TAG) were analysed by using the Infinity Triacylglyceride Assay (ThermoScientific, Vienna, Austria). Circulating leptin, insulin, thyridiodine (T3) and thyroxine (T4) concentrations were measured with the Mesoscale Multiplex Array Elisa System (Mesoscale Diagnostics, Rockville, Maryland, USA). All measurements were performed according to the manufacturer's instructions. (Kaineder et al., IJO 2017, unpublished results).

4.3.9 Statistical Analysis

Data are expressed as mean ± SEM compared to the corresponding control or treatment group. Shapiro-Wilk test was used to scrutinize normal distribution. Either unpaired Student two-tailed t-test or Mann-Whitney U test was used to determine statistical significance when comparing two groups. *P*-values were corrected for multiple testing using the Benjamini-Hochberg procedure. To evaluate homogeneity of variances we used Leven's test and Mauchley's test of sphericity. For repeated body weight measurements, we used two-way repeated measures mixed model ANOVA plus Bonferroni post hoc analysis. Corrected *P*-values <0.05 were considered statistically significant. The calculations were performed in GraphPad Prism Mac 5.0b software (La Jolla, CA, USA) and SPSS Statistics version 23 (IBM, Ehningen, Germany). Relative gene expression levels (mRNA) were analysed using the $2^{(-\Delta\Delta Ct)}$ method[114]. (Kaineder et al., IJO 2017, unpublished results).

Parts of this thesis are adapted from the publication Kaineder et al. "Continuous intrahypothalamic rather than subcutaneous liraglutide administration leads to reduced body weight gain and stimulation of melanocortin system", published 2017 in the *International Journal of Obesity*.

4.4 Results

4.4.1 Chronic intrahypothalamic liraglutide treatment leads to profound weight loss and adipose tissue loss

IH treatment resulted in a significant body weight loss of 4% at day 7 (P<0.05) and 5% at day 9 (P<0.05) compared to baseline. Compared to the control group (IH control), chronic IH liraglutide treatment significantly reduced body weight gain by 6% at day 7 (P<0.05), 8% at day 9 (P<0.01), 6% at day 14 and day 16 (P<0.05) (Figure 9A). A 3% reduction in body weight gain was maintained from day 21 to day 28 compared to IH control (Figure 9A). IH liraglutide treated rats had significantly reduced epididymal and inguinal fat mass compared to IH control (P<0.05) (Figure 9B). (Kaineder et al., IJO 2017, unpublished results).

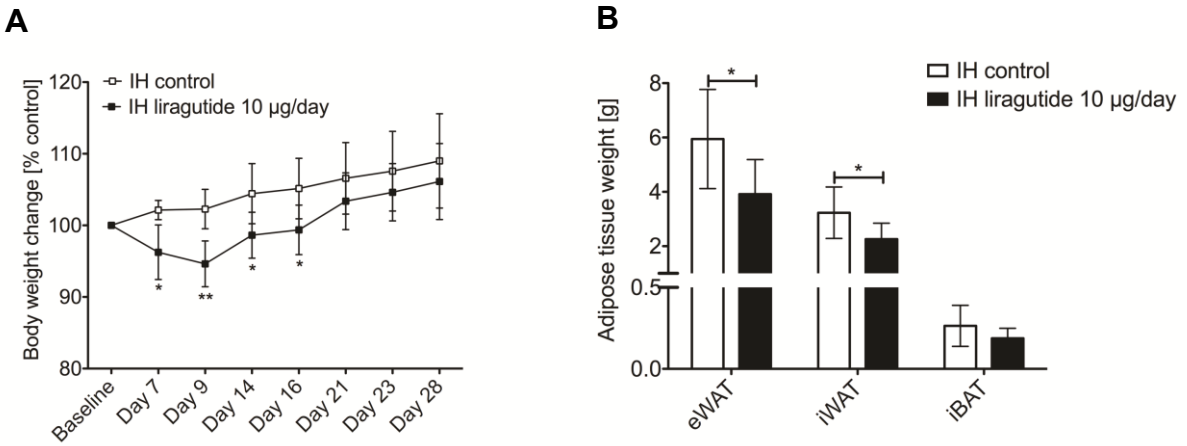

Figure 9 – Chronic intrahypothalamic liraglutide treatment leads to body weight loss and adipose tissue mass loss. (A) Body weight loss over 16 days and a reduced body weight gain from day 21 to day 28 triggered by continuous IH liraglutide treatment (IH 10 µg/day) compared to control group (IH control, aCSF). **(B)** Adipose tissue mass loss from eWAT (epididymal), iWAT (inguinal) white adipose tissue depots and from iBAT (interscapular) brown adipose tissue depot after 28 days of IH liraglutide treatment. Interaction p=0.0025, Time p<0.0001, Treatment p<0.0210. Data are presented as mean ± SEM of 7-8 animals per group. (*p<0.05, **p<0.01). IH – intrahypothalamic; SC - subcutaneous.

4.4.2 Chronic subcutaneous liraglutide treatment does not affect body weight and adipose tissue mass

Chronic subcutaneous administration of liraglutide did neither affect body weight (Figure 10A), nor did it reduce adipose tissue mass (Figure 10B). (Kaineder et al., IJO 2017, unpublished results).

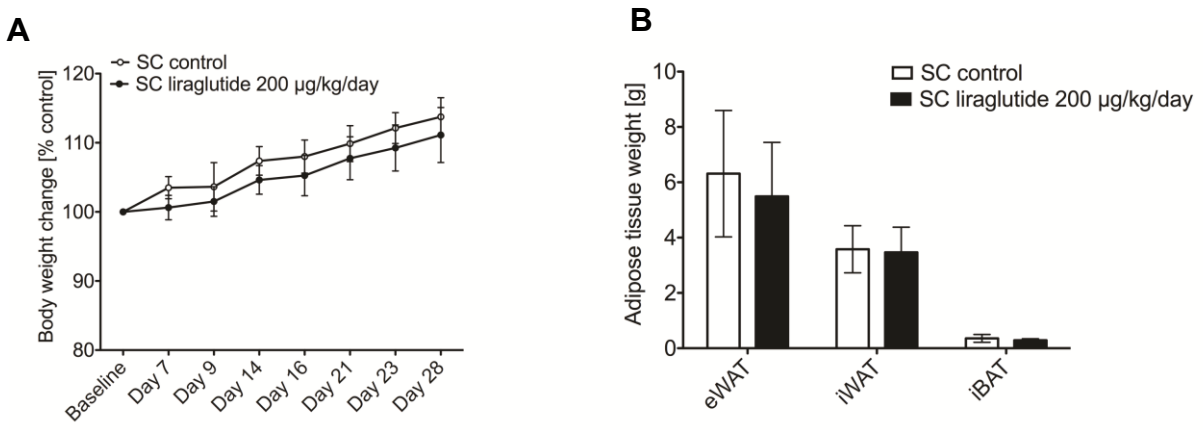

Figure 10 – Chronic subcutaneous liraglutide treatment does not lead to body weight and adipose tissue mass loss. (A) No change in body weight over 28 days of SC liraglutide treatment (200 µg/kg/day) compared to corresponding control group (SC control, 0.9% NaCl). **(B)** No change in adipose tissue weights from eWAT, iWAT and iBAT depots after 28 days of SC liraglutide treatment. Interaction p=0.3379, Time p<0.0001, Treatment p=0.0295. Data are presented as mean ± SEM of 7-8 animals per group. IH – intrahypothalamic; SC - subcutaneous. (Kaineder et al., IJO 2017, unpublished results)

4.4.3 Chronic intrahypothalamic rather than subcutaneous liraglutide treatment leads to body weight loss and adipose tissue loss

Compared to the SC liraglutide treatment group, chronic IH liraglutide treatment induced a significant body weight loss at day 9 (P<0.001), at day 14 and 16 (P<0.01), at day 23 and 28 (P<0.05) (Figure 11A). IH liraglutide treatment resulted in a significant reduction of inguinal white and interscapular brown adipose tissue compared to SC liraglutide treatment (P<0.01) (Figure 11B). (Kaineder et al., IJO 2017, unpublished results).

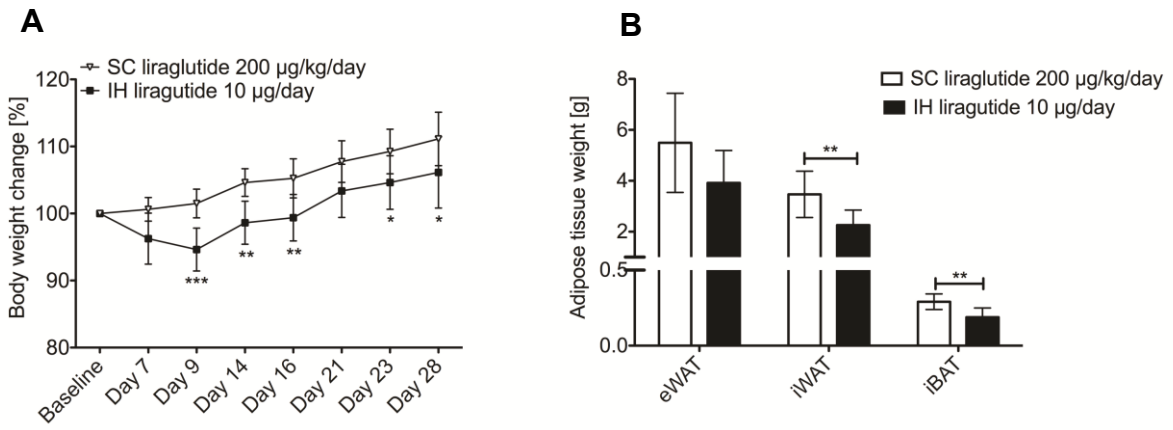

Figure 11 – Chronic intrahypothalamic liraglutide treatment leads to body weight and adipose tissue loss and a reduced body weight gain. (A) Body weight loss over 16 days and a reduced body weight gain from day 21 to day 28 after chronic IH liraglutide treatment (10 µg/day) compared to SC liraglutide treatment (200 µg/kg/day). **(B)** Loss of adipose tissue mass from eWAT, iWAT, iBAT after 28 days of IH liraglutide versus SC liraglutide treatment. Interaction p=0.0010, Time p<0.0001, Treatment p=0.0024. Data are presented as mean ± SEM of 7-8 animals per group. (*p<0.05, **p<0.01, ***p<0.001). IH – intrahypothalamic; SC - subcutaneous. (Kaineder et al., IJO 2017, unpublished results)

4.4.4 Chronic intrahypothalamic liraglutide treatment reduces the size of brown adipocytes

Chronic IH liraglutide treatment showed a significant reduction in brown adipocyte size compared to the control group (IH control) (P<0.05) (Figure 12A, 12B). We found a trend towards reduced adipocyte size in eWAT (epidiymal) and iWAT (inguinal) compared to control group (Figure 12A, 12B). (Kaineder et al., IJO 2017, unpublished results).

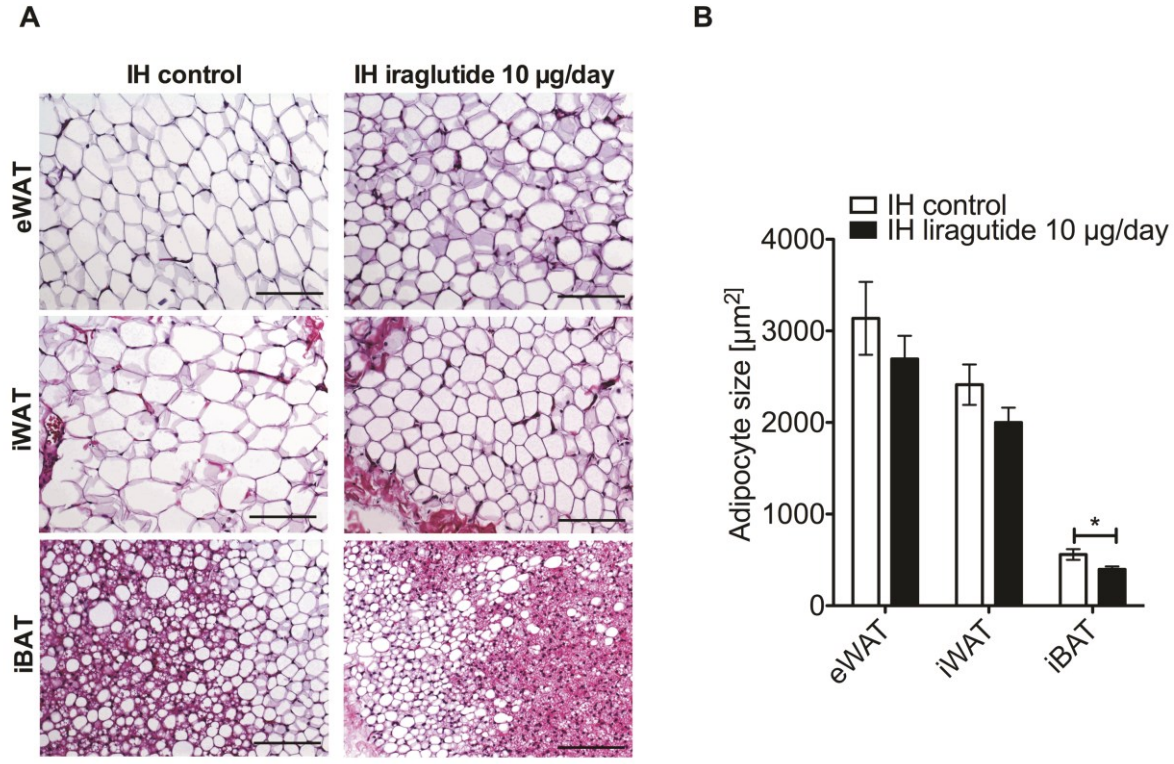

Figure 12 – Chronic intrahypothalamic liraglutide treatment leads to reduction in brown adipocyte size. (A) Adipocyte size after 28 days of IH liraglutide treatment (IH 10 µg/day). **(B)** Representative H&E stainings of adipose tissues (eWAT, iWAT, iBAT) 28 days after IH liraglutide injection compared to IH control; 20X magnification, scale bar = 200 µm. Data are given in mean + SD of 7-8 animals. (*p<0.05). (Kaineder et al., IJO 2017, unpublished results)

4.4.5 Chronic intrahypothalamic liraglutide treatment reduces gain of visceral adipose tissue volume

After 28 days of IH liraglutide treatment we found a 10% reduction of visceral adipose tissue (VAT) compared to the control group (IH control) (P<0.05) (Figure 13A). The subcutaneous adipose tissue (SAT) volume showed a trend towards reduced adipose tissue volume by IH liraglutide treatment compared to IH control (Figure 13B). Overall we observed a reduced visceral and subcutaneous adipose tissue gain from baseline to day 28 after IH liraglutide treatment. (Kaineder et al., IJO 2017, unpublished results).

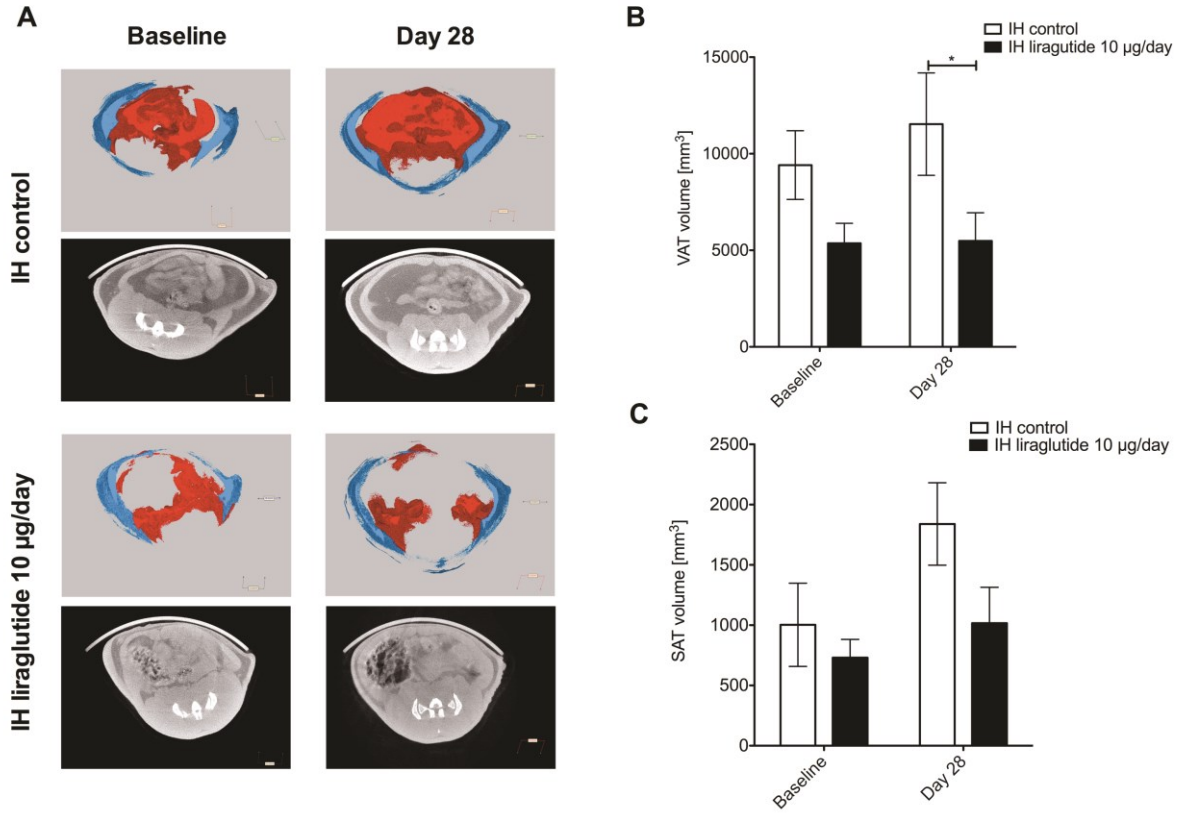

Figure 13 – Chronic intrahypothalamic liraglutide treatment reduces visceral adipose tissue depot. (A) micro-CT calculated VAT volume (mm^3) at baseline (after pump initialisation) and at day 28 after IH liraglutide treatment compared to IH control. **(B)** micro-CT calculated SAT volume (mm^3) from baseline to day 28 after IH liraglutide treatment compared to IH control. **(C)** Fully segmented 3D micro-CT images (xyz) of the abdominal region VAT (red) and SAT (blue). Black/white images show transverse axial micro-CT images of rat abdomen at level L5-S1 inter-vertebral disk. VAT = visceral adipose tissue; SAT = subcutaneous adipose tissue; Data are expressed as mean ± SEM of 7-8 animals. (*p<0.05). (Kaineder et al., IJO 2017, unpublished results)

4.4.6 Chronic subcutaneous liraglutide treatment does not affect adipose tissue volume

We observed no reduction of visceral and subcutaneous adipose tissue gain from baseline to day 28 after SC liraglutide treatment (Figure 14A, Figure 14B). Visceral and subcutaneous adipose tissue volumes showed a trend towards reduction by SC liraglutide treatment compared to SC control on day 28 (Figure 14A, Figure 14B). SC liraglutide treatment compared to IH liraglutide treatment showed a higher gain in visceral and subcutaneous adipose tissue.

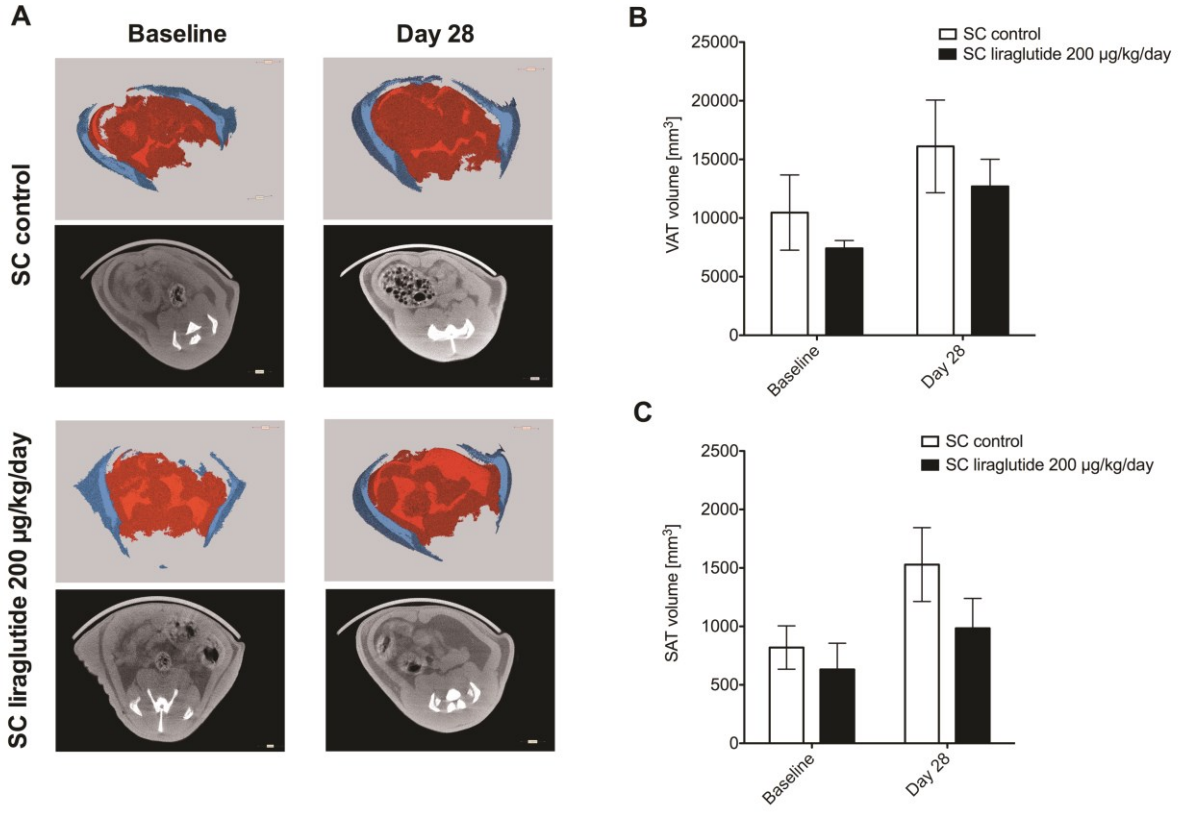

Figure 14 - Chronic subcutaneous liraglutide treatment does not reduce adipose tissue volume. (A) micro-CT calculated VAT volume (mm^3) at baseline (after pump initialisation) and at day 28 after SC liraglutide treatment compared to SC control. **(B)** micro-CT calculated SAT volume (mm^3) from baseline to day 28 after SC liraglutide treatment compared to SC control. **(C)** Fully segmented 3D micro-CT images (xyz) of the abdominal region VAT (red) and SAT (blue). Black/white images show transverse axial micro-CT images of rat abdomen at level L5-S1 inter-vertebral disk. VAT = visceral adipose tissue; SAT = subcutaneous adipose tissue; Data are expressed as mean ± SEM of 7-8 animals.

4.4.7 The chronic intrahypothalamic liraglutide-induced body weight and adipose tissue mass loss is independent of thermogenesis and browning

Chronic IH liraglutide treatment did not affect expression of brown adipocyte marker *ucp1* in iBAT (Figure 19). Chronic IH liraglutide treatment did not change expression of browning, adipogenesis, lipolysis and beta-oxidation markers (*prdm16, cidea, cidec fgf21, tnfrsf9, zic1, bmp7, cebpb, cebpa, ppargc1a, pparg, ldlr, lpl, adrb1, cpt1a*) in eWAT, iWAT and iBAT (Figure 15, Figure 17, Figure 19). Mitochondrial cytochrome c oxidase subunit 3 (*mtco3*) in eWAT was significantly increased with IH liraglutide treatment compared to the control group ($P<0.05$) but no effect was observed on other markers for mitochondrial respiration (*cox4i1, cycs, mtco3*) (Figure 15). We observed a trend towards reduction of leptin mRNA levels in eWAT and iWAT with IH liraglutide treatment compared to the control group, whereas adiponectin was unaffected (Figure 15, Figure 17). Chronic SC liraglutide treatment did not affect expression of brown adipocyte marker *ucp1* in iBAT, and expression of browning, adipogenesis, lipolysis and beta-oxidation markers (*prdm16, cidea, cidec, fgf21, tnfrsf9, zic1, bmp7, cebpb, ppargc1a, pparg, ldlr, lpl, adrb1, cpt1a*) in eWAT, iWAT and iBAT (Figure 16, Figure 18, Figure 20). The gene for the enzyme *dio* was unaffected by chronic IH liraglutide treatment compared to the IH control group (Figure 20). (Kaineder et al., IJO 2017, unpublished results).

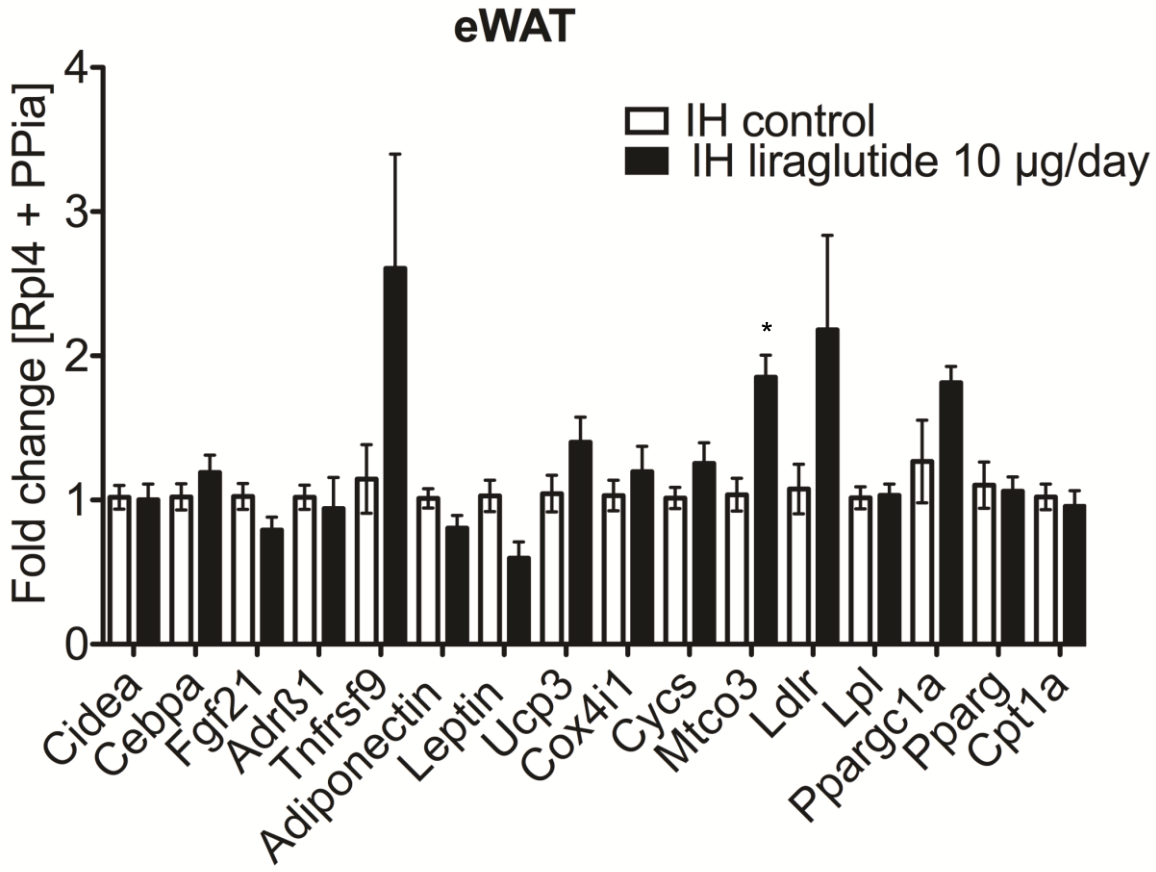

Figure 15 – Chronic intrahypothalamic liraglutide treatment does not induce thermogenesis and browning of the eWAT. Relative mRNA levels (fold changes) in eWAT after 28 days of IH liraglutide treatment compared to control group (IH control). *Rpl4* and *PPia* were used as reference genes. Data are given in mean ± SEM of 7-8 animals per group. (**p*<0.05). (Kaineder et al., IJO 2017, unpublished results)

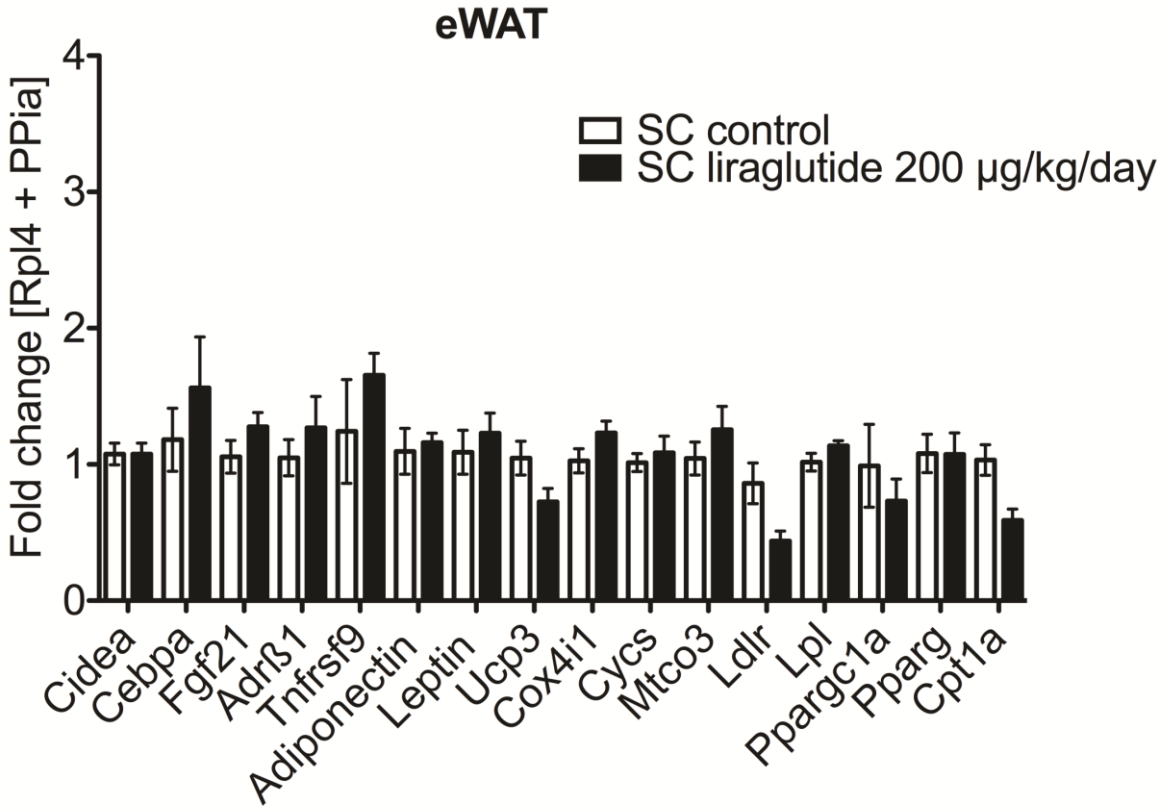

Figure 16 – Chronic subcutaneous liraglutide treatment does not affect browning or thermogenesis in eWAT. Relative mRNA levels (fold changes) in eWAT after 28 days of SC liraglutide treatment compared to control group (SC control). *Rpl4* and *PPia* were used as reference genes. Data are presented as mean ± SEM of 7-8 animals per group. (Kaineder et al., IJO 2017, unpublished results)

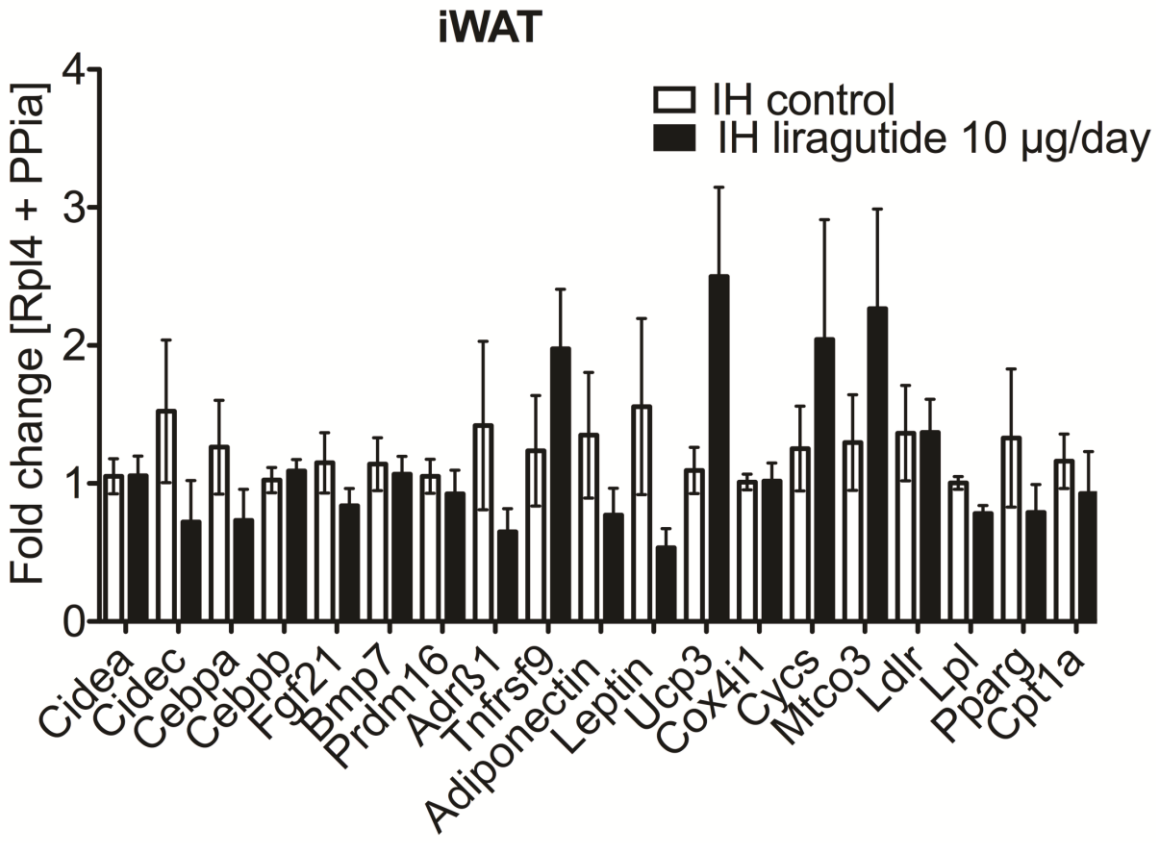

Figure 17 - Intrahypothalamic liraglutide treatment does not induce thermogenesis and browning of the iWAT. Relative mRNA levels (fold changes) in iWAT after 28 days of IH liraglutide treatment compared to control group (IH control). *Rpl4* and *PPia* were used as reference genes. Data are presented as mean ± SEM of 7-8 animals per group. (Kaineder et al., IJO 2017, unpublished results)

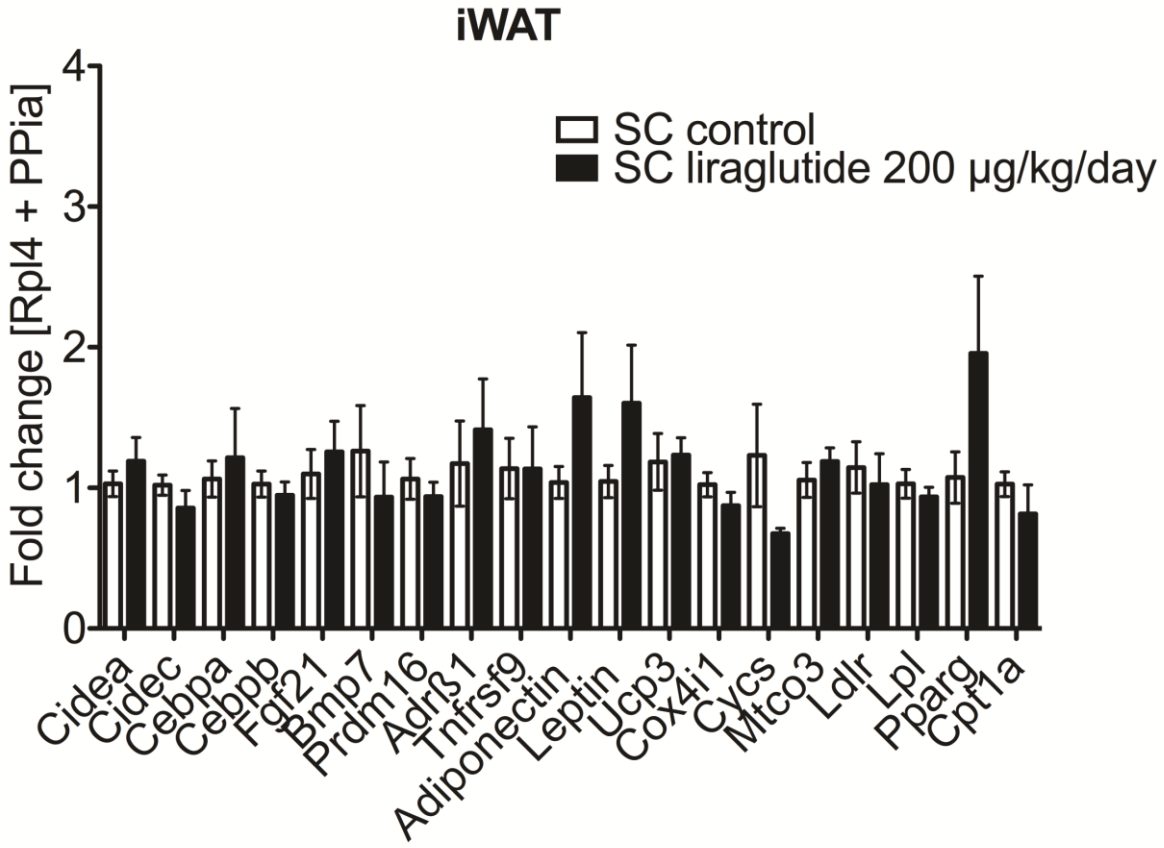

Figure 18 – Chronic subcutaneous liraglutide treatment does not affect browning or thermogenesis in iWAT. Relative mRNA levels (fold changes) in iWAT after 28 days of SC liraglutide treatment compared to control group (SC control). *Rpl4* and *PPia* were used as reference genes. Data are presented as mean ± SEM of 7-8 animals per group.

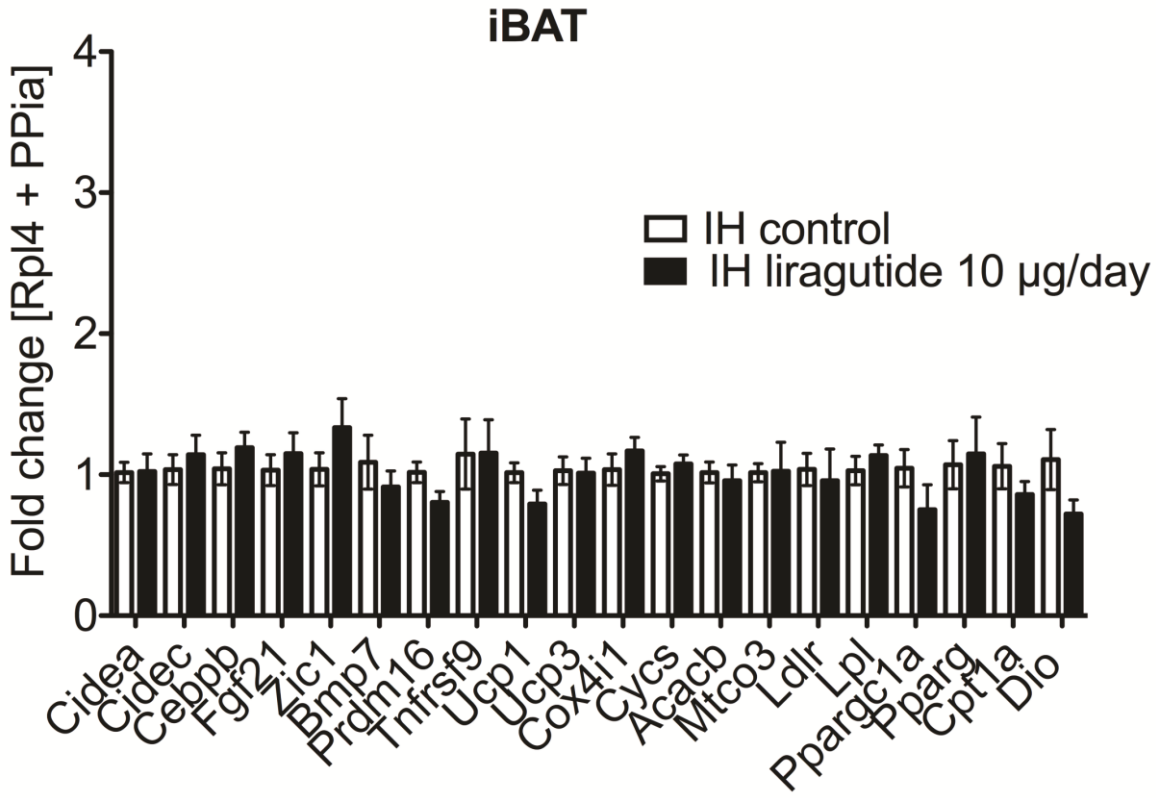

Figure 19 – Chronic intrahypothalamic liraglutide treatment does not induce thermogenesis and browning of the iBAT. Relative mRNA levels (fold changes) in iWAT after 28 days of IH liraglutide treatment compared to control group (IH control). *Rpl4* and *PPia* were used as reference genes. Data are presented as mean ± SEM of 7-8 animals per group. (Kaineder et al., IJO 2017, unpublished results)

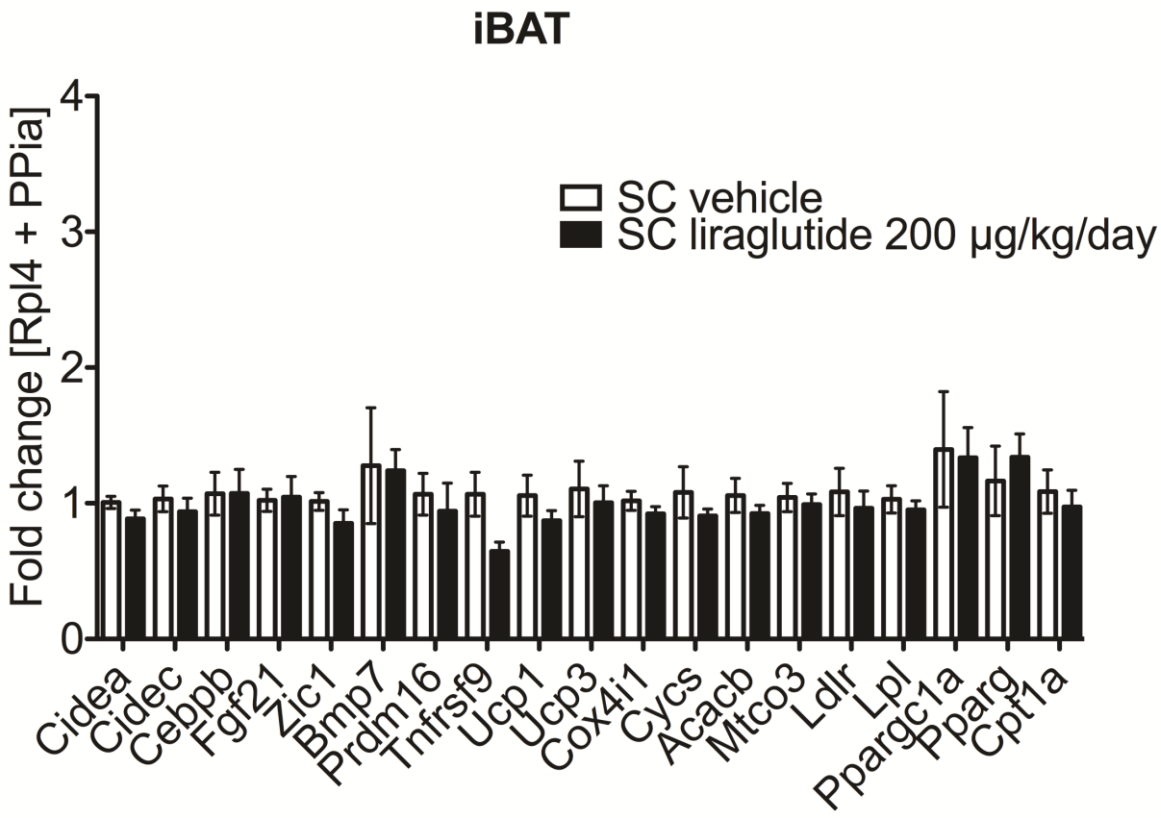

Figure 20 – Chronic subcutaneous liraglutide treatment does not affect browning or thermogenesis in iBAT. Relative mRNA levels (fold changes) in iBAT after 28 days of SC liraglutide treatment compared to control group (SC control). *Rpl4* and *PPia* were used as reference genes. Data are presented as ± SEM of 7-8 animals per group.

4.4.8 Chronic intrahypothalamic liraglutide treatment stimulates the central melanocortin (MC4R) system

Chronic IH treatment with liraglutide led to an 18-fold induction of the hypothalamic melanocortin 4 receptor gene expression (*mc4r*) compared to the control group (P<0.01) (Figure 21) but no further changes were found in any genes regulating appetite and satiety in the hypothalamus (*mc3r, bdnf, pomc, agrp, npy, lepr, pc1, glp1r*). Expression of genes of the pituitary-thyroid axis (*tsh, trh, dio2*) was likewise unaffected by IH liraglutide treatment except the slight increase in *tsh* mRNA levels (Figure 21). Expression of markers for appetite neurons, like *a-msh* and *sosc3* was undetectable. Expression patterns of neuronal appetite markers were undetectable in SC liraglutide treated group. (Kaineder et al., IJO 2017, unpublished results).

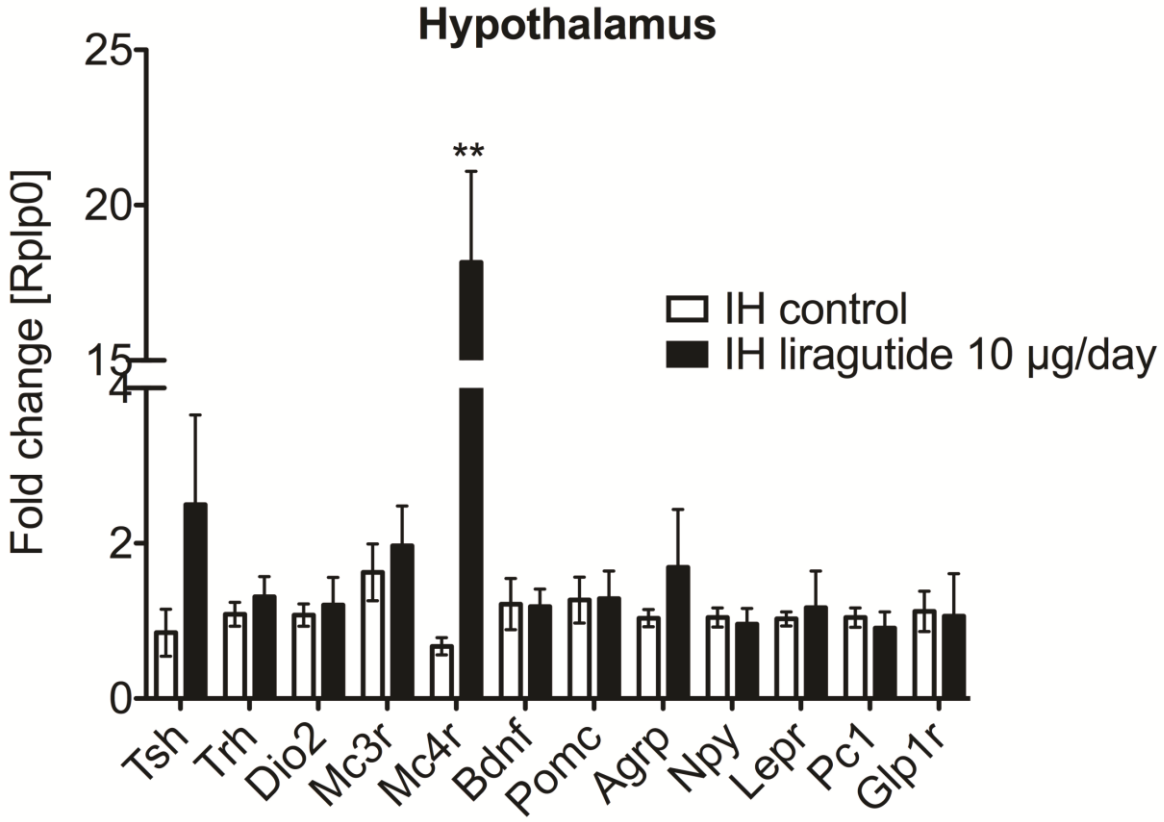

Figure 21 – Chronic intrahypothalamic liraglutide treatment stimulates an 18-fold induction of *mc4r* levels. Relative mRNA expression levels (fold changes) of genes involved in thyroid-pituitary axis (*tsh, trh, dio2*) and energy homeostasis (*bdnf, pomc, agrp, npy, lepr, pc1, glp1r, mc3r, mc4r*) in the hypothalamus. *Rplp0* was used as reference gene. Data are presented as mean ± SEM of 7-8 animals per group compared to their corresponding control group. (**p<0.01). (Kaineder et al., IJO 2017, unpublished results)

4.4.9 Chronic intrahypothalamic liraglutide treatment increases thyroxine levels

Chronic IH liraglutide treatment led to a 1.4-fold increase in circulating concentrations of the thyroid hormone thyroxine (T4) compared to the control group (IH control) (P<0.05) (Table 5). Neither IH liraglutide nor SC liraglutide treatment affected any circulating factor of glucose metabolism (insulin, glucose) or fatty acid metabolism (leptin, NEFA, FG, TAG) at day 28. We observed normal TSH levels for all groups at baseline, treatment day 14 and treatment day 21 compared to control groups (Table 6). (Kaineder et al., IJO 2017, unpublished results).

Table 5 – Chronic intrahypothalamic liraglutide treatment leads to increased T4 concentrations. Circulating plasma levels of markers for glucose metabolism (glucose, insulin), fatty acid metabolites (leptin, NEFA, TAG, FG) and thyroid hormones (T3,T4) at day 28 after chronic IH (10 µg/day) and SC (200 µg/kg/day) liraglutide treatment. Data are given as mean ± SEM of 7-8 animals per group. (*p<0.05); FG, free glycerol; NEFA, non-esterified fatty acids; TAG, triglyceride; T3, triiodothyronine; T4, thyroxine; (Kaineder et al., IJO 2017, unpublished results)

	IH control	IH liraglutide [10 µg/day]	SC control	SC liraglutide [200 µg/kg/day]
FG (µmol/ml)	13.21 ± 2.94	13.43 ± 2.73	11.98 ± 1.54	11.39 ± 1.71
NEFA (µmol/ml)	14.67 ± 4.14	15.54 ± 5.4	15.85 ± 5.0	17.76 ± 5.77
TAG (µmol/l)	0.08 ± 0.02	0.08 ± 0.03	0.10 ± 0.03	0.10 ± 0.04
Leptin (ng/ml)	25.20 ± 14.0	14.96 ± 13.54	8.20 ± 5.74	8.18 ± 5.48
Insulin (ng/ml)	1.71 ± 0.61	1.23 ± 0.45	1.24 ± 0.57	1.07 ± 0.12
Glucose (mmol/l)	7.04 ± 0.33	7.29 ± 0.69	7.90 ± 0.63	6.56 ± 0.89
T3 (ng/dl)	24.35 ± 5.6	25.95 ± 7.3	24.99 ± 8.6	24.34 ± 7.8
T4 (ng/dl)	**57.78 ± 8.2**	**80.61 ± 23.3***	61.0 ± 12.6	58.42 ± 14.8

Table 6 - TSH (ng/ml) levels at baseline, 14 days and 21 days after intrahypothalamic or subcutaneous liraglutide administration. We observed no changes in TSH levels neither in intrahypothalamic nor in subcutaneous treated groups. Data are given in mean ± SD. TSH – thyroid stimulating hormone; IH – intrahypothalamic, SC - subcutaneous.

	IH vehicle	IH liraglutide [10 µg/day]	SC vehicle	SC liraglutide [200 µg/kg/day]
Baseline	0.81 ± 0.18	0.94 ± 0.26	1.65 ± 1.16	1.32 ± 0.60
Day 14	1.32 ± 0.44	1.08 ± 0.17	2.29 ± 2.17	1.04 ± 0.41
Day 21	1.20 ± 0.30	1.12 ± 0.35	1.75 ± 1.20	1.20 ± 0.31

5 Discussion

This study aimed to identify different effects of chronic central and peripheral liraglutide treatment on body weight. Chronic central application of liraglutide induced a significant body weight loss and overall reduction in body weight gain, which was supported by a significant loss of adipose tissue mass. Chronic central liraglutide treatment led to a reduction in brown adipocyte size and reduced gain of visceral fat. Furthermore, chronic central liraglutide treatment led to a significant activation of hypothalamic *mc4r* mRNA expression and a significant increase in plasma T4 concentrations.

Chronic intrahypothalamic (IH) liraglutide administration induced a significant reduction in body weight during the first 16 days of treatment. We observed a light gain in body weight after day 16 of IH liraglutide treatment, but body weight gain was still low compared to control group. At day 9 of IH liraglutide treatment the biggest loss in body weight was observed. Compared to peripheral liraglutide treatment, we found that central injection of liraglutide induced a significant body weight loss from day 9 to day 28 and a significant loss in adipose tissue mass (iWAT, iBAT) after 28 days. To our knowledge, this is the first study on chronic central liraglutide treatment continuously for 28 days in animal trials. The observed body weight regain at the end of our study (day 21 to day 28) could be caused by GLP-1 receptor desensitization (tachyphylaxis) upon continuous stimulation[117] supported by the unaffected GLP-1R expression in the hypothalamus in our study after chronic central liraglutide treatment. Other physiological mechanisms such as reduced energy expenditure, increased appetite seen as an increase in ghrelin[118], reduced satiety or a reduction in plasma leptin could be further explanations for the observed body weight regain[119–122]. We observed a trend towards reduced plasma leptin levels after chronic central liraglutide treatment, which has been suggested to increase food intake[119,122]. An increased food intake might explain the observed body weight regain at the end of our study upon chronic central liraglutide administration. As we investigated the chronic liraglutide effects in a healthy lean animal model without leptin resistance, the body weight regain seems to be a natural protective counter-regulatory physiological response after weight loss also seen in humans[66]. (Kaineder et al., IJO 2017, unpublished results).

In humans, 3 mg liraglutide causes a moderate weight loss of 7.2 kg in obese individuals with slight weight regain[66,79]. Our animal study did not result in any reduction in body weight gain after peripheral chronic administration of liraglutide while similar subcutaneous liraglutide treatment has led to anorectic effects and body weight loss in diet-induced obese rats on high-fat diet[35]. Similar studies in diet-induced obese are expected to result in a more pronounced anorectic effect[73,123] compared to our study design with lean rats on normal diet. However, our primary aim was to test the chronic physiological effect of liraglutide in the hypothalamus of a healthy animal model. (Kaineder et al., IJO 2017, unpublished results).

In contrast to other studies, we did not observe any changes on body weight by peripheral liraglutide administration. Considering the total liraglutide concentration in plasma at baseline and day 28 (Appendix), we assume that the continuous subcutaneous dosing of liraglutide in our study was not effective enough to stimulate the hypothalamic GLP-1R to trigger body weight loss compared to a more effective bolus administration in other studies[35,124]. Moreover, the liraglutide-induced anorectic effect and body weight loss are affected by the dosing regimen[63,66,124], the maximum dose of liraglutide used as obesity treatment is 3.0 mg. Such high dosing is necessary to decrease caloric intake and reduce body weight in humans. To exert anorexigenic effects in rodents, even higher dosing of liraglutide is necessary because of the shorter half-life of liraglutide in rodents[80,125]. (Kaineder et al., IJO 2017, unpublished results).

Combining our results on body weight development and adipose tissue mass we demonstrated that liraglutide mediates its body weight reducing effects more potently via central rather than peripheral mechanisms. (Kaineder et al., IJO 2017, unpublished results).

Shown by a recent acute study, administration of liraglutide led to increased thermogenesis in brown adipose tissue and browning of white adipose tissue through the AMP-activated protein kinase pathway in the ventromedial hypothalamus (VMH) independent of caloric intake[38]. In contrast, we found no significant changes in gene expressions of bona fide brown adipocyte marker *ucp1*, transcription factors for browning (*prdm16, ppargc1a*), browning enriched markers (*cidea, cidec, tnfrsf9, zic1, adrß1*) and browning activators (*fgf21, bmp7*)[126–130]. Therefore, our study does not support the involvement of increased thermogenic or browning capability in liraglutide-induced weight loss but this could be due to differences in the delivery site

and duration of treatment[38]. Several animal and human studies have attributed the weight reducing effects mediated by liraglutide to caloric intake rather than to increased energy expenditure[35,60,72,131]. (Kaineder et al., IJO 2017, unpublished results).

Similar to the extensive reduction in body weight gain, the chronic central liraglutide treatment in our study led to a sustained reduction of eWAT and iWAT mass as well as a reduced gain in visceral adipose tissue volume, but we found no such effect after chronic peripheral liraglutide treatment. Subcutaneous adipose tissue volume was slightly increased on day 28 compared to baseline after central liraglutide treatment, but less increased than in the control group. We observed a trend towards reduced size of white adipocytes in eWAT and iWAT after central liraglutide administration. iBAT mass was unaffected while iBAT adipocytes were significantly reduced in size after chronic central liraglutide treatment. We hypothesize that a reduced food intake is responsible for the observed reduction in adipocyte size and adipose tissue mass since we did not observe any changes in fatty acid metabolism after central liraglutide treatment. A previous study, where diet-induced obese mice where treated with liraglutide for 14 days has attributed the observed fat mass reduction to central GLP-1 receptor signaling[60]. This supports our assumption that the decline in visceral fat depot is mainly mediated by hypothalamic neural mechanisms as indicated by the clear difference between the effects of central and peripheral liraglutide administration found in our study. (Kaineder et al., IJO 2017, unpublished results).

As expected, peripheral and central liraglutide treatment left hormonal parameters for glucose metabolism and fatty acid metabolism largely unaffected, as we investigated the liraglutide effect on healthy lean animals. But we observed a significant increase in circulating T4 concentrations without changes in TSH levels after chronic central liraglutide treatment. However, we can exclude that changes in the thyroxine binding globulin are responsible (TBG) for the increase in T4 levels, as it was reported that rats lack TBG[134,135]. In humans, weight loss and maintenance of body weight have been associated with increased peripheral conversion of T4 to the bioactive enantiomer reverse T3[121,132] but we found no changes in the expression of the enzyme type II iodothyronine deiodinase (DIO2) in iBAT which is essential for the intracellular conversion of T4 to T3[133]. Although we found an increase in T4 levels,

we did not observe any changes in the mRNA expression of *trh* and *tsh* in the hypothalamus. (Kaineder et al., IJO 2017, unpublished results).

Moreover, we examined the effect of chronic central liraglutide administration on neuronal populations known to regulate caloric intake and energy homeostasis. Contrary to other studies, we observed no change in the mRNA expression of hypothalamic orexigenic (*agrp/npy*) or anorexigenic (*pomc/a-msh*) neurons but we found a significant 18-fold induction of *mc4r* mRNA in the hypothalamus after chronic central liraglutide administration. These results indicate an alternative pathway for liraglutide to activate the anorectic MC4R system, besides the previously described POMC/CART produced melanocyte-stimulating hormone α-MSH signalling in the hypothalamus[136–138]. Also the previously identified downstream of the MC4R signalling, the neurotrophin brain derived neurotrophic factor (BDNF) was unaffected by chronic liraglutide stimulation, which again indicates an alternative signalling mechanism for liraglutide to stimulate the melanocortin system[139]. To our knowledge, we show for the first time that continuous, chronic liraglutide administration in the hypothalamus leads to a significant activation of the MC4R. Recently, a 5-day combination therapy including the MC4R agonist RM-493 and liraglutide in diet-induced obese mice showed improved body weight, fat mass reduction and a minimized receptor desensitization compared to monotherapy[140]. There is also evidence that the melanocortin signalling is involved in the brain's reward system (amygdala)[141], which was previously reported as high-fat fed or candy fed rats prefer low-fat or chow diet after administration of MC4R agonists (MTII)[142,125]. (Kaineder et al., IJO 2017, unpublished results).

We hypothesize that liraglutide possibly modulates the activity of dopamine producing neurons and their neuronal projections to regions involved in rewarding processes underlying appetite. Therefore it would be interesting to further investigate the role of liraglutide in combination with the MC4R agonist on the dopamine driven reward system.

CHAPTER 3

The pharmacological effect of acute liraglutide treatment in the hypothalamus on energy homeostasis

6 The pharmacological effect of acute liraglutide treatment on energy homeostasis

6.1 Abstract

Liraglutide, a long-acting GLP-1R agonist stimulates satiety, which leads to reduced caloric intake and body weight loss. Acute studies have shown that liraglutide exerts differential effects on energy balance when administered to different sites in the hypothalamus. The underlying mechanisms that mediate the body weight loss elicited by central and acute liraglutide are still not entirely clear.

We aimed to assess the role of acute (24 h) liraglutide administration in the hypothalamus on body weight and whether the melanocortin system or thermogenesis is activated. 16 healthy lean Sprague Dawley rats were separated in treatment (IH liraglutide) and control group (IH control) and treated either with a single dose of liraglutide (10 µg) or placebo (aCSF). We analysed the genetic expression of markers for browning, thermogenic, and adipocyte differentiation in various adipose tissue depots. mRNA signature of hypothalamic neurons, which regulate appetite were analysed by qPCR. We measured parameters in plasma for glucose and fat metabolism.

Acute central liraglutide treatment did not reduce body weight. Metabolic profiles were unaffected by acute central liraglutide treatment. We did not observe any effects on the melanocortin system.

6.2 Aim

In combination to the chronic effect of liraglutide on body weight and adipose tissue composition, an acute study with central liraglutide treatment (24 h) should reveal whether a loss of body weight and adipose tissue mass as well as the activation of the central melanocortin system are also an early response to liraglutide treatment.

6.3 Introduction

We showed that liraglutide exerts its chronic anorectic effects more potently through GLP-1 receptors in the brain rather than via peripheral GLP-1R. A recent study has shown that a single central injection of liraglutide decreased caloric intake and body weight and increased energy expenditure after 24 h and this effect remitted after 48 hours[38]. In addition the authors observed higher temperatures in the brown

adipose tissue depot and increased browning and thermogenic capability of white and brown adipocytes after 24 hours[38]. To elucidate the hypothalamic area(s) specific for these energy homeostatic effects of liraglutide Beiroa et al. injected a single dose of liraglutide in hypothalamic nuclei, known to play a major role in appetite regulation, such as the PVN, DMH, ARC, LHA, and VMH[38]. Liraglutide exerts its body weight and food intake reducing effects via the ARC, the PVN and the LHA without influencing energy expenditure in terms of adipose tissue browning and thermogenesis[38]. An acute stimulation of the GLP-1R with centrally injected liraglutide in the VMH induces thermogenesis of the brown adipose tissue and browning of white adipocytes via activation of the AMPK pathway[38]. ICV administration of liraglutide dose-dependently reduces food intake and body weight after 24 hours in fasted rodents[61]. In contrast, it was reported that acute liraglutide administration causes a modest reduction in caloric intake at 4 hours but not at 24 hours in chow-fed mice[60]. The inconsistency among studies needs to be clarified by further elucidating the acute effect of liraglutide and other long-acting GLP-1R agonists on central energy regulation.

6.4 Research design and methods

6.4.1 Animal models

Male Sprague Dawley (S.D.) rats (12–15 weeks old, 400–450 g; Charles River Laboratories) were housed under conditions of controlled temperature (23°C) and illumination (12-h light/dark cycle). Rats were allowed ad libitum access to water and standard laboratory chow. Animals were sacrificed by decapitation and tissue samples (hypothalamus, adipose tissues) were removed and immediately frozen in liquid nitrogen, and stored at -80°C until analysis. All animal experiments were approved by the Austrian Federal Government (BMWF-66.010/0010-WF/V/3b/2015) and were performed in consent with Directive 2010/63/EU on the protection of animals used for scientific purposes. (Kaineder et al., IJO 2017, unpublished results).

6.4.2 Study design

16 male Sprague Dawley rats were assigned to one of two groups according to their body weight (each group N=8) (Table 7). Liraglutide (IH liraglutide; 10 µg per animal) or aCSF (IH control) were injected directly into the hypothalamus (AP – 1.7, ML 0.6, DV – 7.6 mm) via syringe (5 µl, Hamilton, Bonaduz, Switzerland).

Table 7 - Treatment and application site of four different groups. Each group was comprised of 8 rats and was treated for 24 hours. AP (anterior -posterior), ML (medial – lateral), DV (dorsal – ventral); stereotactic coordinates: (AP – 1.7, ML 0.6, DV – 7.6 mm).

Group number	Group name	Treatment	Application site
1	IH liraglutide	Liraglutide 10 µg/rat	Hypothalamus
2	IH control	aCSF	Hypothalamus

6.4.3 Surgical implantation of intrahypothalamic cannula

Before implantation, rats were individually placed in an anesthesia induction chamber (Rothacher, Heitenried, Switzerland) induced with 4 vol% isoflurane (Isoflo, Esteve Farma, Carnaxide, Portugal) in 100% oxygen with a delivery rate of 5 l/min until loss

of righting reflex. Rats were anesthetized using an injectable anesthetic (0.1 ml/kg; 0.5 mg/kg Midazolam, 5 µg/kg Fentanyl, 5 mg/kg Domitor; ERWO Pharma GmbH, Hameln pharma plus GmbH, Vienna, Austria). Anesthesia was maintained with isoflurane in 100% oxygen at a flow of 1.5 l/min. The head was fixed in a small animal stereotactic frame (Model 900, David Kopf Instruments, California, USA) and rats were prepared for surgery by shaving the head and disinfecting the skin with 70% ethanol. A spherical dental drill was used to drill a 1 mm hole into the skull leaving the dura intact. The dura was then punctured with fine forceps in order to create a defined opening of the meninges[96]. The cannula (PlasticsOne, Bilaney Consultants, Düsseldorf, Germany) was inserted slowly to a depth of 7.6 mm (intrahypothalamically) via a 1 mm hole drilled into the skull 1.7 mm lateral to the bregma and 0.6 mm from midline and fixed to the skull using four anchor screws and biocompatible dental cement (iCEM Self Adhesive; Heraeus, Hanau, Germany). After surgery, rats received analgesics and anti-inflammatory drugs once (50 mg/kg Claforan, Sanofi-Aventis GmbH, Vienna, Austria; 50 mg/ml Carprofen; Pfizer Corporation Austria GmbH, Vienna, Austria). (Kaineder et al., IJO 2017, unpublished results).

6.4.4 Assessment of body weight and adipose tissue mass

Body weight was continuously assessed on a precise laboratory scale (Competence CP3202S-0CE, Sartorius AG, Göttingen, Germany). After 24 hours rats were sacrificed and freshly excised adipose tissue depots (inguinal WAT, epididymal WAT, interscapular BAT) were weighed on an analytical balance (M-Power AZ214, Sartorius AG, Göttingen, Germany). Epididymal (eWAT) and inguinal (iWAT) white adipose tissue and interscapular brown adipose tissue (iBAT) were isolated, fixed in 4% paraformaldehyde over night at room temperature and embedded in paraffin. Embedded tissues were cut in 5-µm-thick sections and stained with haematoxylin and eosin (H&E). (Kaineder et al., IJO 2017, unpublished results).

6.4.5 RNA isolation, cDNA transcription and RT-qPCR

QIAzol Lysis Reagent (QIAGEN GmbH, Hilden, Germany) was used for tissue lysis. Total RNA content was isolated from homogenized adipose and hypothalamic tissue by using the RNeasy Mini Kit (QIAGEN GmbH, Hilden, Germany) including on-column DNase I treatment. RNA quantity was measured on NanoDrop (NanoDrop 2000c, ThermoFisherScientific GmbH, Vienna, Austria) and 1 µg total RNA was

reversely transcribed by using the iScript advanced cDNA synthesis kit (Bio-Rad Laboratories, Vienna, Austria). Gene expression analysis via qPCR was performed using TaqMan Universal PCR Master Mix (Life Technologies, Carlsbad, California, USA) or LightCycler 480 SYBR Green I Master Mix (Roche, Vienna, Austria) according to the manufacturer's instructions on a Roche LightCycler 480 Instrument (Roche Austria, Vienna, Austria). Sequences of primers and probes are listed in the Appendix. (Kaineder et al., IJO 2017, unpublished results).

6.4.6 Examination of metabolic and hormonal parameters

Plasma glucose levels were measured by using the Accu-Check Performa system (Roche Diabetes Care Austria GmbH, Vienna, Austria). Non-esterified free fatty acids (NEFA) were measured via the enzymatic colorimetric NEFA-HR(2) assay kit (WAKO Diagnostics, Richmond, Virginia, USA). Plasma free glycerol (FG) content was quantified colorimetrically using free glycerol reagent (Sigma Aldrich, Vienna, Austria). Plasma triglyceride levels (TAG) were analysed by using the Infinity Triglycerides Assay (ThermoScientific, Vienna, Austria). All measurements were performed according to the manufacturer's instructions. (Kaineder et al., IJO 2017, unpublished results).

6.4.7 Statistical Analysis

Data are expressed as mean ± SEM compared to the corresponding control. Shapiro-Wilk test was used to scrutinize normality of the data. Either unpaired two-tailed Student t-test or Mann-Whitney U test were used to determine statistical significance when comparing two groups. For repeated body weight measurements, we used two-way repeated measures ANOVA. *P*-values <0.05 were considered statistically significant. The calculations were performed in GraphPad Prism Mac 5.0b software (La Jolla, CA, USA). Relative gene expression levels (mRNA) were analysed using the $2^{(-\Delta\Delta Ct)}$ method[114].

6.5 Results

6.5.1 Acute intrahypothalamic liraglutide treatment does not affect body weight

We observed no change in body weight 24 hours after IH liraglutide treatment (10 µg) neither compared to baseline nor compared to control group (Figure 22). (Kaineder et al., IJO 2017, unpublished results).

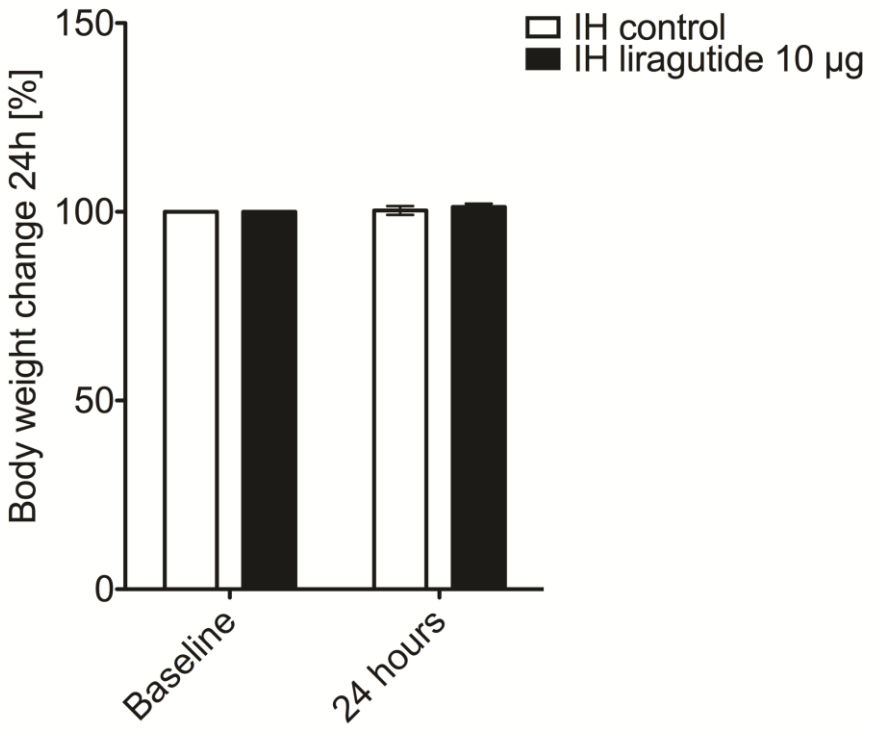

Figure 22 – Acute intrahypothalamic liraglutide treatment does not lead to body weight loss. Body weight at baseline (before treatment) and 24 hours after IH liraglutide treatment (10 µg) compared to IH control. Interaction p=0.1724, Time p=0.0207, Treatment p=0.1724. Results are indicated as mean ± SEM, 7-8 animals per group. IH – intrahypothalamic. (Kaineder et al., IJO 2017, unpublished results)

6.5.2 Acute liraglutide treatment does not reduce adipose tissue mass

We observed no change in weight of epididymal, inguinal white and interscapular brown adipose tissue 24 hours after IH liraglutide treatment compared to control group (Figure 23). (Kaineder et al., IJO 2017, unpublished results).

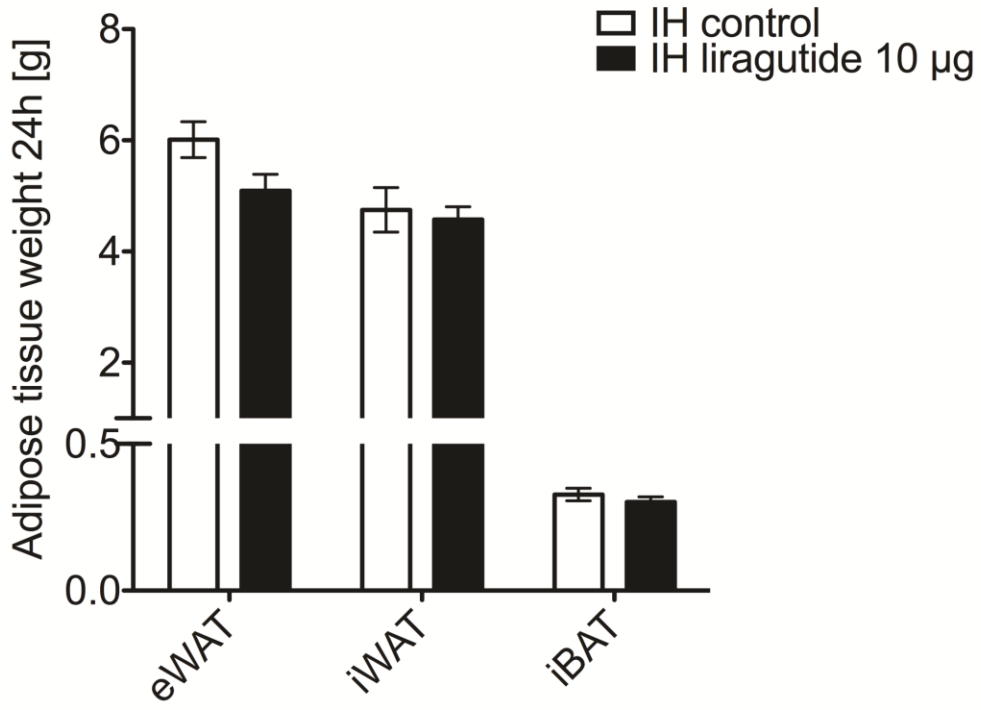

Figure 23 – Acute liraglutide treatment does not lead to adipose tissue weight loss. Adipose tissue mass of eWAT, iWAT, iBAT 24 hours after IH liraglutide treatment (10 µg) compared to control group. Data are represented as mean ± SEM of 7-8 animals per group. IH – intrahypothalamic. (Kaineder et al., IJO 2017, unpublished results)

6.5.3 Acute intrahypothalamic liraglutide treatment does not affect expression of markers for thermogenesis and adipose tissue morphology

Acute IH liraglutide treatment did not affect expression of brown adipocyte marker (*ucp3*), and expression of browning and adipogenesis markers (*prdm16, cidea, cebpa, fgf21)* in iWAT and eWAT compared to control group (Figure 24 and Figure 25). The brown adipocyte marker *ucp1* was undetectable in iWAT. Immunohistochemical stainings of eWAT, iWAT, and iBAT did not show morphological differences after 24 hours central liraglutide treatment (Figure 24, 25, 26). The morphology of inguinal and epididymal white adipose tissue as well as interscapular brown adipose tissue was unaffected after IH liraglutide treatment, which is indicated by H&E stainings. (Kaineder et al., IJO 2017, unpublished results).

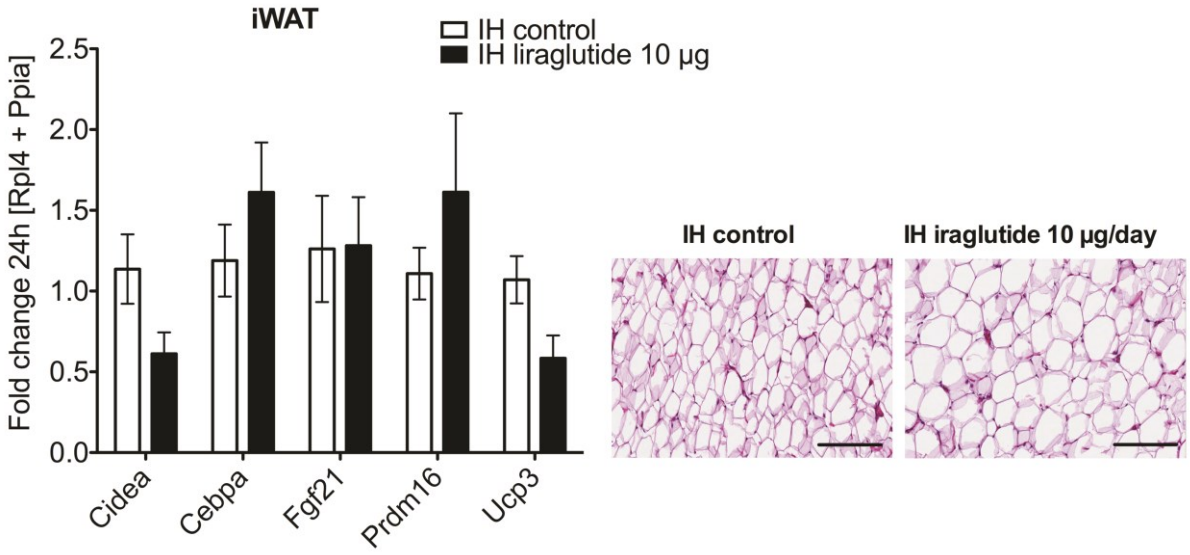

Figure 24 – Acute liraglutide treatment does not affect thermogenesis and browning in iWAT. Relative mRNA levels (fold changes) in iWAT 24 hours after IH liraglutide treatment compared to control group (IH control). *Rpl4* and *PPia* were used as reference genes. Scale bar = 10X magnification. Data are given in mean ± SEM of 7-8 animals per group.

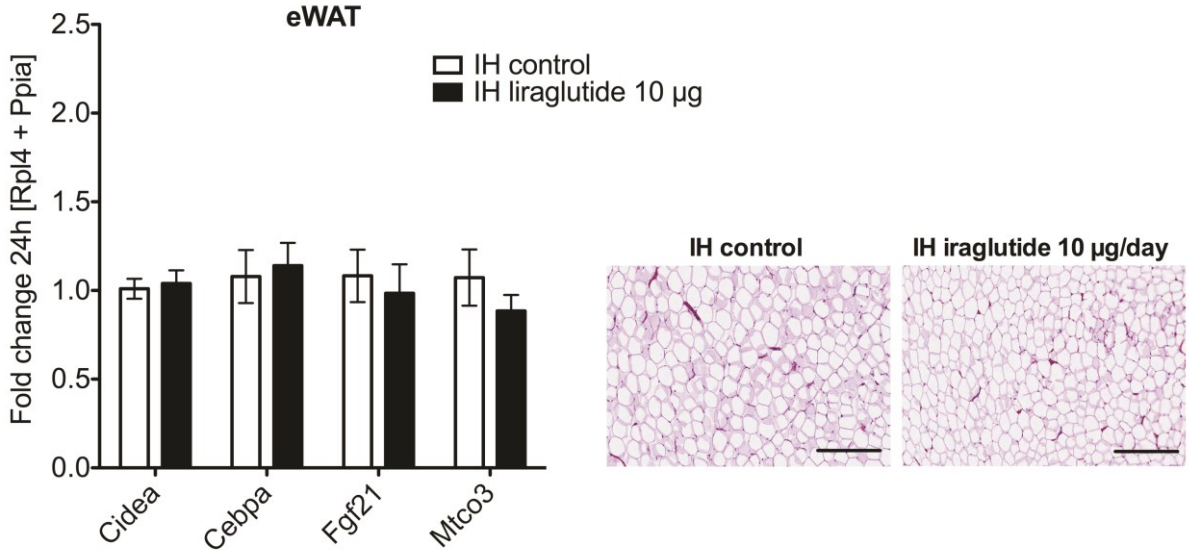

Figure 25 - Acute liraglutide treatment does not affect thermogenesis and browning in eWAT. Relative mRNA levels (fold changes) in eWAT 24 hours after IH liraglutide treatment compared to control group (IH control). *Rpl4* and *PPia* were used as reference genes. Scale bar = 10X magnification. Data are given in mean ± SEM of 7-8 animals per group.

Acute IH liraglutide treatment did not affect expression of brown adipocyte markers (*ucp3, ucp1*), and expression of browning and adipogenesis markers (*prdm16, cidea, fgf21,adrß1)* in iBAT compared to control group (Figure 26). (Kaineder et al., IJO 2017, unpublished results).

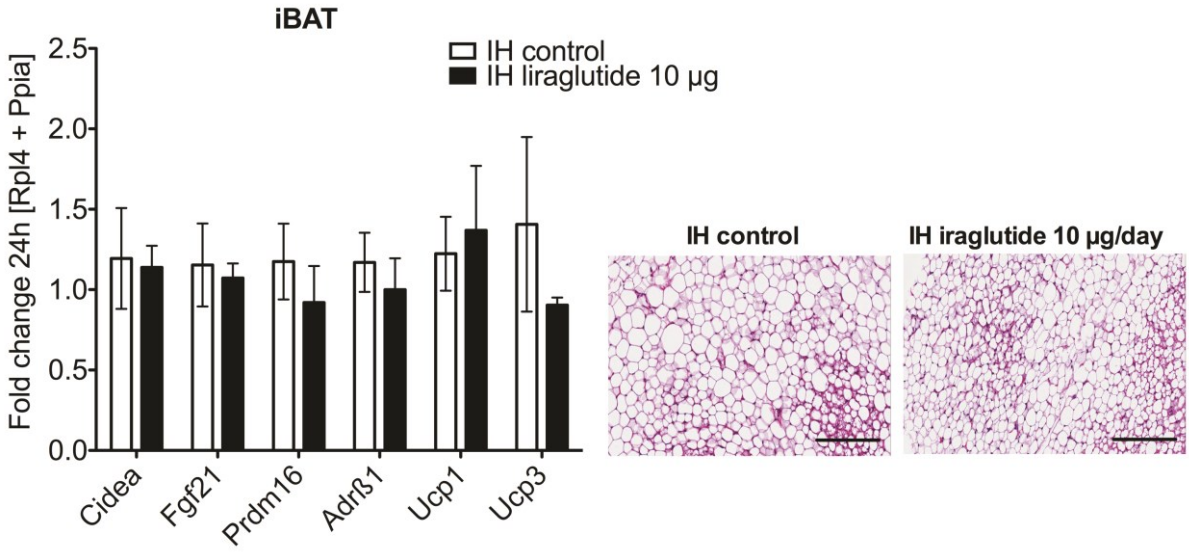

Figure 26 – Acute liraglutide treatment does not affect thermogenesis and browning in iBAT. Relative mRNA levels (fold changes) in iBAT 24 hours after IH liraglutide treatment compared to control group (IH control).

Rpl4 and *PPia* were used as reference genes. Scale bar = 10X magnification. Data are given in mean ± SEM of 7-8 animals per group.

6.5.4 Acute intrahypothalamic liraglutide treatment does not affect the regulation of hypothalamic appetite neurons

Acute IH treatment with liraglutide led to unchanged expression of melanocortin 4 receptor gene (*mc4r*) compared to the control group (Figure 27). We did not observe any changes to expression level of the orexigenic neuropeptide *npy* and anorexigenic neuropeptide *pomc* (Figure 27). mRNA expressions of *glp1r*, *agrp* and *lepr* were undetectable in the hypothalamus after 24 hours liraglutide administration. (Kaineder et al., IJO 2017, unpublished results).

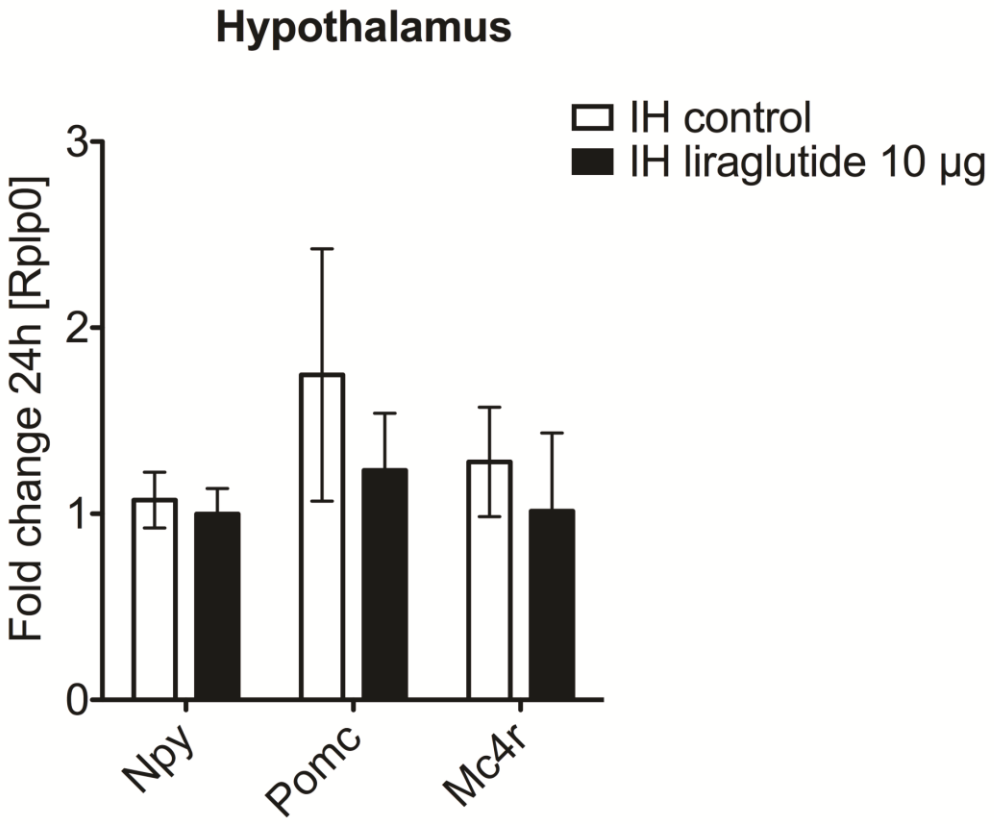

Figure 27 - Acute liraglutide treatment does not trigger appetite neurons in the hypothalamus. Relative hypothalamic mRNA expression levels (fold changes) 24 hours after IH liraglutide treatment. *Rplp0* was used as reference gene. Data are given as mean ± SEM of 7-8 animals per group compared to their corresponding control group. (Kaineder et al., IJO 2017, unpublished results)

6.5.5 Acute intrahypothalamic liraglutide treatment does not affect glucose and fatty acid metabolite levels

We observed no changes in plasma glucose levels and also not in plasma levels of fatty acid metabolites (FG, NEFA, TAG) 24 hours after IH liraglutide treatment (Table 8). (Kaineder et al., IJO 2017, unpublished results).

Table 8 – Acute liraglutide treatment does not affect adipose markers and also not glucose concentrations. Circulating plasma levels of glucose (glucose, insulin), of fatty acid metabolites (NEFA, TAG, FG) 24 hours after IH (10 µg) liraglutide treatment. Data are given as mean ± SEM of 7-8 animals per group. FG, free glycerol; NEFA, non-esterified fatty acids; TAG, triglyceride; (Kaineder et al., IJO 2017, unpublished results)

	IH control	IH liraglutide [10 µg]
FG (µmol/ml)	22.05 ± 2.40	23.80 ± 6.26
NEFA (µmol/ml)	33.96 ± 2.91	54.46 ± 11.21
TAG (mmol/l)	4.15 ± 0.29	3.50 ± 0.28
Glucose (mmol/l)	7.98 ± 0.22	8.06 ± 0.22

6.6 Discussion

This study aimed to investigate the acute effect of liraglutide on body weight and the central melanocortin system (POMC/MC4R). Central (IH) liraglutide treatment did not induce body weight loss and no change in adipose tissue mass after 24 hours. Expression patterns of browning and thermogenic markers in adipose tissues were unaffected by central liraglutide administration. Similar, mRNA expression of markers for appetite neurons in the hypothalamus was unchanged after acute central liraglutide treatment. In addition glucose and fatty acid metabolism were unaffected by acute central liraglutide treatment.

In contrast to chronic central liraglutide treatment, acute central liraglutide administration did not trigger a reduction in body weight and adipose tissue weight in our study. A recent acute study observed a body weight loss after liraglutide injection after 24 hours, but this effect remitted after 48 hours[38]. It was shown that acute liraglutide administration causes a modest reduction in caloric intake and body weight loss at 4 hours but not at 24 hours[60].

Similar to our data for chronic liraglutide administration, mRNA expression of browning and thermogenic markers (*cidea, cebpa, fgf21, prdm16, ucp1, ucp3, adrß1*) in interscapular brown adipose tissue (iBAT), and inguinal white adipose tissue (iWAT) were largely unaffected by central acute liraglutide treatment. In contrast a recent acute study associated the administration of liraglutide with increased thermogenesis in brown adipose tissue and browning of white adipose tissue through the AMP-activated protein kinase pathway in the ventromedial hypothalamus (VMH)[38]. Our study does not support the involvement of increased thermogenic or browning capability in acute liraglutide treatment but this could be due to differences in delivery site (IH vs. VMH) and differences in dosing[38].

We observed no change in mRNA expression of markers for anorexigenic (*pomc, mc4r*) and orexigenic (*npy*) neurons by acute central liraglutide injection. This supports our data on body weight, adipose tissue weight and energy expenditure (in terms of browning and thermogenesis).

7 Conclusion

To summarise my PhD thesis, I want to highlight the most important findings from the previous 3 chapters.

In general, we examined the chronic and acute pharmacological effects of the GLP-1 receptor agonist liraglutide on energy homeostasis in the hypothalamus. This was accomplished by establishing a drug delivery system reliable for chronically targeting the hypothalamus without causing severe tissue damage.

Our first study showed that PEEK performed best of all 3 tested materials for focal drug delivery system to the hypothalamus because it did not influence body weight development and was biocompatible with the surrounding brain areas. We observed no severe tissue damage caused by the cannula and were able to focally deliver sodium fluorescein to the hypothalamus. These results built a solid basis for further investigations on the chronic and acute pharmacological effect of liraglutide treatment on energy homeostasis in the hypothalamus.

Considering the results from our second study about continuous chronic intrahypothalamic liraglutide treatment on energy homeostasis we conclude that central liraglutide treatment rather than peripheral liraglutide treatment leads to reduction of body weight and adipose tissue weight. In addition, the tremendous activation of the anorectic MC4R shows that central chronic liraglutide is a potent regulator of energy homeostasis and that there is an alternative pathway for liraglutide to stimulate the melanocortin system other than POMC/α-MSH.

Our third study aimed to clarify whether the observed anorectic effect of liraglutide is also an early response, and if thermogenesis and browning of adipose tissue and the activation of the melanocortin system are involved. To our surprise and contrary to other acute studies we could not observe any changes on body weight or changes to mRNA signature of markers for thermogenesis, browning and appetite regulating neurons after acute central liraglutide treatment. We conclude that the different delivery sites of liraglutide in the hypothalamus mainly contribute to the observed inconsistencies among studies.

8 Future perspective

Future studies will further investigate the chronic effect of liraglutide on energy homeostasis, by evaluating the contribution of caloric intake and energy expenditure to the observed body weight loss. First we will perform a dose-response study, thereby elucidating the threshold dose of central and peripheral liraglutide for body weight loss. We will use our continuous focal delivery technique to investigate the chronic central effects of liraglutide in diet induced obese rats. We want to identify novel anorectic targets in the hypothalamus triggering the melanocortin system and its downstream system. This can help to develop safe low-dose combination therapies to reduce side effects and improve the chronic weight management and metabolic control.

Table 9 – Future projects. cOFM – cerebral open flow microperfusion; DIO – diet induced obese; PK – pharmacokinetics; PD – pharmacodynamics; EE – energy expenditure; FI – food intake;

Future projects	**Rat model**
cOFM + osmotic pumps	*In vitro*
PK/PD Studies – Appearance rate in CSF of long-acting GLP-1R agonists (IV; SC)	DIO
IH & SC liraglutide action on EE/FI: • Liraglutide concentration (CSF & Plasma) • Neurotransmitter/Metabolomics profiling(CSF) • FA/glucose metabolites (plasma) • µCT/adipocyte size/adipose tissue mass • FI/EE • Gene expression profile (hypothalamus/adipose tissue)	DIO
Target homeostatic brain regions (hypo nuclei) + liraglutide: • Identify downstream targets of MC4R	DIO
Target non-homeostatic brain regions (thalamus, frontal cortex, NAc) + liraglutide: • Learning/Memory/Motivation → Reward	DIO

Bibliography

1. WHO. Obesity and overweight [Internet].Fact sheet. 2016 [cited 2016 Nov 17]. Available from: http://www.who.int/mediacentre/factsheets/fs311/en/

2. Wang Y, Beydoun MA. The obesity epidemic in the United States - Gender, age, socioeconomic, racial/ethnic, and geographic characteristics: A systematic review and meta-regression analysis. *Epidemiol Rev* 2007;**29**:6–28.

3. Ng M, Fleming T, Robinson M, Thomson B, Graetz N, Margono C, et al. Global, regional, and national prevalence of overweight and obesity in children and adults during 1980 – 2013: a systematic analysis for the Global Burden of Disease Study 2013. *Lancet* 2014;**384**:766–81.

4. Ogden CL, Carroll MD, Curtin LR, Mcdowell MA, Tabak CJ, Flegal KM. Prevalence of overweight and obesity in the US, 1999-2004. *JAMA* 2016;**295**:1549–55.

5. Kelly T, Yang W, Chen C-S, Reynolds K, He J. Global burden of obesity in 2005 and projections to 2030. *Int J Obes (Lond)* 2008;**32**:1431–7.

6. Gesundheit B für. Overweight and Obesity in Austria. 2012. p. 5–6.

7. Ladenheim EE. Liraglutide and obesity: A review of the data so far. *Drug Des Devel Ther* 2015;**2015**:1867–75.

8. Calling S. Obesity and cardiovascular disease. Aspects of methods and susceptibility. 2006.

9. Haslam DW, James WPT. Obesity. *Lancet* 2005;**366**:1197–209.

10. Mctigue KM, Hess R, Ziouras J, Kathleen M, Hess R. Obesity in Older Adults: A Systematic Review of the Evidence for Diagnosis and Treatment. *Obesity* 2006;**14**:1485–97.

11. Guh DP, Zhang W, Bansback N, Amarsi Z, Birmingham CL, Anis AH. The incidence of co-morbidities related to obesity and overweight: a systematic review and meta-analysis. *BMC Public Health* 2009;**9**:88.

12. Morton GJ, Meek TH, Schwartz MW. Neurobiology of food intake in health and

disease. *Nat Rev Neurosci* 2014;**15**:356–72.

13. Edholm OG, Fletcher JG, Widdowson EM, McCance RA. The Energy Expenditure and Food Intake of Individual Men. *Br J Nutr* 1955;**9**:286–300.

14. Schneeberger M, Gomis R, Claret M. Hypothalamic and brainstem neuronal circuits controlling homeostatic energy balance. *J Endocrinol* 2014;**220**:25–46.

15. Lenard NR, Berthoud H. Central and Peripheral Regulation of Food Intake and Physical Activity: Pathways and Genes. *Obesity (Silver Spring)* 2009;**16**:S11–22.

16. Pang G, Xie J, Chen Q, Hu Z. Energy intake, metabolic homeostasis, and human health. *Food Sci Hum Wellness* 2014;**3**:89–103.

17. Martin K, Mani M, Mani A. New targets to treat obesity and the metabolic syndrome. *Eur J Pharmacol* 2015;1–11.

18. Hetherington A, Ranson S. The relation of various hypothalamic lesions to adiposity in the rat. *J Comp Ne* 1942;**76**:475–99.

19. Kennedy GC. The hypothalamic control of food intake in rats. *Proc R Soc London Ser B, Biol Sci* 1950;**137**:535–49.

20. Anand BK, Brobeck JR. Hypothalamic control of food intake in rats and cats. *Yale J Biol Med* 1951;**24**:123–40.

21. Rexford SA, Antwi DA. Brain regulation of appetite and satiety. *Endocrinol Metab Clin North Am* 2008;**37**:811–23.

22. Gropp E, Shanabrough M, Borok E, Xu AW, Janoschek R, Buch T, et al. Agouti-related peptide-expressing neurons are mandatory for feeding. *Nat Neurosci* 2005;**8**:1289–91.

23. Luquet S. NPY/AgRP Neurons Are Essential for Feeding in Adult Mice but Can Be Ablated in Neonates. *Science (80-)* 2005;**310**:683–5.

24. Huszar D, Lynch CA, Fairchild-Huntress V, Dunmore JH, Fang Q, Berkemeier LR, et al. Targeted Disruption of the Melanocortin-4 Receptor Results in Obesity in Mice. *Cell* 1997;**88**:131–41.

25. Yaswen L, Diehl N, Brennan MB, Hochgeschwender U. Obesity in the mouse model of pro-opiomelanocortin deficiency responds to peripheral melanocortin. *Nat Med* 1999;**5**:1066–70.

26. Stephens TW. Life without neuropeptide Y. 1996. p. 377–8.

27. Qian S, Chen H, Weingarth D, Myrna E, Novi DE, Guan X, et al. Neither Agouti-Related Protein nor Neuropeptide Y Is Critically Required for the Regulation of Energy Homeostasis in Mice. *Society* 2002;**22**:5027–35.

28. Corander MP, Rimmington D, Challis BG, O'Rahilly S, Coll AP. Loss of agouti-related peptide does not significantly impact the phenotype of murine POMC deficiency. *Endocrinology* 2011;**152**:1819–28.

29. Elmquist JK, Bjørbaek C, Ahima RS, Flier JS, Saper CB. Distributions of Leptin Receptor mRNA Isoforms in the Rat Brain. *J Comp Neurol* 1998;**395**:535–47.

30. Marks JL, Porte D, Stahl WL, Baskin DG. Localization of insulin receptor mRNA in rat brain by in situ hybridization. *Endocrinology* 1990;**127**:3234–6.

31. Zigman JM, Jones JE, Lee CE, Saper CB, Elmquist JK. Expression of Ghrelin Receptor mRNA in the Rat and the Mouse Brain. *J Comp Neurol* 2006;**494**:528–48.

32. Spanswick D, Smith M a, Groppi VE, Logan SD, Ashford ML. Leptin inhibits hypothalamic neurons by activation of ATP-sensitive potassium channels. *Nature* 1997;**390**:521–5.

33. Schwartz MW, Seeley RJ, Woods SC, Weigle DS, Campfield LA, Burn P, et al. Leptin increases hypothalamic pro-opiomelanocortin mRNA expression in the rostral arcuate nucleus. *Diabetes* 1997;**46**:2119–23.

34. Ueno H, Nakazato M. Mechanistic relationship between the vagal afferent pathway, central nervous system and peripheral organs in appetite regulation. *J Diabetes Investig* 2016;**7**:812–8.

35. Secher A, Jelsing J, Baquero AF, Hecksher-Sorensen J, Cowley MA, Dalboge LS, et al. The arcuate nucleus mediates GLP-1 receptor agonist liraglutide-dependent weight loss. *J Clin Invest* 2014;**124**:4223–6.

36. Wu Q, Boyle MP, Palmiter RD. Loss of GABAergic Signaling by AgRP Neurons to the Parabrachial Nucleus Leads to Starvation. *Cell* 2009;**137**:1225–34.

37. Ollmann MM, Wilson BD, Yang YK, Kerns JA, Chen Y, Gantz I, et al. Antagonism of central melanocortin receptors in vitro and in vivo by agouti-related protein. *Sci (New York, NY)* 1997;**278**:135–8.

38. Beiroa D, Imbernon M, Gallego R, Senra A, Herranz D, Villarroya F, et al. GLP-1 agonism stimulates brown adipose tissue thermogenesis and browning through hypothalamic AMPK. *Diabetes* 2014;**63**:3346–58.

39. Rezai-Zadeh K, Yu S, Jiang Y, Laque A, Schwartzenburg C, Morrison CD, et al. Leptin receptor neurons in the dorsomedial hypothalamus are key regulators of energy expenditure and body weight, but not food intake. *Mol Metab* 2014;**3**:681–93.

40. Maejima Y, Sedbazar U, Suyama S, Kohno D, Onaka T, Takano E, et al. Nesfatin-1-Regulated Oxytocinergic Signaling in the Paraventricular Nucleus Causes Anorexia through a Leptin-Independent Melanocortin Pathway. *Cell Metab* 2009;**10**:355–65.

41. Stricker EM. Influence of saliva on feeding behavior in the rat. *J Comp Physiol Psychol* 1970;**70**:103–12.

42. Ahima RS, Saper CB, Flier JS, Elmquist JK. Leptin regulation of neuroendocrine systems. *Front Neuroendocrinol* 2000;**21**:263–307.

43. Yeo GS, Farooqi IS, Challis BG, Jackson RS, O'Rahilly S. The role of melanocortin signalling in the control of body weight: evidence from human and murine genetic models. *QJM* 2000;**93**:7–14.

44. Fan W, Boston B a, Kesterson R a, Hruby VJ, Cone RD. Role of melanocortinergic neurons in feeding and the agouti obesity syndrome. *Nature* 1997;**385**:165–8.

45. Xu B, Goulding EH, Zang K, Cepoi D, Cone RD, Jones KR, et al. Brain-derived neurotrophic factor regulates energy balance downstream of melanocortin-4 receptor. *Nat Neurosci* 2003;**6**:736–42.

46. Holst JJ. The Physiology of Glucagon-like Peptide 1. *Physiol Rev* 2007;**87**:1409–39.

47. Roed SN, Wismann P, Underwood CR, Kulahin N, Iversen H, Cappelen KA, et al. Real-time trafficking and signaling of the glucagon-like peptide-1 receptor. *Mol Cell Endocrinol* 2014;**382**:938–49.

48. Vilsbøll T, Holst JJ. Incretins, insulin secretion and Type 2 diabetes mellitus. *Diabetologia* 2004;**47**:357–66.

49. Punjabi M, Arnold M, Geary N, Langhans W, Pacheco-López G. Peripheral glucagon-like peptide-1 (GLP-1) and satiation. *Physiol Behav* 2011;**105**:71–6.

50. Turton MD, O'Shea D, Gunn I, Beak SA, Edwards CMB, Meeran K, et al. A role for GLP-1 in the central regulation of feeding. *Nature* 1996;**379**:69–72.

51. Schmidt H, Gutzwiller J, Schmidt H, Rohrer B. GLP-1 promotes satiety and reduces food intake in patients with T2DM. *Am J Physiol* 1999;**276**:1541–4.

52. Nuffer WA, Trujillo JM. Liraglutide: A New Option for the Treatment of Obesity. *Pharmacotherapy* 2015;**35**:926–34.

53. Janssen P, Rotondo A, Mulé F, Tack J. Review article: a comparison of glucagon-like peptides 1 and 2. *Aliment Pharmacol Ther* 2012;

54. Flint A, Nazzal K, Jagielski P, Hindsberger C, Zdravkovic M. Influence of hepatic impairment on pharmacokinetics of the human GLP-1 analogue, liraglutide. *Br J Clin Pharmacol* 2010;**70**:807–14.

55. Deacon CF, Nauck MA, Toft-nielsen M, Pridal L, Willms B, Hoist JJ. Both Subcutaneously and Intravenously Administered Glucagon-Like Peptide I Are Rapidly Degraded From the NH2-Terminus in Type II Diabetic Patients and in Healthy Subjects. *Diabetes* 1995;**44**:1126–31.

56. Malm-Erjefält M, Bjørnsdottir I, Vanggaard J, Helleberg H, Larsen U, Oosterhuis B, et al. Metabolism and Excretion of the Once-Daily Human Glucagon-Like Peptide-1 Analog Liraglutide in Healthy Male Subjects and Its In Vitro Degradation by Dipeptidyl Peptidase IV and Neutral Endopeptidase. *Drug Metab Dispos* 2010;**38**:1944–53.

57. Dunphy JL, Taylor RG, Fuller PJ. Tissue distribution of rat glucagon receptor and GLP-1 receptor gene expression. *Mol Cell Endocrinol* 1998;**141**:179–86.

58. Tornehave D, Kristensen P, Rømer J, Knudsen LB, Heller RS. Expression of the GLP-1 receptor in mouse, rat, and human pancreas. *J Histochem Cytochem* 2008;**56**:841–51.

59. Göke R, Larsen PJ, Mikkelsen JD, Sheikh SP. Distribution of GLP-1 binding sites in the rat brain: evidence that exendin-4 is a ligand of brain GLP-1 binding sites. *Eur J Neurosci* 1995;**7**:2294–300.

60. Sisley S, Gutierrez-Aguilar R, Scott M, D'Alessio DA, Sandoval DA, Seeley RJ. Neuronal GLP1R mediates liraglutide's anorectic but not glucose-lowering effect. *J Clin Invest* 2014;**124**:2456–63.

61. Sisley S, Smith K, Sandoval DA, Seeley RJ. Differences in acute anorectic effects of long-acting GLP1R agonists in rats. *Peptides* 2014;**58**:1–6.

62. Williams DL, Baskin DG, Schwartz MW. Evidence that intestinal glucagon-like peptide-1 plays a physiological role in satiety. *Endocrinology* 2009;**150**:1680–7.

63. Hayes MR, Kanoski SE, Alhadeff AL, Grill HJ. Comparative effects of the long-acting GLP-1 receptor ligands, liraglutide and exendin-4, on food intake and body weight suppression in rats. *Obesity* 2011;**19**:1342–9.

64. Flint A, Raben A, Astrup A, Holst JJ. Glucagon-like peptide 1 promotes satiety and suppresses energy intake in humans. *J Clin Invest* 1998;**101**:515–20.

65. Verdich C, Flint A, Gutzwiller J-P, Naslund E, Beglinger C, Hellstrøm PM, et al. A Meta-Analysis of the Effect of Glucagon-Like Peptide-1 (7 – 36) Amide on Ad Libitum Energy Intake in Humans. *J Clin Endocrinol Metab* 2001;**86**:4382–9.

66. Astrup A, Rössner S, Van Gaal L, Rissanen A, Niskanen L, Al Hakim M, et al. Effects of liraglutide in the treatment of obesity: a randomised, double-blind, placebo-controlled study. *Lancet* 2009;**374**:1606–16.

67. Davies MJ, Bergenstal R, Bode B, Kushner RF, Lewin A, Skjøth TV, et al. Efficacy of Liraglutide for Weight Loss Among Patients With Type 2 Diabetes The SCALE Diabetes Randomized Clinical Trial. *Jama* 2015;**314**:687–99.

68. Wadden TA, Hollander P, Klein S, Niswender K, Woo V, Hale PM, et al. Weight maintenance and additional weight loss with liraglutide after low-calorie-diet-induced weight loss : The SCALE Maintenance randomized study. *Int J Obes* 2013;**37**:1443–51.

69. Pi-Sunyer X, Astrup A, Fujioka K, Greenway F, Halpern A, Krempf M, et al. A Randomized, Controlled Trial of 3.0 mg of Liraglutide in Weight Management. *N Engl J Med* 2015;**373**:11–22.

70. Knudsen LB, Madsen LW, Andersen S, Almholt K, De Boer AS, Drucker DJ, et al. Glucagon-like peptide-1 receptor agonists activate rodent thyroid C-cells causing calcitonin release and C-cell proliferation. *Endocrinology* 2010;**151**:1473–86.

71. Waser B, Beetschen K, Pellegata NS, Reubi JC. Incretin receptors in non-neoplastic and neoplastic thyroid C cells in rodents and humans: Relevance for incretin-based diabetes therapy. *Neuroendocrinology* 2011;**94**:291–301.

72. Can J, Sloth B, Jensen C, Flint A, Blaak E, Saris W. Effects of the once-daily GLP-1 analog liraglutide on gastric emptying, glycemic parameters, appetite and energy metabolism in obese, non-diabetic adults. *Int J Obes* 2013;**38**:784–93.

73. Alhadeff AL, Baird J-P, Swick JC, Hayes MR, Grill HJ. Glucagon-like Peptide-1 receptor signaling in the lateral parabrachial nucleus contributes to the control of food intake and motivation to feed. *Neuropsychopharmacology* 2014;**39**:2233–43.

74. Dickson SL, Shirazi RH, Hansson C, Bergquist F, Nissbrandt H, Skibicka KP. The glucagon-like peptide 1 (GLP-1) analogue, exendin-4, decreases the rewarding value of food: a new role for mesolimbic GLP-1 receptors. *J Neurosci* 2012;**32**:4812–20.

75. Bloemendaal L Van, Ijzerman RG, Kulve JS, Barkhof F. GLP-1 receptor activation modulates appetite- and reward-related brain areas in humans. *Diabetes* 2014;**63**:4786–4196.

76. Larsen PJ, Tang-Christensen M, Jessop DS. Central administration of

glucagon-like peptide-1 activates hypothalamic neuroendocrine neurons in the rat. *Endocrinology* 1997;**138**:4445–55.

77. Tang-Christensen M, Larsen PJ, Göke R, Fink-Jensen A, Jessop DS, Moller M, et al. Central administration food and water intake of GLP-1- (7-36) in rats amide inhibits food and water intake in rats. *Am J Physiol* 1996;**271**:R848–56.

78. Tang-Christensen M, Sparre-Ulrich AH, Hartmann B, Grevstad U, Rosenkilde MM, Holst JJ, et al. Transfer of liraglutide from blood to cerebrospinal fluid is minimal in patients with type 2 diabetes. *Int J Obes* 2015;**39**:1651–4.

79. Iepsen EW, Torekov SS, Holst JJ. Liraglutide for Type 2 diabetes and obesity: a 2015 update. *Expert Rev Cardiovasc Ther* 2015;**13**:753–67.

80. Knudsen LB. Liraglutide: the therapeutic promise from animal models. *Int J Clin Pract* 2010;**64**:4–11.

81. Kanoski SE, Fortin SM, Arnold M, Grill HJ, Hayes MR. Peripheral and central GLP-1 receptor populations mediate the anorectic effects of peripherally administered GLP-1 receptor agonists, liraglutide and exendin-4. *Endocrinology* 2011;**152**:3103–12.

82. Clinton SM, Sucharski IL, Finlay JM. Desipramine attenuates working memory impairments induced by partial loss of catecholamines in the rat medial prefrontal cortex. *Psychopharmacology (Berl)* 2006;**183**:404–12.

83. Di Benedetto M, Feliciani D, D'Addario C, Izenwasser S, Candeletti S, Romualdi P. Effects of the selective norepinephrine uptake inhibitor nisoxetine on prodynorphin gene expression in rat CNS. *Mol Brain Res* 2004;**127**:115–20.

84. Cunningham MG, O'Connor RP, Wong SE. Construction and Implantation of a Microinfusion System for Sustained Delivery of Neuroactive Agents. *J Vis Exp* 2008;1–8.

85. Hauss-Wegrzyniak B, Dobrzanski P, Stoehr JD, Wenk GL. Chronic neuroinflammation in rats reproduces components of the neurobiology of Alzheimer's disease. *Brain Res* 1998;**780**:294–303.

86. Marchalant Y, Rosi S, Wenk GL. Anti-inflammatory property of the cannabinoid

agonist WIN-55212-2 in a rodent model of chronic brain inflammation. *Neuroscience* 2007;**144**:1516–22.

87. Zhang X, Lee TH, Xiong X, Chen Q, Davidson C, Wetsel WC, et al. Methamphetamine induces long-term changes in GABAA receptor alpha2 subunit and GAD67 expression. *Biochem Biophys Res Commun* 2006;**351**:300–5.

88. Naert G, Ixart G, Tapia-Arancibia L, Givalois L. Continuous i.c.v. infusion of brain-derived neurotrophic factor modifies hypothalamic-pituitary-adrenal axis activity, locomotor activity and body temperature rhythms in adult male rats. *Neuroscience* 2006;**139**:779–89.

89. Radecki DT, Brown LM, Martinez J, Teyler TJ. BDNF protects against stress-induced impairments in spatial learning and memory and LTP. *Hippocampus* 2005;**15**:246–53.

90. Soria-Gómez E, Massa F, Bellocchio L, Rueda-Orozco PE, Ciofi P, Cota D, et al. Cannabinoid type-1 receptors in the paraventricular nucleus of the hypothalamus inhibit stimulated food intake. *Neuroscience* 2014;**263**:46–53.

91. Burghardt PR, Krolewski DM, Dykhuis KE, Ching J, Pinawin AM, Britton SL, et al. Nucleus accumbens cocaine-amphetamine regulated transcript mediates food intake during novelty conflict. *Physiol Behav* 2016;**158**:76–84.

92. Bayon A. In Vivo Perfusion and Release of Neuroactive Substances: Methods and Strategies. 2012. 250 p.

93. Sofroniew M V., Vinters H V. Astrocytes: Biology and pathology. *Acta Neuropathol* 2010;**119**:7–35.

94. Kincaid-Colton CA, Streit WJ. The Brain's Immune System. *Sci Am* 1995;**275**:54–61.

95. Mofid MM, Thompson RC, Pardo CA, Manson PN, Vander Kolk CA. Biocompatibility of fixation materials in the brain. *Plast Reconstr Surg* 1997;**100**:14–20.

96. Birngruber T, Ghosh A, Hochmeister S, Asslaber M, Kroath T, Pieber TR, et al.

Long-term implanted cOFM probe causes minimal tissue reaction in the brain. *PLoS One* 2014;**9**:1–7.

97. Black J, Maitin EC, Gelman H, Morris DM. Serum concentrations of chromium, cobalt and nickel after total hip replacement: a six month study. *Biomaterials* 1983;**4**:160–4.

98. Evans EJ, Thomas IT. The in vitro toxicity of cobalt-chrome-molybdenum alloy and its constituent metals. *Biomaterials* 1986;**7**:25–9.

99. French HG, Cook SD, Haddad RJ. Correlation of tissue reaction to corrosion in osteosynthetic devices. *J Biomed Mater Res* 1984;**18**:817–28.

100. Heath JC, Freeman MAR, Swanson SA V. Carcinogenic properties of wear particles from prostheses made in cobalt-chromium alloy. *Lancet* 1971;**297**:564–6.

101. Paxinos G, Watson C. The rat brain in stereotaxic coordinates. 2007. 90 p.

102. Conn PM, Flanagan TR, Winn SR. Methods in Neurosciences: Providing Pharmacological Access to the Brain.Conn PM, editor. 1991. 520 p.

103. CurbellPlastics. Material Selection Guide. 2016. p. 1–7.

104. Seymour JP, Kipke DR. Neural probe design for reduced tissue encapsulation in CNS. *Biomaterials* 2007;**28**:3594–607.

105. Green S, Schlegel J. A polyaryletherketone biomaterial for use in medical implant applications. *Polym Med Ind Proc a Conf held Brussels* 2001;1–7.

106. Spitzer N, Sammons GS, Price EM. Autofluorescent cells in rat brain can be convincing impostors in green fluorescent reporter studies. *J Neurosci Methods* 2011;**197**:48–55.

107. Iepsen EW, Torekov SS, Holst JJ. Liraglutide for Type 2 diabetes and obesity: a 2015 update. *Expert Rev Cardiovasc Ther* 2015;**13**:753–67.

108. Van Bloemendaal L, Ten Kulve JS, La Fleur SE, Ijzerman RG, Diamant M. Effects of glucagon-like peptide 1 on appetite and body weight: Focus on the CNS. *J Endocrinol* 2014;**221**:T1–16.

109. Talsania T, Anini Y, Siu S, Drucker DJ, Brubaker PL. Peripheral exendin-4 and peptide YY3-36 synergistically reduce food intake through different mechanisms in mice. *Endocrinology* 2005;**146**:3748–56.

110. Theeuwes F, Yum SI. Principles of the design and operation of generic osmotic pumps for the delivery of semisolid or liquid drug formulations.Vol. 4, Annals of Biomedical Engineering. 1976. p. 343–53.

111. Alzet. ALZET Osmotic Pumps [Internet]. [cited 2017 Mar 21]. Available from: http://www.alzet.com/products/ALZET_Pumps/howdoesitwork.html

112. Alzet. ALZET Brain Infusion System [Internet]. [cited 2017 Mar 21]. Available from: http://www.alzet.com/products/brain_infusion_kit/how_it_works.html

113. Judex S, Luu YK, Ozcivici E, Adler B, Lublinsky S, Rubin CT. Quantification of Adiposity in Small Rodents using Micro-CT. *Methods* 2010;**50**:243–51.

114. Livak KJ, Schmittgen TD. Analysis of relative gene expression data using real-time quantitative PCR and 2-ddCT method. *Methods* 2001;**25**:402–8.

115. Meeran K, Shea DO, Edwards CMB, Turton MD, Heath MM, Gunn I, et al. Repeated Intracerebroventricular Administration of GLP-1 or exendin alters Body Weight in the Rat. *Endocrinology* 1999;**140**:244–50.

116. Donahey JC, van Dijk G, Woods SC, Seeley RJ. Intraventricular GLP-1 reduces short- but not long-term food intake or body weight in lean and obese rats. *Brain Res* 1998;**779**:75–83.

117. Nauck MA, Kemmeries G, Holst JJ, Meier JJ. Rapid tachyphylaxis of the glucagon-like peptide 1-induced deceleration of gastric emptying in humans. *Diabetes* 2011;**60**:1561–5.

118. Iepsen EW, Lundgren J, Holst JJ, Madsbad S, Torekov SS. Successful weight loss maintenance includes long-term increased meal responses of GLP-1 and PYY3-36. *Eur J Endocrinol* 2016;**174**:775–84.

119. Iepsen EW, Lundgren J, Dirksen C, Jensen J, Pedersen O, Hansen T, et al. Treatment with a GLP-1 receptor agonist diminishes the decrease in free plasma leptin during maintenance of weight loss. *Int J Obes* 2014;**39**:1–8.

120. Sumithran P, Prendergast LA, Delbridge E, Purcell K, Shulkes A, Kriketos A, et al. Long-term persistence of hormonal adaptations to weight loss. *N Engl J Med* 2011;**365**:1597–604.

121. Rosenbaum M, Leibel RL. Adaptive thermogenesis in humans. *Int J Obes* 2010;**34**:47–55.

122. Kissileff HR, Thornton JC, Torres MI, Pavlovich K, Mayer LS, Kalari V, et al. Leptin reverses declines in satiation in weight-reduced obese humans. *Am J Clin Nutr* 2012;**95**:309–17.

123. Alhadeff AL, Rupprecht LE, Hayes MR. GLP-1 neurons in the nucleus of the solitary tract project directly to the ventral tegmental area and nucleus accumbens to control for food intake. *Endocrinology* 2012;**153**:647–58.

124. Jelsing J, Vrang N, Hansen G, Raun K, Knudsen LB. Liraglutide: short-lived effect on gastric emptying - long lasting effect on body weight. *J Diabetes, Obes Metab* 2012;**14**:531–8.

125. Raun K, Voss P, Gotfredsen CF, Golozoubova V, Rolin B, Knudsen LB. Liraglutide, a long-acting glucagon-like peptide-1 analog, reduces body weight and food intake in obese candy-fed rats, whereas a dipeptidyl peptidase-IV inhibitor, vildagliptin, does not. *Diabetes* 2007;**56**:8–15.

126. Harms M, Seale P. Brown and beige fat: development, function and therapeutic potential. *Nat Med* 2013;**19**:1252–63.

127. Seale P, Conroe HM, Estall J, Kajimura S, Frontini A, Ishibashi J, et al. Prdm16 determines the thermogenic program of subcutaneous white adipose tissue in mice. *J Clin Invest* 2011;**121**:96–105.

128. Wu J, Boström P, Sparks LM, Ye L, Choi JH, Giang A, et al. Beige Adipocytes are a Distinct Type of Thermogenic Fat Cell in Mouse and Human. *Cell* 2013;**150**:366–76.

129. Kopecky J, Clarke G, Enerbäck S, Spiegelman B, Kozak LP. Expression of the mitochondrial uncoupling protein gene from the aP2 gene promoter prevents genetic obesity. *J Clin Invest* 1995;**96**:2914–23.

130. Petrovic N, Walden TB, Shabalina IG, Timmons JA, Cannon B, Nedergaard J. Chronic peroxisome proliferator-activated receptor γ (PPARγ) activation of epididymally derived white adipocyte cultures reveals a population of thermogenically competent, UCP1-containing adipocytes molecularly distinct from classic brown adipocytes. *J Biol Chem* 2010;**285**:7153–64.

131. Flint A, Raben A, Rehfeld JF, Holst JJ, Astrup A. The effect of glucagon-like peptide-1 on energy expenditure and substrate metabolism in humans. *Int J Obes* 2000;**24**:288–98.

132. Rosenbaum M, Hirsch J, Murphy E, Leibel RL. Effects of changes in body weight on carbohydrate metabolism, catecholamine excretion, and thyroid function. *Am J Clin Nutr* 2000;**71**:1421–32.

133. Lockie SH, Heppner KM, Chaudhary N, Chabenne JR, Morgan D a., Veyrat-Durebex C, et al. Direct control of brown adipose tissue thermogenesis by central nervous system glucagon-like peptide-1 receptor signaling. *Diabetes* 2012;**61**:2753–62.

134. Choksi NY, Jahnke GD, St. Hilaire C, Shelby M. Role of Thyroid Hormones in Human and Laboratory Animal Reproductive Health. *Birth Defects Res Part B - Dev Reprod Toxicol* 2003;**68**:479–91.

135. EPA. US. Assessment of thyroid follicular cell tumors. *US Environ Prot Agency, Washington, DC* 1998;**EPA/630/R**:13.

136. Adan RA, Cone RD, Burbach JP, Gispen WH. Differential effects of melanocortin peptides on neural melanocortin receptors. *Mol Pharmacol* 1994;**46**:1182–90.

137. Caruso C, Carniglia L, Durand D, Gonzalez P V., Scimonelli TN, Lasaga M. Melanocortin 4 receptor activation induces brain-derived neurotrophic factor expression in rat astrocytes through cyclic AMP - Protein kinase A pathway. *Mol Cell Endocrinol* 2012;**348**:47–54.

138. Ramírez D, Saba J, Carniglia L, Durand D, Lasaga M, Caruso C. Melanocortin 4 receptor activates ERK-cFos pathway to increase brain-derived neurotrophic factor expression in rat astrocytes and hypothalamus. *Mol Cell Endocrinol*

2015;**411**:28–37.

139. Xu B, Goulding EH, Zang K, Cepoi D, Cone RD, Jones KR, et al. Brain-derived neurotrophic factor regulates energy balance downstream of melanocortin-4 receptor. *Nat Neurosci* 2003;**6**:736–42.

140. Clemmensen C, Finan B, Fischer K, Tom RZ, Legutko B, Sehrer L, et al. Dual melanocortin-4 receptor and GLP-1 receptor agonism amplifies metabolic benefits in diet-induced obese mice. *EMBO Mol Med* 2015;**7**:288–98.

141. Tapinc DE, Ilgin R, Kaya E, Gozen O, Ugur M, Koylu EO, et al. Gene expression of pro-opiomelanocortin and melanocortin receptors is regulated in the hypothalamus and mesocorticolimbic system following nicotine administration. *Neurosci Lett* 2016;**24**:30901–6.

142. Boghossian S, Park M, York DA. Melanocortin activity in the amygdala controls appetite for dietary fat. *Am J Physiol Regul Integr Comp Physiol* 2010;**298**:R385–93.

9 Appendix

9.1 SYBR and TaqMan primer sequences used for RT-PCR analysis

The primers were used to analyse thermogenic and browning gene expression patterns in the epididymal, inguinal white and interscapular brown adipose tissue and for assessment of mRNA levels of appetite regulators in the hypothalamus. (Kaineder et al., IJO 2017, unpublished results).

Table 10- Primer sequences designed by using NCBI Blast (Standard Nucleotide BLAST); all self-designed primers were tested for performance by agarose gel electrophoresis.

Oligo name	5'3' Primer
Rplp0	FW *AAGCAAAGGAAGAGTCGGAGG* RV *TGCAAATGGATGCGAGCAAG*
B2m	FW *GTGCTTAGCAGCCTAGCAGT* RV *GATGAAAACCGCACACAGGC*
Mc4r	FW *CGGGTCAGAAACCATCGTCA* RV *TGCAAATGGATGCGAGCAAG*
Mc3r	FW *TTATCCGACGCTGCCTAACC* RV *CATCAGACTGACGATGCCCA*
Pc1	FW *AGTAAAGCAACCCAGAGCCAG* RV *CTTTGCTTCATGGCTCGCAC*
Pomc	FW *GACCTCACCACGGAAAGCAA* RV *TGACCCATGACGTACTTCCG*
Agrp	FW *AGGAAGTAGTCACGTGTGGG* RV *GGACACAGCTCAGCAACATT*
aMsh	FW *GCGATCTAGAACCCGACTGT* RV *GAGGCTCACATCTGCATGGT*
Socs3	FW *AGAACCTACGCATCCAGTGC* RV *GGTTCCGTCGGTGGTAAAGA*
Lepr	FW *CCTGCTGGAGTCCCAAACAA* RV *GCGGAGCAGTTTTGACCTTG*
Trh	FW *ACTCTTCAGCTCAGCATCTTGG* RV *AGGGTGAAGATCAAAGCCAGA*

Dio2	FW *AAGTGTCCCCTTCGGTTTCC* RV *ATGGTACGCGCACATTACCT*
Tsh	FW *GAAATACCGGGATGCCCACA* RV *TCTGTGGCTTGGTGCAGTAG*
Glp1r	FW *ACAGGTCTCTTCTGCAACCG* RV *ATGCCCTTGGAGCACACTAC*

Oligo name	5'3' Primer – TaqMan probes Commercially primers provided by Life Technologies
Ppia	Rn00690933_m1
Rpl4	Rn00821091_g1
Hprt	Rn01527840_m1
Ucp1	Rn00562126_m1
Ucp3	Rn00565874_m1
Cidea	Rn04181355_m1
Cidec	Rn01421167_m1
Fgf21	Rn00590706_m1
Cebpa	Rn00560963_s1
Cebpb	Rn00824635_s1
Adrß1	Rn00824536_s1
Ppargc1α	Rn00580241_m1
Pparγ	Rn00440945_m1
Adiponectin	Rn00595250_m1

Leptin	Rn00565158_m1
Prdm16	Rn01516224_m1
Zic1	Rn00575376_m1
Bmp7	Rn01528889_m1
Mtco3	Rn03296820_s1
Ldlr	Rn00598442_m1
Lpl	Rn00561482_m1
Cox4i1	Rn00665001_g1
Cpt1a	Rn00580702_m1
Cycs	Rn01410227_g1
Acacb	Rn00588290_m1

9.2 Total liraglutide concentrations in plasma

Table 11 - Plasma concentration of liraglutide in SC treatment group. Total liraglutide concentration at baseline and day 28 is shown from four animals chosen on sample availability. Data is given as mean ± SD in pmol/l

	SC liraglutide [200 µg/kg/day]
Baseline (N=4)	1785 ± 1054 pmol/l
Day 28 (N=4)	2000 ± 975 pmol/l